Scour at Culvert Outlets in Mixed Bed Materials

Offices of Research
and Development
Washington, D.C. 20590

Report No.
FHWA/RD-82/011

Final Report
September 1982

U.S. Department
of Transportation

Federal Highway Administration

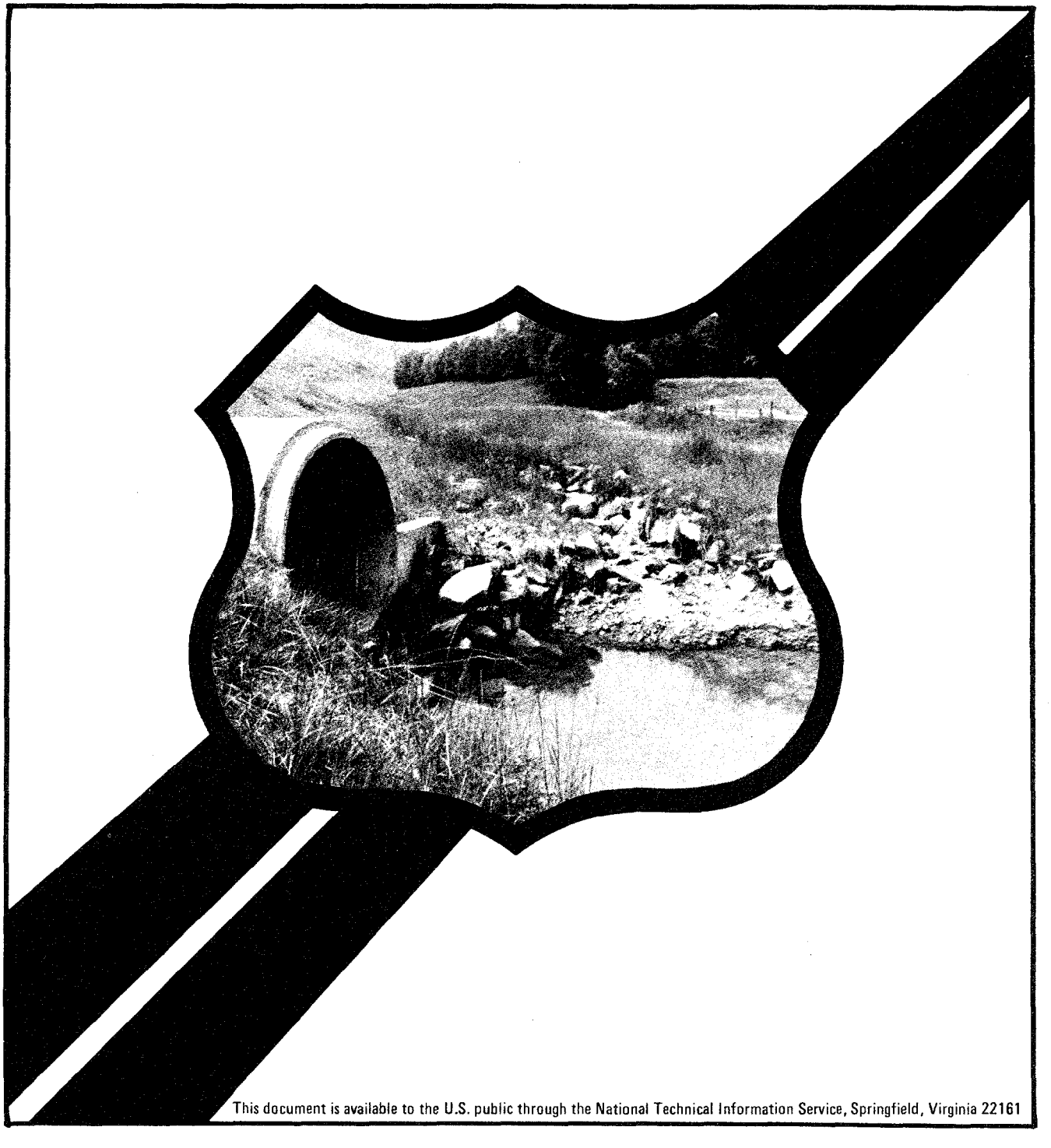

FOREWORD

This report describes laboratory tests of scour in various types of soils at culvert outlets. The tests provide a basis for including soil properties in the estimate of culvert outlet scour and will improve the technique of determining the need for energy dissipators.

Sufficient copies of this report are being distributed to provide a minimum of two copies to each FHWA regional office, one copy to each division office, and one copy to each State highway agency. Direct distribution is being made to the division office.

Charles F. Scheffey
Director, Office of Research
Federal Highway Administration

Technical Report Documentation Page

1. Report No.	2. Government Accession No.	3. Recipient's Catalog No.
FHWA/RD - 82/011		

4. Title and Subtitle	5. Report Date
Scour at Culvert Outlets in Mixed Bed Materials	September 1982
	6. Performing Organization Code
7. Author(s) J. F. Ruff, S. R. Abt, C. Mendoza, A. Shaikh, and R. Kloberdanz	8. Performing Organization Report No.
9. Performing Organization Name and Address Colorado State University Engineering Research Center Fort Collins, Colorado 80523	10. Work Unit No. (TRAIS) FCP 35H1-172
	11. Contract or Grant No. DOT-FH-11-9227
12. Sponsoring Agency Name and Address Office of Research and Development Federal Highway Administration U.S. DOT Washington, DC 20590	13. Type of Report and Period Covered Final Report 1/17/77 to 1/30/82
	14. Sponsoring Agency Code S01244

15. Supplementary Notes

Contract Manager J. Sterling Jones (HRS-42) HER-10
Project Manager Roy E. Trent (HRS-42) HER-10

16. Abstract

The study of localized scour at culvert outlets has been on-going to control and manage erosion along highway embankments. Herein is presented an investigation of scour at culvert outlets which refines and extends the state-of-the-art of predicting the dimensions of scour holes.

Over 100 experiments ranging from 20 to 1000 minutes in duration were conducted in cohesive and non-cohesive bed materials. Culverts having 4-inch (10.2 cm),10-inch (25.4 cm), 14-inch (35.6 cm) and 18-inch (45.7 cm) diameters were tested with discharges from .11 cfs (.003 cms) to 29.13 cfs (.82 cms). Tailwater elevations were maintained at zero, 0.25D and 0.45D ± 0.05D above the culvert inlet where D is the diameter of the culvert.

The results yielded a series of empirical relationships expressing the depth, width, length and volume of scour as a function of the culvert diameter and discharge. Parameters including the shear number, equivalent depth, pipe shape, soil gradation and extent of scour were investigated. General observations concerning scour, hole formation, growth and stabilization were reported.

17. Key Words	18. Distribution Statement
Scour, culvert, localized erosion	No restriction. This document is available to the public through the National Technical Information Service, Springfield, Virginia 22161

19. Security Classif. (of this report)	20. Security Classif. (of this page)	21. No. of Pages	22. Price
Unclassified	Unclassified	115	

PREFACE

The work in this report was performed under contract DOT-FH-11-9227, entitled "Scour at Culvert Outlets in Mixed Bed Materials" between the Federal Highway Administration and Colorado State University. This research contract developed a procedure for predicting and evaluating localized erosion at culvert outlets in cohesive and noncohesive materials.

TABLE OF CONTENTS

TABLE OF CONTENTS (continued)

LIST OF FIGURES

LIST OF TABLES

LIST OF SYMBOLS

Symbol	Description
a	Constant
A	Semi-transverse axis of the hyperbola
A	Projected surface area of the soil grain
A	Cross-sectional area of flow at culvert outlet
b	Constant
c	Constant
C_d	Drag coefficient
C_1, C_2, C_3	Constants
C_h	Cohesive stress resistance
d	Size of soil particle
d_s	Maximum depth of scour
d_{50}	Mean size of material grains
d_{sc}	Depth of scour
d_s	Minimum grain diameter
d'	Volume of scour
d	Depth of scour
d_o	Depth of flow at pipe outlet
d_s	Maximum scour depth at time t
d_{84}	Sieve diameter of the material for which 84 percent is finer by weight
d_{16}	Sieve diameter of the material for which 16 percent is finer by weight
d_{sm}	Maximum scour depth at t_o
D	Pipe diameter
D_o	Pipe diameter
D_{sm}	Depth of scour

Symbol	Description
D_{sm}	Maximum depth of scour
D_p	Jet diameter at the point where the jet plunges into the tailwater
D_r	Dispersion ratio
D	Mean depth of flow
D_s	Depth of scour
D.I.	Discharge intensity ($D.I. = Qg^{-0.5}D^{-2.5}$)
e	Void ratio
$f_1(P), f_2(P)$	Functions related to plastic properties of cohesive soils
F	Force exerted by the flow upon the sediment particle
F_o	Froude number ($F_o = V_o/\sqrt{gd_o'}$)
F_d	Force tending to cause erosion ($F_d = \tau A$)
F_r	Resisting force holding the soil grain in place ($F_r = S_h A$)
F	Froude number ($F = \bar{V}/\sqrt{gL_c}$)
g	Gravitational acceleration
H	Headwall condition
I_p	Plasticity index
L_{sc}	Length of scour
L_{sm}	Length of scour
L	Length of the scour hole for all tailwater conditions
L_s	Maximum length of scour at time t
L	Horizontal distance along the centerline between any cross section and the culvert outlet
L_{sm}	Maximum scour length at t_o
L_c	Culvert characteristic length
L_{mm}	Maximum mound length
n	Number of grains per unit area

Symbol	Description
n	Porosity
NH	No-headwall condition
P.I.	Plastic index
P_c	Percentage of clay
P	Pressure in the vicinity of particles
Q	Water discharge
R	Resistance of motion of particle
R_H	Hydraulic radius
S	Slope of energy grade line
S_v	Shearing strength
SAR	Sodium absorption ratio
S.G.	Specific Gravity of Materials
S_h	Unit strength resisting the hydraulic shear stress
S_η	Inverted shear number ($S_\eta = \rho\bar{V}^2/\tau_c$)
S_v	Saturated soil shear stress
SI	Scour influence
TW	Tailwater elevation above pipe invert
t	Duration of scour in minutes
T	Time
t	Time less than or equal to the duration of scour
t_o	Time duration of experiment
T_w	Tailwater elevation above pipe invert
U_*	Shear velocity
U_{*c}	Shear velocity of impending motion
U.C.	Uniformity coefficient
U_f	Percent of clay particles less than 0.06 mm
V	Characteristic velocity of the flow

Symbol	Description
Vol	Volume of scoured material
Vol_s	Volume of scour
$\overline{V}_o$	Average velocity
V_o	Discharge velocity
V_*	Shear velocity
V_s	Volume of scour at time t
V_p	Jet velocity
V_1, V_2	Point velocities at distances y_1 and y_2 respectively from the boundary
V	Average fluid velocity
$\overline{V}$	Average velocity of flow at culvert outlet
$\overline{V}_b$	Average velocity in the vicinity of a particle
V_{sm}	Volume of scour at t_o
W_{sc}	Width of scour
W_{sm}	Width of scour
W	Width of scour
W_s	Maximum scour width at time t
W_{sm}	Maximum scour width at t_o
WP	Wetted perimeter
x	Coordinate axis ($x = \log V_p t/D_p$)
x	Independent variable ($y = ax^b$)
y	Depth of flow
y	Coordinate axis ($y = \log Z_m/D_p - \log V_p t/D_p$)
y_1, y_2	Distances from the boundary
y	Dependent variable ($y = ax^b$)
Y_e	Equivalent depth parameter
Z_m	Maximum depth of scour

Symbol	Description
α	Constant
β	Ratio of actual volume to d^3 of particle
γ	Specific weight of fluid
γ_s	Specific weight of bed material
δ	Boundary layer thickness
η	Packing coefficient ($\eta = nd^2$)
θ	Angle of repose of material
λ	Shape factor
μ	Dynamic viscosity of water
ν	Kinematic viscosity of fluid
π	Constant (3.1416)
ρ	Mass density of fluid
ρ_s	Mass density of bed material
σ	Grain standard deviation ($\sigma = \sqrt{d_{84}/d_{16}}$)
σ_w	Standard deviation of fall velocity of particles about mean fall diameter
σ	Intergranular surface stress
τ	Intensity of boundary shear
τ_c	Critical shear stress
τ_o	Bed shear stress
τ	Stress due to viscous drag and turbulent form drag of a moving fluid
ϕ	Function
ϕ_h	Hydraulic stress resisting friction angle
ω	Fall velocity

Chapter I

INTRODUCTION

One of the major considerations in the design and construction of a roadway system is the conveyance of tributary drainage through the roadway embankment. As drainage waters are conveyed through the embankment, flow discharges from the culvert and impinges upon the material beneath the outlet. The impinging jet lifts the material particles and transports those particles downstream of the impact area. The jet impact area is transformed into an energy dissipator and a hole is created at the outlet. The eventual result of this scour and erosive process, if left unchecked, is the degradation of the roadway embankment, degradation of the area beneath and adjacent to the culvert outlet and aggradation of the channel, land areas, or properties downstream of the outlet. Because of these severe and often costly damages, the study of localized scour is an important step in the evaluation, control and management of roadway embankment erosion.

The investigation of scour at culvert outlets has been on-going for several decades. Early studies beginning with Rouse (70) and Laursen (43) attempted to understand the general nature and principles of scour. Scour was observed to be a function of discharge, time and material characteristics. Later studies examined numerous scour parameters that affect the degree of degradation and included the tailwater conditions, gradation of the bed material, degree of armour plating and culvert shape and size.

The most notable studies were those of Bohan (13), Fletcher and Grace (27) of the Waterways Experiment Station. They formulated a series of empirical equations which predicted the length, depth, width and volume of scour as a function of the discharge, culvert diameter and time. Bohan, Fletcher and Grace realized the significant effect the tailwater conditions had upon the ultimate scour hole dimensions. Therefore, their prediction equations were generalized to encompass a spectrum of tailwater conditions. Although several studies followed the Bohan, Fletcher and Grace investigations, their work has been adopted as the most comprehensive design criteria available in the area of scour hole dimension prediction.

The ability to predict the magnitude and geometry of localized scour at culvert outlets is a useful evaluation tool in the control and management of erosion along roadway embankments. However, previously developed equations have been extremely conservative. Therefore, it is advantageous to investigate localized scour in noncohesive and cohesive materials at culvert outlets.

Objectives

The general scope of this study was to observe and analyze scour and erosion holes in noncohesive and cohesive material at culvert outlets and to formulate empirical design criteria for predicting scour hole geometry. However, in order to develop a comprehensive, effective

design procedure, it is necessary that the project scope be multi-objective in nature. Therefore, specific project objectives are as follows:

Primary Objectives:

- Determine the dimensions of natural scour holes at the outlet of highway culverts.
- Provide design criteria for the prediction of natural scour hole dimensions.

Secondary Objectives:

- Perform a comprehensive survey of previous scour and erosion studies.
- Establish a data base of scour parameters and soil characteristics applicable to scour in noncohesive and cohesive materials.
- Identify soil characteristics which appear to indicate the scourability of noncohesive and cohesive material.
- Develop an understanding of the laws of similitude relative to scour modeling.

In order to meet these objectives, a series of model studies were conducted on the research campus of Colorado State University sponsored by the Department of Transportation, Federal Highway Administration under Contract No. DOT-FH-11-9227.

Chapter II

REVIEW OF LITERATURE

In order to to predict, control, and manage scour at culvert outlets, it is necessary to understand the nature of the scour phenomenon. The following studies represent the foundation upon which the state-of-the-art of scour hole estimation is based.

Studies of Noncohesive Materials

A major advancement in the study of sediment movement and bed load transport is Shields' (77) analytical and experimental work. Shields assumed that force F exerted by the flow upon the sediment particle could be expressed in terms of the usual drag relationship

$$F = C_d A \rho \frac{V^2}{2} = \phi_1 (\lambda, \frac{Vd}{\nu}) \rho d^2 V^2 \quad (1)$$

in which C_d is the drag coefficient, A is projected area of the particle, ρ is mass density of the fluid, ν is kinematic viscosity of the fluid, d is the size of the particle, λ is a shape factor, and V is the characteristic velocity of the flow at elevation z above the bed. Elevation z is also assumed to be proportional to the size (d) of particle ($z = \alpha d$). Using the equation of velocity distribution near a rough boundary,

$$V = \sqrt{\tau/\rho} \left[5.75 \log \alpha + \phi_2 \left(\frac{d\sqrt{\tau/\rho}}{\nu}\right)\right] = \sqrt{\tau/\rho}\ \phi_3 \left(\alpha, \frac{d\sqrt{\tau/\rho}}{\nu}\right) \quad (2)$$

in which $\tau = \gamma y S$ is intensity of boundary shear, $\sqrt{\tau/\rho} = u_* = \sqrt{gyS}$ is shear velocity, $\alpha = \frac{z}{d}$ is coefficient of proportionality, γ is specific weight of fluid, S is slope of energy grade line, and y is depth of flow. Combining these relationships

$$F = \tau d^2 \phi (\lambda, \alpha, \frac{du_*}{\nu}) \quad (3)$$

Shields further assumed that the resistance, R, to motion of a particle should only depend upon bed form and the immersed weight of the particle:

$$R = \beta (\gamma_s - \gamma) d^3 \quad (4)$$

where β is a dimensionless friction coefficient that represents the ratio of actual volume of the particle to d^3 and γ_s is specific

weight of the bed material. Equating these forces and assuming a level bed of uniform particle size for the initial movement of the particle Shields found:

$$\frac{\tau_c}{(\gamma_s - \gamma)d} = \phi\left(\frac{u_* d}{\nu}\right) = \phi\left(\frac{d}{\delta}\right) \tag{5}$$

where δ is boundary layer thickness and τ_c is critical shear stress. The form of the function ϕ was determined from experiments. Shields reasoned that shape factors should also influence motion, but no such influence was detected in the experiments.

Some of the early efforts in attempting to understand the scour mechanism were made by Rouse (70) in the early 1940's. Rouse observed the change of scour hole geometry as a function of time using a vertical two-dimensional jet directed downward upon an erodible bed. Based upon his observations, Rouse concluded that scour was a function of discharge and time. Furthermore, he found that the depth of scour in a uniform, cohesionless material is dependent upon the size and velocity of the discharging jet and fall velocity of the sediment. Rouse laid the foundation for a series of studies which followed as a result of his findings.

In 1952, Laursen (43) presented his observations on the nature of scour in both a general and localized sense. Laursen related the following premises as basic principles in the investigation of local scour:

- The rate of scour will equal the difference between the capacity for transport out of the scoured area and the rate of supply of material to that area.
- The rate of scour will decrease as the flow section is enlarged.
- There will be a limiting extent to scour.
- The scour limit will be approached asymptotically.

It was noted that the rate of scour will decrease as the local velocities in the eroding area are reduced to where the surface forces are unable to overcome the resisting force of gravity.

As interest increased in attempting to control scour, Doddiah (22) examined the effects of scour and verified a significant portion of Rouse's work. Then Doddiah extended his findings to incorporate the importance of the tailwater condition. He concluded that not only did the tailwater depth influence the amount of scour that occurred, but also there existed a critical tailwater depth in which any decrease in tailwater caused a decrease in scour depth.

Thomas (88) followed and studied the effect that drop height of the jet has on the scour depth. Thomas found that an increase in the jet discharge had a greater significance in the depth of scour than did an equal percentage increase in drop height of the jet or change in depth of the tailwater.

Hallmark (33) verified some of the findings of his predecessors and then embarked on yet another important aspect of the scour phenomenon, that of armorplating. Hallmark's work was conducted with gravel materials while previous studies were conducted with sand materials. His results lead to the following conclusions:

- The rate of scour decreases with an increase in the amount of armorplate in the scour hole.
- A relatively small amount of armorplating material will cause a relatively large decrease in the rate of scour.
- Graded armorplating material decreases the rate of scour more effectively than uniform material of the same median size.
- The minimum size of the armorplate should be about the same as the maximum size of the bed material.
- A uniform size of aggregate slightly larger than the largest particle size of the bed material reduced the rate of scour.

Hallmark's work was perhaps the best concentrated effort toward understanding and controlling scour since Rouse. However, Hallmark was unable to directly relate the depth of scour to the material size.

Smith (82,83) expanded Rouse's work and found that although the depth of the scour hole was dependent upon the initial jet impingement, a final scour condition evolved independently of the initial state. Smith further concluded that the cavity width, eddy currents and slope of the cavity banks effect the rate of scour. Smith noted that for tailwater depths above the critical tailwater depth, a given increase in jet energy will produce a smaller increase in volume of scour than with a tailwater depth less than critical.

Sometime after Smith, L. M. Laushey (44) performed a series of in-depth studies on the scour phenomenon and made a few observations which were confirmed in other studies. Laushey found that the maximum depth of the scour hole at equilibrium was a function of the cube root of the volume of the material scoured, $d_s = \phi\ (3\sqrt{Vol})$. He further noted that the depth and volume scoured in short periods of time were large percentages of the ultimate scour hole dimensions. He also performed work relating the culvert tailwater depth to a critical erosion velocity which initiated scour. Laushey concluded that submergence of the outlet pipe by an amount less than one half of the pipe diameter did not change the incipient scour velocity.

White (95) suggested that when forces on a sand grain are in equilibrium and the grain is on the verge of moving (see Figure 1), the horizontal force F on each exposed particle by the fluid is

$$F = \tau d^2/\eta \tag{6}$$

where $\eta = nd^2$ is a packing coefficient, n is number of grains per unit area, τ is mean shear applied to the bed, and d is diameter of particle. White also assumed that resistance force R to motion is the submerged weight of the particle.

$$R = \frac{\pi}{6} (\gamma_s - \gamma) d^3 \tan \theta \tag{7}$$

where γ_s and γ are the specific weight of particle and fluid respectively. When the forces acting on the particle are in equilibrium,

$$\tan \theta = \frac{\tau d^2/\eta}{\frac{\pi}{6} (\gamma_s - \gamma) d^3} \tag{8}$$

or

$$\tau = \eta \frac{\pi}{6} (\gamma_s - \gamma) d \tan \theta \tag{9}$$

where θ is the angle of repose. By his experiments White found that rounded sand grains subjected to a steady viscous drag (where $\frac{u_* d}{\nu} < 3.5$) begin to move when,

$$\tau = 0.18 (\gamma_s - \gamma) d \tan \theta \tag{10}$$

He also stated that for high speed flow where $\frac{u_* d}{\nu} > 3.5$, drag on a particle due to viscous stresses is negligible compared with form drag due to normal pressure differences. These forces on individual grains fluctuate irregularly.

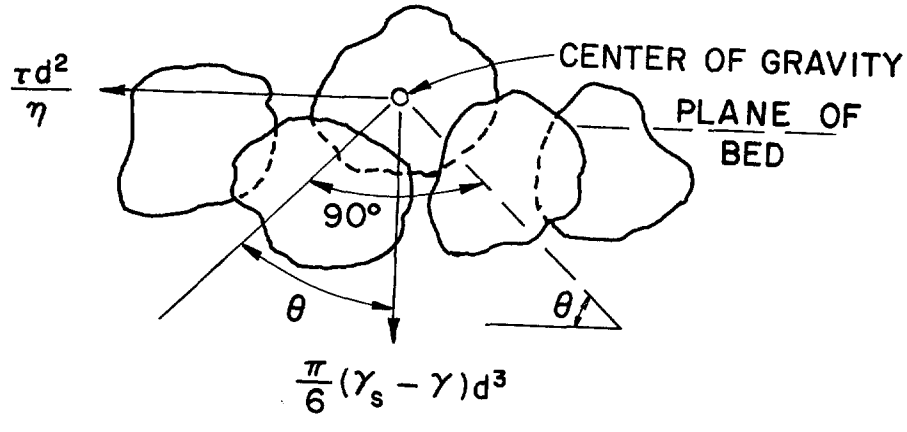

Figure 1. Forces on an individual sand grain.

At about the same time, the T. R. Opie (61) study produced data which in part paralleled Laushey's results. Opie's study produced the following:

- There exists a correlation between the length of scour, depth of scour, width of scour and volume of scour with the pipe diameter and discharge.
- The depth of scour was reduced greatly by increasing the tailwater to approximately the level of the top of the pipe.
- For depths of tailwater below the center of the pipe, TW < D/2, the effect of tailwater depth on the depth of scour was small.
- A slightly different geometry of scour hole was observed for angular material compared with that of rounded material.

Opie established a set of design relationships for computing the approximate scour hole parameters based upon the scour depth, material shape and the use of a transition at the culvert outlet. Experimental results were based on using rock and gravel materials with d_{50} ranging from 25 mm to 204 mm. His design equations are as follows:

	Rounded	Angular
Transition	$L_{sc} = 8.0\ d_{sc}$	$L_{sc} = 6.9\ d_{sc}$
	$W_{sc} = 11.5\ d_{sc}$	$W_{sc} = 11.5\ d_{sc}$
No Transition	$W_{sc} = 6.8\ d_{sc}$	$W_{sc} = 6.0\ d_{sc}$
Transition	$\sqrt[3]{Vol} = 3.2\ d_{sc}$	$\sqrt[3]{Vol} = 3.5\ d_{sc}$
No Transition	$\sqrt[3]{Vol} = 2.6\ d_{sc}$	$\sqrt[3]{Vol} = 2.3\ d_{sc}$

(11)

The Opie equations define d_{sc} as the depth of scour, L_{sc} as the length of scour, W_{sc} as the width of scour and Vol as the volume of scour.

M. A. Stevens (86) followed Opie and analyzed scour in riprap at culvert outlets. Stevens worked with materials with mean diameters ranging from 0.049 ft (15 mm) to 0.613 ft (187 mm) and concluded that the minimum rock size needed to insure that scour would not occur was a mean riprap diameter of one third the pipe diameter. Perhaps one notable finding was that he related the importance of the mound which formed downstream of the scour hole. According to Stevens, if the scour mound is removed, the amount of scour caused by the impinging jet is significantly greater than if the scour mound is left in place.

Bohan (13), at the Waterways Experiment Station, performed a series of scour studies where the flow from the culvert discharge freely onto a channel bed of noncohesive, sand material. The sand had a mean diameter of 0.22 mm and a standard deviation of 1.31. Bohan examined and

correlated the scour hole parameters in accordance with the tailwater conditions, the culvert diameter, the time of discharge and the Froude number ($\bar{V}_o\ g^{-0.5}\ D^{-0.5}$). Bohan developed the following scour design equations:

Minimum Tailwater (depth < $D_o/2$)

$$\begin{aligned} L_{sm} &= 4D_o t^{0.15}\ (1 + 5 \log F_o) \\ W_{sm} &= 2D_o t^{0.2}\ \ (1 + 7 \log F_o) \\ D_{sm} &= D_o\ t^{0.1}\ \ (1.3 + 1.4 \log F_o) \\ Vol_s &= 10\ D_o^{\ 3}\ t^{0.4}\ F_o^{\ 2} \end{aligned} \tag{12}$$

Maximum Tailwater (depth $\geq D_o/2$)

$$\begin{aligned} L_{sm} &= 3D_o t^{0.1}\ \ (2 + 13 \log F_o) \\ W_{sm} &= 2D_o t^{0.05}\ (2 + 5 \log F_o) \\ D_{sm} &= D_o t^{0.1}\ \ \ (0.5 + 3 \log F_o) \\ Vol_s &= 19D_o^{\ 3}\ t^{0.3}\ F_o^{\ 1.7} \end{aligned} \tag{13}$$

where D_o is the pipe diameter, F_o is the Froude number, L_{sm} is the length of scour, W_{sm} is the width of scour, D_{sm} is the depth of scour, Vol_s is the volume of scour, $\bar{V}_o$ is the average velocity and t is the duration of scour in minutes. After several tests, Bohan also found that the minimum grain diameter (d_s) necessary to resist scour was:

$$d_s = 0.25\ D_o\ F_o \qquad \text{Minimum Tailwater} \tag{14}$$

$$d_s = D_o\ (0.25\ F_o - 0.15) \qquad \text{Maximum Tailwater} \tag{15}$$

Bohan continued his work to establish a design criterion to minimize scour through implementation of a horizontal stone blanket. Through use of a $Q/D^{5/2}$ parameter, the following general equation was developed to determine the blanket mean stone size,

$$d_{50}/D_o = 0.020\ \frac{D_o}{T_w}\ (Q/D_o^{\ 5/2})^{4/3} \tag{16}$$

where T_w is the tailwater depth.

A. R. Robinson (67) examined scour under cantilevered outlets in hopes of establishing a design criterion for scour hole prediction. His study centered on the scour on non-cohesive sands with mean grain

diameters of 0.71 mm to 5.66 mm with a standard deviation of 1.20. Robinson conducted his testing with discharges ranging from 5 to 30 cubic feet per second for durations of up to four days. After extensive testing, Robinson concluded:

- The rate of scour will decrease as the flow section is enlarged by erosion.
- There exists a linear relation between the relative width of the scour cavity and the flow parameter $Q/D^{2.5}$ for each material.
- The rate of change of scour depth with flow rate decreases as the flow rate increases.

Most of his results duplicated earlier findings. However, Robinson formulated three relationships for the volume of scour (d'), width of scour (W) and depth of scour (d), based upon the discharge velocity (V_o), shear velocity (V_*), time (T) and pipe diameter (D).

$$\text{Volume:} \quad \frac{d'}{D} = \frac{52.9\left(\frac{V_o}{V_*}\right)^{-1/2} + \log\frac{V_o T}{D} - 7}{196\left(\frac{V_o}{V}\right)^{-3/2}} \tag{17}$$

$$\text{Width:} \quad \frac{W}{D} = \left[\frac{52.9\left(\frac{V_o}{V_*}\right)^{-1/2} + \log\frac{V_o T}{D} - 7}{153\left(\frac{V_o}{V_*}\right)^{-3/2}}\right]^{4/3} \tag{18}$$

$$\text{Depth:} \quad \frac{d}{D} = \left[\frac{52.9\left(\frac{V_o}{V_*}\right)^{-1/2} + \log\frac{V_o T}{D} - 7}{270\left(\frac{V_o}{V_*}\right)^{-3/2}}\right]^{4/5} \tag{19}$$

Fletcher and Grace (27) of the Waterways Experiment Station extended Bohan's study and compiled a guidance procedure for the estimation and control of scour. Their data analysis revealed that the maximum scour depth under a culvert outlet occurred at approximately 0.4 L, where L is the length of the scour hole for all tailwater conditions. Furthermore, they concluded that the $Q/D^{2.5}$ parameter was an extremely important factor and that the depth width, length and volume of the scour cavity could be expressed as a function of the same parameter. Based on these findings, Fletcher and Grace produced a series of design guidelines:

Tailwater < 0.5 D

$$\frac{D_{sm}}{D} = 0.80 \left(\frac{Q}{D^{2.5}}\right)^{0.375} t^{0.10}$$

$$\frac{W_{sm}}{D} = 1.00 \left(\frac{Q}{D^{2.5}}\right)^{0.915} t^{0.15}$$

$$\frac{L_{sm}}{D} = 2.40 \left(\frac{Q}{D^{2.5}}\right)^{0.71} t^{0.125} \qquad (20)$$

$$\frac{V_s}{D} = 0.73 \left(\frac{Q}{D^{2.5}}\right)^{2} t^{0.375}$$

Tailwater $\geq$ 0.5 D

$$\frac{D_{sm}}{D} = 0.74 \left(\frac{Q}{D^{2.5}}\right)^{0.375} t^{0.15}$$

$$\frac{W_{sm}}{D} = 0.72 \left(\frac{Q}{D^{2.5}}\right)^{0.915} t^{0.15}$$

$$\frac{L_{sm}}{D} = 4.10 \left(\frac{Q}{D^{2.5}}\right)^{0.71} t^{0.125} \qquad (21)$$

$$\frac{V_s}{D} = 0.62 \left(\frac{Q}{D^{2.5}}\right)^{2} t^{0.325}$$

where D_{sm} is the maximum depth of scour, V_s the volume of scour, L_{sm} the length of scour, W_{sm} the width of scour, D the pipe diameter, Q the discharge and t the test duration in minutes.

Ettema (24) attempted to examine the local clear water scour mechanism with relation to the bed material gradation as depicted by the grain standard deviation ($\sigma = \sqrt{d_{84}/d_{16}}$) and uniformity coefficient (u.c. = d_{60}/d_{10}). His tests were performed on bed materials ranging from 0.55 mm to 6.00 mm in mean grain size with sediment grading (σ/d_{50} from 0.2 to 1.6 and uniformity coefficients of 1.33 to 2.90. Ettema concluded that the maximum depth of clearwater scour is:

- a function of the standard deviation of the grain size distribution such that as the standard deviation increased the depth of scour decreases.

- not dependent on the grain size when coarse sands and gravels have a uniform grain size (standard deviations approaching zero).

Ettema noted the principal cause for the decrease in the final depth of scour is the formation of armoring in graded materials. He found that scour took a longer time to reach equilibrium in clear water than in sediment laden waters.

Blaisdell et al. (12) presented an analytical method to compute the final depth of scour based on experimental observations made during the early stage of the scouring process. The method defines a relationship between the logarithm of the average velocity of scour and the logarithm of time, by using a limb of a vertically-oriented rectangular hyperbola with the origin of the hyperbola offset from the y-axis. The form of equation for the hyperbola is

$$(y - y_o)^2 - x^2 = A^2 \qquad (22)$$

in which A = the semitransverse axis,

$x = \log V_p t/D_p$,

$y = \log Zm/D_p - \log V_p t/D_p$,

V_p = jet velocity,

D_p = jet diameter at the point where the jet plunges into the tailwater,

Zm = maximum depth of scour,

t = time from the beginning of scour.

A can be computed by assuming values for y_o and using experimental values of x and y. The best value of A is that value for which the standard error of estimate is a minimum.

Studies of Cohesive Materials

Similar studies of scour in cohesive soils have not been conducted. Information pertaining to the prediction of the dimensions of natural scour cavities as well as subsequent aggradation and degradation in cohesive materials at culvert outlets are not available. Therefore, the following references cite research on cohesive materials which denote specific trends, indicators or conclusions that may relate to localized scour and erosion at culvert outlets.

The erodibility of cohesive materials has been of major concern for many decades. The majority of erosion studies have concentrated in the areas of a) rill, sheet and gully erosion, b) general erosion of river

and streams and c) local erosion at bridge piers and spillways. However, the effects of localized scour at culvert outlets, particularly in cohesive materials, have thus far been neglected.

The study of basic soil characteristics and how those characteristics influence soil erodibility can be traced to work performed in the early 1930s by H. E. Middleton (53). However, one of the first notable efforts in relating soil properties to erosion was that by T. C. Peele (64) in 1937. Peele compiled several studies of the era and proposed that the soil properties of percolation rate, suspension percentage and dispersion ratio appeared to be good indicators for relative soil erodibility. Although Peel's work was quite general, it seemingly opened the door to an endless series of investigations.

Investigations by G. W. Musgrave (60) and H. W. Anderson (7) followed Peele's ground work and quantitatively investigated several soil characteristics. For example, Anderson portrayed the dispersion ratio, the ratio of the total weight of silt and clay sized aggregates to the total weight of silt and clay sized materials, as a significant erosion indicator such that a soil is classified erodible when the dispersion ratio (D_r) exceeds 10.

In 1956, Sundborg (87) indicated that the shearing strength of a material is proportional to the cohesive resistive force of a soil acting in a direction opposite to the fluid force. From this conclusion resulted the relationship for critical shear stress of a cohesive material on a horizontal bed.

$$\tau_c = \frac{c_1 \, a_1}{c_2 \, a_2} (\gamma_s - \gamma) \, d_s \tan \theta + c_3 \, S_v \qquad (23)$$

where S_v is the shearing strength, c_1 and c_2 are known constants and c_3 is an unknown constant.

I. S. Dunn (23) also attempted to relate the soil resistance to hydraulic shear stresses by determining a critical shear stress at which soil particles would lift away from a cohesive surface. To determine the critical shear stress (critical tractive shear), Dunn applied stress by a vertical jet impinging upon a submerged soil sample. Several experiments were performed using a variety of sandy clay and silty clay cohesive materials.

Dunn presumed that the amount of fine material in a soil would be an indicator of the resistance to the tractive forces. Therefore, as fine particles are added to a soil, it is reasonable to expect that the cohesive properties will increase. Dunn further concluded that the plasticity index (I_p), the numerical difference between the liquid limit and the plastic limit, is a useful indicator for predicting soil erodibility for soils of plasticity index of 5 to 16. Furthermore, the

grain size of a cohesive material may also be a good parameter for soil resistance to erosion. The culmination of this study was the formulation of the following equations:

$$\tau_c = 0.20 + \frac{(S_v + 180)}{1000} \tan (30 + 1.73\ I_p) \tag{24}$$

and

$$\tau_c = 0.02 + \frac{(S_v + 180)}{1000} \tan (0.06\ U_f) \tag{25}$$

where the critical tractive shear is a function of the soil shear strength (S_v), the percent of clay particles (U_f) less than 0.06 mm by weight and the plasticity index (I_p).

Smerdon and Beasley (81) continued investigating the critical tractive force theory testing a variety of cohesive farm soils, primarily silty loam and clay in nature, in a tilting flume. They believed that the plasticity index, dispersion ratio, mean particle size and the percent of clay were the critical physical properties to identifying the erosibility of a cohesive material. However, they concluded that the critical shear force is best correlated to the plasticity index, dispersion ratio and percentage of clay. The resulting Smerdon and Beasley tractive force equations for computing the magnitude of the tractive force (τ) for uniform flow is:

$$\tau = \gamma DS \tag{26}$$

where τ is the tractive force in pounds per square foot, D is the mean depth of flow and S is the channel gradient. An equation derived from the logarithmic velocity equation for computing the magnitude of the tractive force (τ) for turbulent flow is:

$$\tau = \rho\ ((V_2 - V_1)/5.75\ \log_{10}\ (y_2/y_1))^2 \tag{27}$$

where ρ is the density of water, V_1 and V_2 are point velocities at distances y_1 and y_2 respectively from the boundary.

A large number of notable studies occurred during the early 1960s which broadened the avenues for future investigations. For example, Martin (51) examined cohesive materials in a wetted state and determined that soil characteristics such as water content, salt content and ion exchange were indicators to clay strength. Abdel-Rahman (1) tested clay sediments and concluded that a possible chemical reaction occurs when water is introduced to a cohesive material. The resulting chemical reaction between the water and soil can stabilize the material from further erosion.

While the critical tractive force theory was in the midst of development, Moore and Masch (58) performed experiments on the local scour of cohesive sediments. It was determined that the scour of a

cohesive sediment depends on the flow characteristics of the fluid causing scour as well as the resistance or cohesiveness of the material. Some of their resulting conclusions are:

- The depth of scour is proportional to the logarithm of time.
- Most natural sediments are inherently non-uniform and therefore do not scour in symmetrical patterns.
- The relatively large discontinuities in the uniform scour rate was a result of large pieces of sediment breaking off and being carried away.
- The mean depth of scour may be considered to be proportional to the cube root of the volume of scoured material.
- The depth of scour is seen to be a function of the fluid property, jet geometry, jet velocity, time of the test and sediment characteristics.

The Moore and Masch study is one of the first attempts relating the local scour of cohesive soils to both material and fluid characteristics.

Flaxman (26) studied a group of stable channels in the Western United States. He noted that the unconfined compressive strength of saturated cohesive materials was a good indicator of how fast a soil erodes. Contrary to Anderson's work, Flaxman observed fluvial sediments with small or negligible plastic indexes that were quite stable. Flaxman concluded that the plasticity index alone was not a decisive erosion indicator.

Grissinger, Asmussen and Espey (31) reviewed and discussed Flaxman's study extensively. Particular attention was given to the time period that cohesive materials were exposed to available free water. It was noted that during an erosive event, cohesive materials absorb water thereby decreasing interparticle forces and increasing the rate of erosion during material hydration. However, if the soil samples were exposed to free water and then allowed to age before erosion began, the average rate of erosion decreased due to the stabilizing effect of adsorbed layers of water molecules on the clay surfaces.

Partheniades (63) also conducted a series of tests in a flume with cohesive clay soils. Partheniades found that the minimum scouring shear stresses and rates of erosion are independent of the bed strength. Moreover, the scouring of clay particles was controlled by the hydraulic fluid forces and the material resistive forces (electro-chemical). Apparently, the shear strength is a function of the clay particle bonding strength and the degree of consolidation.

Extending the critical tractive force theory one step, Lyle and Smerdon (50) tested a group of sandy loams, silty clays and clay materials in a hydraulic flume. Lyle and Smerdon correlated the plasticity index, dispersion ratio, mean particle size and percentage of clay to the critical tractive force. However, they found that

additional soil characteristics such as percent organic matter, vane shear strength, cation exchange capacity (CEC) and calcium-sodium ratio might also be erosive indicators of cohesive materials. Their study culminated with the formulation of three equations for computing the critical tractive shear force as follows:

$$\cdot\ \tau_c = 0.00771 + 0.0233\ (1.2\text{-}e) + (0.00079 + 0.00035\ (e\text{-}1.2))\ I_p \tag{28}$$

$$\cdot\ \tau_c = (0.0141 + 0.00075\ (1.2\text{-}e))10^{0.0062(P_c)} \tag{29}$$

and

$$\cdot\ \tau_c = (0.0322 + 0.0086\ (1.2\text{-}e))10^{-nD_r} \tag{30}$$

where e is the void ratio, I_p is the plasticity index, P_c is the percentage of clay, D_r is the dispersion ratio and n is

$$n = 0.00452\ (10)^{0.32\ (e\text{-}1.2)} \tag{31}$$

These equations, indicating the relationships of τ_c and the soil properties, are to be applied according to the available data.

Grissinger (32) continued in his quest of relating basic soil characteristics to soil erosive resistance. A series of soil samples were molded and placed in a horizontal flume. Water flowed over the sample producing a shear stress (erosive force) on the soil. Grissinger found that for a given clay sample, as the bulk density and antecedent water content increased, the stability of the material increased. He reasoned that as the water content increases, the clay particles become oriented resulting in a more stable sample. However, as Grissinger tested a greater number of clays, it was noted that an increase in density and water content does not necessarily stabilize all clay indicators; the clay mineral orientation and the type of clay material.

In 1970, Paaswell (62) reviewed and summarized many of the significant findings concerning the erosion of cohesive materials for the Highway Research Board. He collected and classified the soil characteristics as previously cited into three categories; physical, physiochemical and mechanical. His primary conclusion was that as the plasticity index increased, the erodibility of the soil decreased.

Christensen and Das (18) studied the hydraulic erosion of cohesive soils by lining a sample tube with the cohesive material and allowing water to flow through the clay lined tube. They concluded:

- The erosion rate of material was a function of the shear stress, temperature, density, soil moisture content, clay type, percentage clay and cation concentration.
- Decreasing the surface roughness was as important as increasing the density for reducing erosion.

When the critical tractive shear stress was significantly exceeded, large clusters of soils were removed from the tube.

Liou (46,47) and Sargunam, Riley and Arulanandan and Krone (71) concentrated their efforts in studying the physio-chemical factors in the erosion of cohesive soils. Sargunam et al. introduced the sodium adsorption ratio (SAR) as an erosion indicator and found that as the SAR decreased, the cohesive properties of the material increased. Furthermore, it was noted that calcium ions cause soils to have a higher critical shear stress than do sodium ions.

Arulanandan, Loganathan and Krone (9) continued in the investigation of the physio-chemical influence in the erosion process of cohesive soils. It was found that clays with high concentrations of calcium or magnesium bond more firmly than clays with high concentrations of sodium. The concentration of salts in the eroding water can have a significant effect on the critical shear stress for surface erosion. Arulanandan reinforced the use of the sodium adsorption ratio as a critical shear stress indicator. The pH was tested as an erosive indicator but was not seen as a significant erosive parameter.

Sargent, Houskins and Beckwith (75) performed a series of pinhole tests on a cohesive embankment soil. The fluids used during testing had pH's of 7.0, 4.0, 2.0 and 1.0. The results revealed that the soil was nondispersive in all tests except for the liquid having a pH of 1.0. Therefore, the acidic nature of a fluid may accelerate erosion.

In 1976, Kuti and Yen (41) reported their findings after performing a series of scour tests at the toe of a spillway using cohesive soils comprised of from 20 to 80 percent clay. Kuti and Yen concentrated a significant portion of the study relating the time and scour parameters as a function of the percent of clay material in the soil. They noted that soils with a high percentage of clay take a longer time to reach a state of equilibrium than soils with a low percentage of clay at the same void ratio. Furthermore, the change in void ratio only affects the time at which scouring reaches an equilibrium state. Therefore, the scour parameters remain constant for a given flow condition and cohesive material. When the percent of clay by weight decreases in a soil while the void ratio remains constant, the volume of soil scoured decreases. A significant conclusion was that for any finite flow condition, the extent of scour is limited.

Jack (38) performed an analysis studying local scour at culvert outlets. Utilizing the work of Bohan, Jack developed a depth of scour estimation equation as a function of the depth of flow at the pipe outlet (d_o) and of the Froude number ($F_o = V_o/\sqrt{gd_o}$) when the tailwater exceeds one half of the culvert diameter. Jack's equation for estimating the depth of scour is:

$$D_s = 0.75\, d_o\, (\sqrt{40.51 - (F_o - 5.66^2)} - 2.93) \qquad (32)$$

Jack suggested that the equation was applicable to not only cohesionless sands, but to all the Soil Conservation Service Hydrologic Soil Groups as shown in Table 1. The estimated scour depth is determined by multiplying the adjustment factor corresponding to the appropriate soil group by the depth of scour. Jack's equation is based on tests of two hours in duration. Jack concluded that culvert outlet scour problems are mostly associated with structures operating under inlet control conditions with outlet velocities of approximately nine feet per second or greater.

Table 1. SCS Hydrologic Soil Groups

SCS Hydrologic Soil Group	Description	Adjustment Factor
A	Sand	1.00
B	Silty Loam	0.70
C	Firm Loam	0.60
D	Stiff Loam	0.50

The Louisiana Department of Highways (LDH) (49) published a scour prediction methodology based upon the Bohan and Jack studies. The LDH investigation indicated the following:

- Culverts without headwalls are more vulnerable to scour than culverts with headwalls.
- Scour at the outlet will be above 0.7 of the maximum depth of scour for tailwater elevations less than 0.5D.
- There exists a critical velocity at which scour commences and the cavity requires protection for all soils as shown in Table 2.

Table 2. Critical Scour Velocities

Soil Type	Critical Scour Velocity (fps)
A	1.5
B	3.0
C	3.5
D	4.5 - 5.0

Murray (59) studied the erodibility of a coarse sand-clayey silt in a small hydraulic flume. Murray identified two regimes of sediment transport, low and high, and expressed both regimes as a function of the bed shear stress. The values of parameters were empirically derived from the experimental tests. The following equation was determined:

$$\tau_o = \frac{\rho \bar{V}^2}{190} \tag{33}$$

where ρ is the fluid density and $\bar{V}$ is the average fluid velocity. The low regime transport rate was determined to be proportional to the 16 power of the bed shear stress while the high regime transport rate was proportional to the 2.5 power of the bed shear stress. The transport rate was also directly proportional to the percentage fines in the soil mixture.

Ariathurai and Arulanandan (8) continued in the identification of the principal physical and chemical factors relating to the rate of erosion of saturated cohesive soils. They concentrated their efforts on the factors affecting critical shear stress to include type and percentage clay, chemical composition of pore and eroding fluids, temperature presence of organic matter and soil stress history. Ariathuria and Arulanandan performed tests on over 200 natural and made-up soil samples. Their conclusions can be summarized as follows:

- Low SAR increases interparticle attraction and subsequent flocculation whereas high SAR causes particles to repel and remain dispersed.

- The types and concentrations of ions in pore and eroding fluids have a pronounced effect on the erodibility of cohesive soils.

- Increasing fluid temperature reduces interparticle attraction and enhances erosion rates.

The prediction of localized scour at culvert outlets requires a thorough understanding of hydraulic and soil characteristics in conjunction with the erosive properties. As can be seen from the literature review, the literature abounds with studies that deal with erosive properties of soils but few studies attempted to formulate design criteria for expected scour at culvert outlets. Those studies that did formulate design criteria were made for non-cohesive material and designers, like Jack (38), were confronted with the need to extend the criteria to all materials. Additional studies are needed, therefore, to systematically extend design criteria to a full range of soil conditions encountered by designers.

Chapter III

EXPERIMENTAL FACILITIES AND PROCEDURES

Introduction

The investigation of scour at culvert outlets in mixed-bed materials was conducted using six materials under a variety of conditions. Materials were tested in two facilities with culverts ranging from 4 inches (10.2 cm) to 18 inches (45.7 cm) in diameter. Test periods ranged from 316 minutes to 1000 minutes in duration with discharges of .11 cfs (.003 cms) to 29.3 cfs (0.83 cms). A summary of the experimental materials, models, discharges and test durations is presented in Table 3 and the remainder of this chapter.

Experimental Facilities

Two hydraulic flumes were utilized for conducting the scour investigation. The initial testing program was conducted in an outdoor, concrete flume. The scope of the study was expanded to incorporate a smaller, indoor flume. The indoor facility was a 1:5 Froude scale model of the outdoor flume. Characteristics of each facility are as follows.

Description of the 4 Foot (1.2 Meter) Indoor Facility

The indoor, recirculating flume was constructed of steel and plywood with dimensions, 4 ft. (1.2 m) in width, 2 ft. (0.6 m) in depth, and 15 ft. (4.5 m)in length. The flume was divided into upper and lower reaches. The upper reach was 12 ft. (3.6 m)long and 4 ft. (1.2 m)width, with bed material placed throughout at a depth of 1.5 ft. (0.45 m). The lower reach was used as a sediment trap 2.5 ft. (0.75 m) in length placed immediately downstream of the upper reach. An adjustable tailgate weir was at the downstream end of the trap to control the water surface elevation.

A 4 inch (10.2 cm) steel pipe used to model the culvert was anchored at the upstream wall of the upper reach. The axis of the culvert coincided with the centerline of the flume and its invert was placed adjacent to the initial bed level. Water was recirculated by pumping from a sump at the downstream end of the flume after having flowed through the model. The water discharge was measured by inserting an orifice plate in the circulation system and determining the differential head across an orifice with a vertical manometer. The manometer resolution was 0.01 ft. (0.305 cm). The discharge was controlled with a butterfly valve.

The headwall was constructed of plywood and was placed perpendicular to the flume walls at the end of the cantilevered culvert as shown in Figure 2. The headwall formed the upstream boundary of the flume.

To fill the tailwater basin and establish tailwater conditions, a 3/4 inch (1.91 cm) flexible pipe was installed into the pipe network. The flexible pipe extended from the pump discharge to the tailwater basin outside of the flume bypassing the material basin.

Table 3. Summary of Test Program Parameters

Material	d_{50} (mm)	Model	Pipe Diameter (ft)	Discharge Range (cfs)	Times of Data Collection (minutes)	TW* x D
Uniform Sand	1.86	20'	0.333	0.11-1.14	31,100,316	0.45
Uniform Sand	1.86	20'	0.85	1.15-7.65	31,100,316	0.00
Uniform Sand	1.86	20'	0.85	1.15-7.65	31,100,316	0.25
Uniform Sand	1.86	20'	0.85	1.89-9.45	31,100,316,1000	0.45
Uniform Sand	1.86	20'	1.13	3.85-19.26	31,100,316,1000	0.45
Uniform Sand	1.86	20'	1.46	7.31-29.23	31,100,316,1000	0.45
Uniform Sand	1.86	4'-w/o headwall	0.333	0.16-0.91	31,100,316,1000	0.45
Uniform Sand	1.86	4'-w headwall	0.333	0.16-0.91	31,100,316,1000	0.45
Uniform Sand	1.86	4'	4"x4" square	0.25-1.16	31,100,316	0.45
Bohan	0.22	4'	0.333	0.11-0.18	14,20	0.45
Graded Sand	2.0	4'	0.333	0.18-0.73	31,100,316	0.45
Uniform Gravel	7.62	20'	0.35	1.91-7.65	31,100,316	0.0
Uniform Gravel	7.62	20'	0.35	1.91-7.65	31,100,316	0.25
Uniform Gravel	7.62	20'	0.35	1.91-7.65	31,100,316	0.45
Graded Gravel	7.34	20'	0.85	1.91-7.65	31,100,316	0.45
Cohesive	0.15	20'	0.85	1.91-7.65	31,100,316,1000	0.45
Cohesive	0.15	20'	1.13	3.81-15.23	31,100,316,1000	0.45
Cohesive	0.15	20'	1.33	7.28-29.13	31,100,316,1000	0.45

*TW is tailwater elevation; numbers given are the water depth as a portion of the culvert diameter.

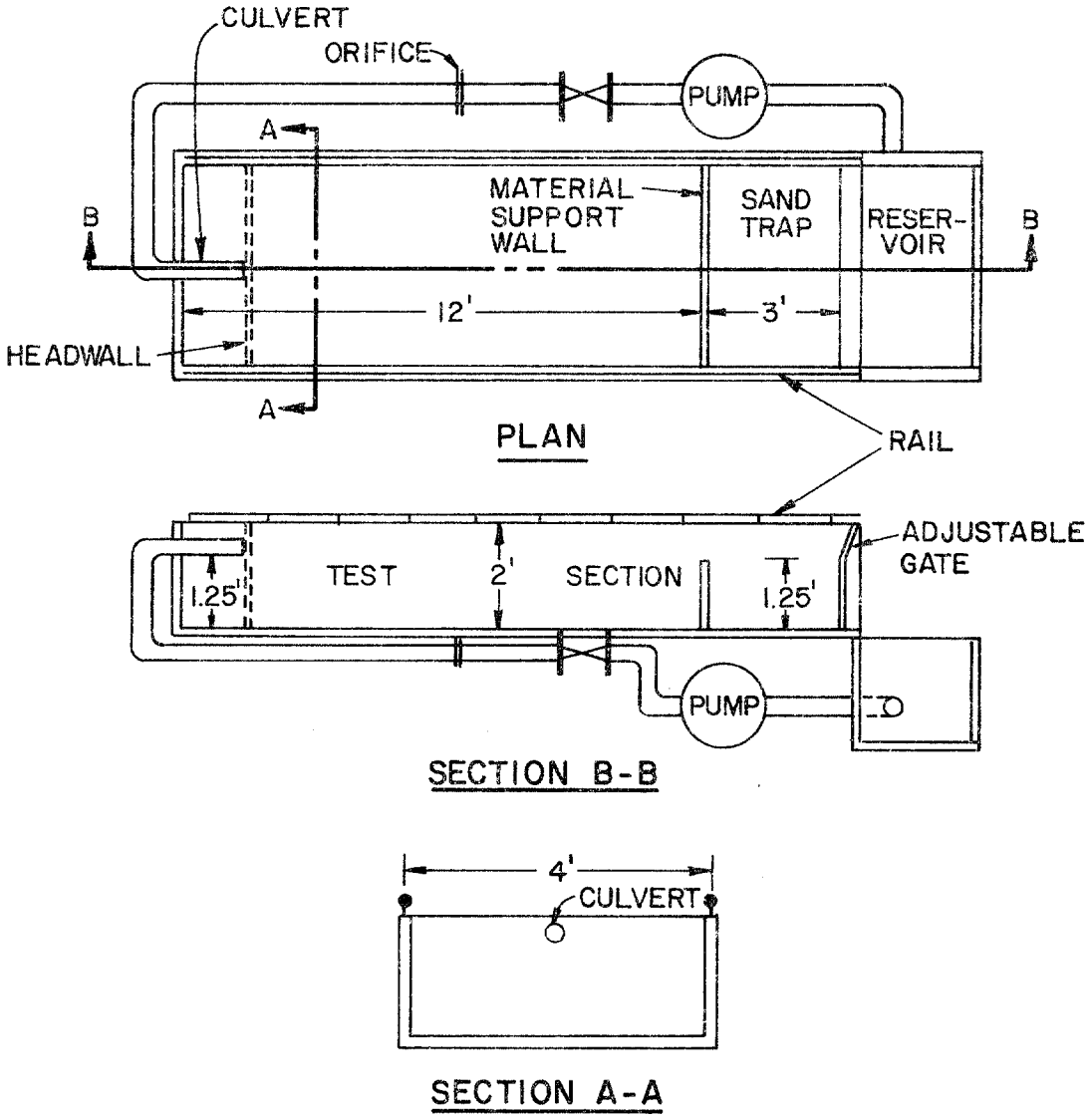

Figure 2. Schematic drawing of 4-foot indoor flume.

A point gage was installed onto a cart which was mounted on rails on top of the flume walls. The gage resolution was .001 ft (0.03 cm) A grid system was establised to accurately locate the point gage within the flume. The grid system was comprised of markings .1 ft (3.05 cm) on center starting at the headwall in the longitudinal direction and markings .1 ft (3.05 cm) on center originating at the flume centerline in the traverse directions.

Description of the 20 Foot (6.1 Meter) Outdoor Facility

As outdoor, concrete flume was utilized with dimensions of 100 ft (3.05) in length, 20 ft (6.1 m) in width and 8 ft (2.4 m) in depth as shown in Figure 3. The flume was divided into two reaches, an upper reach and a lower reach, spanning 63 ft (19.2 m) and 37 ft (11.3 m) respectively. The upper reach of the flume was used as the bed material basin in which all scour tests were conducted. The lower reach was used as a tailwater control and material recovery basin.

Smooth, circular steel pipes (culverts) were each cantilevered horizontally through the flume inlet headboards and extended 6 ft (1.83 m)to 9 ft (2.74 m) downstream of the headwall. The culverts were 4 inches (10.2 cm), 10 inches (25.4 cm) , 14 inches (35.6 cm) , and 18 inches (45.7 cm) in diameter. Each culvert was centered between the flume sidewalls and was placed to maintain a minimum bed material thickness of 6 ft (1.83 m) measured from the pipe invert to the bottom of the flume.

All tests were conducted with water pumped from a nearby water reservoir on the Colorado State University Research Campus. Water was pumped through a 24-inch (61 cm) pipeline using a 300 horsepower motor and pump to the outdoor facility. Discharges into the flume were controlled through a pipe network with a 12-inch (30.5 cm) butterfly valve and a 24-inch (61 cm) butterfly valve located approximately 30 ft (9.1 m) upstream of the flume headwall. Flow rates were established and monitored with orifices mounted in the 12-inch and 24-inch pipelines. Tailwater depths were controlled with stop logs at the flume outlet.

To expedite the filling of the tailwater basin and to establish the required tailwater conditions, a 4-inch (10.2 cm) bypass pipeline and gate valve were installed into the 24-inch pipe between the 24-inch butterfly valve and the 16 7/8 inch (42.9 cm) orifice. A 4 inch (10.2 cm), flexible pipe was then attached to the valve. The flexible pipe extended from the valve house to the tailwater basin along the outside of the flume bypassing the material basin.

To facilitate data collection, a motorized carriage traversed the longitudinal axis of the flume on rails mounted on the top of the flume walls. The carriage was equipped with a small motorized cart which traversed the transverse axis of the flume. The carriage and cart enabled the collection of data at nearly any position in the upper reach of the flume.

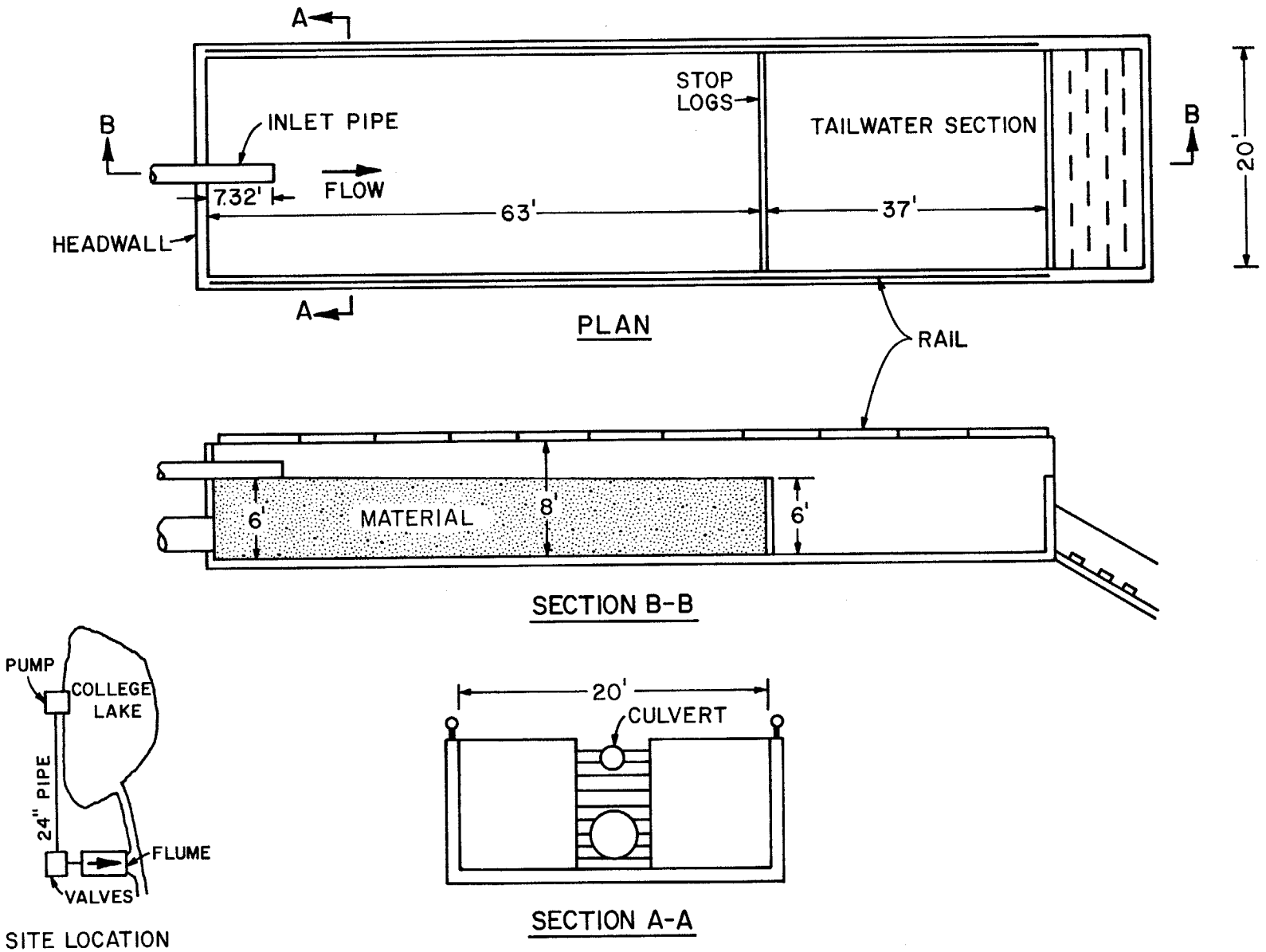

Figure 3. Schematic drawing of 20-foot outdoor flume.

A point gage was mounted to the motorized cart. The gage resolution was 0.01 ft (0.3 cm) A grid system was established to accurately locate the point gage within the flume. The grid system was comprised of markings 1.0 ft (30.5 cm) on center starting at the headwall in the longitudinal direction and markings of 0.5 feet (15.2 cm) on center originating at the flume centerline in the transverse directions.

Description of Bed Materials

Five noncohesive materials and one cohesive soil were used as bed materials for this scour investigation. Soil properties of each bed material were obtained and recorded in accordance with procedures outlined in the American Society for Testing and Materials (ASTM) specifications.

Noncohesive Materials. The five noncohesive materials tested included uniform sand, uniform gravel, graded sand, graded gravel and a fine sand similar to that used in the Bohan study. The non-cohesive material soil properties are summarized in Table 4. The specific gravity (S.G.) of the non-cohesive material source was tested to be 2.65.

Table 4. Summary of Noncohesive Material Properties

Soil Type	d_{50} (mm)	*σ	Unit Weight, γ_{soil} (psf)	Angle of Repose (degrees)	Fall Velocity (cm/s)	**Critical Shear Stress, τ_c (psf)	**Critical Shear Velocity, u_{*c} (ft/s)
Uniform Sand (fine)	0.22	1.26	79.9	34.8	2.7	.006	.056
Uniform Sand (medium)	1.86	1.33	93.8	34.8	27.1	.089	.214
Graded Sand	2.00	4.38	105.9	31.8	27.3	.119	.248
Uniform Gravel	7.62	1.32	94.4	37.3	63.0	.408	.459
Graded Gravel	7.34	4.78	117.9	37.3	64.0	.682	.594

*Standard deviation (σ) is $(d_{84}/d_{16})^{\frac{1}{2}}$

**$\tau_c = 0.67\ (\gamma_{soil}-\gamma)d_{50}\tan\theta$; $u_{*c} = (\tau_c/\rho)^{\frac{1}{2}}$; Sediment Transport Technology, Simons and Senturk (80).

In these relationships τ_c, γ_{soil}, γ & d_{50} must have consistent units. The mass density of water, ρ, is 1.935 slugs/ft^3 (English system) or 1 gm/cm^3 (metric system) at 20°C. If τ_c is in gmf/cm^2, one should beware that the unit gmf (grams of force) is no longer recommended and that the "f" is often omitted. 1 gmf = 980.6 gm cm/s^2

Cohesive Bed Material The cohesive material was derived from a residual, Colorado expansive clay mixed with a graded sand. The

tan-green sandy clay mixture is classified as an SC soil type in accordance with the Unified Soil Classification System. An agricultural analysis further catagorized the material as a sandy loam comprised of 58% sand, 27% clay and 15% silts and organic matter. The cohesive material properties are summarized in Table 5.

Table 5. Summary of Cohesive Material Properties

Characteristic	Characteristic Value
Soil Type	SC
Texture	Sandy loam
Atterberg Limits	
liquid limit	34
plastic limit	19
plastic index	15
Soil Composition	
organic matter	1%
sand	58%
silt	14%
clay	27%
pH	7.8
Mean grain size	0.15 mm
Uniformity coefficient	300
Fall velocity (d_{50})	0.08 fps (2.4 cm/sec)
Cation exchange capacity	9.0 meg/100 g
Soil fabric	Dispersed
Dispersivity of the colloid fraction	Non-dispersive
Permeability	6.4×10^{-6} cm/sec

Placement of Bed Materials

Noncohesive Bed Materials. Each non-cohesive bed material was placed in the upper reach (material basin) of the flume in which each test was conducted. The material was roughly leveled to coincide with the culvert invert. The bed material was inundated and drained to induce settlement of the bed prior to the initial experiment. Additional material was then placed and leveled until the bed surface was horizontal to within $\pm$ 0.10 ft (3 cm)of the culvert invert.

Cohesive Bed Material. The placement of the cohesive material into the outdoor testing facility required a multi-step process to insure

material uniformity throughout the scour bed. The material was placed at a density of 90% ± 2% of the maximum dry unit density. To meet this requirement, the following procedure was established:

1) A 4-inch (10.2 cm) gravel bed was placed and leveled in the bottom of the material basin to facilitate drainage.

2) A portion of the cohesive material was placed into the upper basin so that when distributed, a 5-inch (12.7 cm) to 6-inch (15.2 cm) layer of material covered the previous material layer.

3) A six hundred pound, motor driven sheep's foot roller then rolled the bed from 4 to 6 times depending upon the antecedent soil moisture conditions. The vibratory and compactive action of the roller provided a means for densifying the material. The roller spikes were 6 inch (15.2 cm) long to allow penetration between adjacent material layers. The repetitive rolling action minimized the layering effect during testing due to the material placement procedure.

4) After a material layer had been placed and rolled, a sand cone density test was performed. If density requirements were not met, the layer was again rolled and tested.

5) A moisture content determination of the material was made. If the moisture content of the material was less than approximately 11 percent, water was uniformly applied with a sprinkler until the soil water content reached approximately 11 percent.

6) Steps 2-5 were repeated until the bed grade reached the culvert invert elevation. The bed surface was then rolled with a 150 pound, smooth drum roller to compact, shape and level the bed surface to within ± 0.10 ft (3 cm)of the culvert invert.

Test Procedure

Once preparations were completed, the scour test was initiated by starting the pump, opening the bypass line and adjusting the tailwater control thereby allowing the tailwater basin to fill with water. When the tailwater basin filled to the level of the channel bed, water spilled onto the channel bed inundating the bed material. Water temperatures ranged from approximately 64 degrees to 85 degrees Fahrenheit depending upon the facility and source of water. The flume filled until the desired tailwater surface elevation was attained. Tailwater elevations ranged from the pipe invert to approximately 0.45 times the culvert diameter.

Upon establishment of the proper tailwater level, the bypass line was closed. Then, the valve controlling the flow to the culvert was opened and adjusted to provide the pre-determined discharge. Simultaneously, the tailwater control was adjusted to maintain the desired tailwater elevation.

Data Collection

During each test, culvert flows were stopped at times summarized in Table 3 to facilitate intermediate data collection. The data collection procedure was as follows:

1) The valve controlling the culvert was closed while the bypass line was opened in order to maintain the desired tailwater surface elevation.

2) The carriage and cart were positioned at the culvert outlet and the pipe invert reading was taken to calibrate the point gage.

3) The carriage was moved to the nearest grid mark downstream of the culvert outlet. The cart was traversed across the flume obtaining and recording data at desired intervals. The carriage was then advanced downstream and the procedure repeated.

4) When the data collection was completed, the bypass line was closed and the culvert flow was resumed.

At the conclusion of the test run, the scour cavity was dewatered. A series of photographs and written comments were recorded to document the scour hole and the surrounding bed.

Chapter IV

ANALYSIS OF SCOUR

Scour at the outlet of a culvert is a complex process which encompasses the variable flow patterns of a discharging jet that impinges upon a horizontal bed as well as the entrainment and transport of erodible bed materials. Thus far, there has not been an analytical solution development which describes this scour mechanism. However, on the basis of the experimental investigation presented herein, a series of empirical relationships can be formulated to depict scour cavity characteristics. The development of these relationships will be portrayed using a series of dimensionless parameters.

Dimensional Analysis

A fundamental dimensional analysis was performed using the π-Theorem. The variables used in the analysis are elements of the soils, fluid and models. The variables included in the analysis are given below and are described in the List of Symbols in the Preface. For noncohesive soils

$$f\,[d_s,\ D,\ L_s,\ W_s,\ V_s,\ \mu,\ \gamma,\ d_{50},\ \sigma,\ \lambda,\ \omega,\ \sigma_\omega,\ \tau_c,\ U_{*c},\ Q,\ \bar{V},\ \gamma_s,\ \rho,$$
$$\rho_s,\ \bar{V}_b,\ P,\ t,\ \theta,\ n,\ g,\ t_o,\ TW,\ R_H] = 0 \qquad (34)$$

and for cohesive soils

$$f\,[d_s,\ D,\ L_s,\ W_s,\ V_s,\ \mu,\ \gamma,\ \bar{V},\ g,\ \rho,\ Q,\ \ ,\ R_H,\ TW,\ \tau_c,$$
$$t_o,\ t,\ U_{*c},\ \gamma_s,\ n,\ \rho_s] = 0 \qquad (35)$$

A schematic diagram of the culvert outlet and scour cavity variables are shown in Figure 4. By systematically combining these variables a series of expressions containing force, length and time terms can be evaluated. The results of these variable manipulations is the generation of a comprehensive set of dimensionless parameters. The parameters significant in the analysis of scour cavity development are for the cohesionless soils

$$F\,[\frac{d_s}{D},\ \frac{W_s}{D},\ \frac{L_s}{D},\ \frac{V_s}{D^3},\ \frac{Tw}{D},\ \frac{d_{50}}{D},\ \sigma,\ \frac{\Delta\gamma D}{\rho V^2},\ \frac{\bar{V}}{\sqrt{gD}},\ \frac{Q}{g^{1/2}D^{5/2}},\ \frac{t}{t_o}] = 0 \qquad (36)$$

and for cohesive soil

$$F\,[\frac{d_s}{D},\ \frac{R_H}{D},\ \frac{W}{D},\ \frac{L}{D},\ \frac{V_s}{D^3},\ \frac{T_w}{D},\ \frac{Q}{g^{1/2}\ D^{5/2}},\ \frac{\tau_c}{\rho V^2},\ \frac{t}{t_o}] = 0 \qquad (37)$$

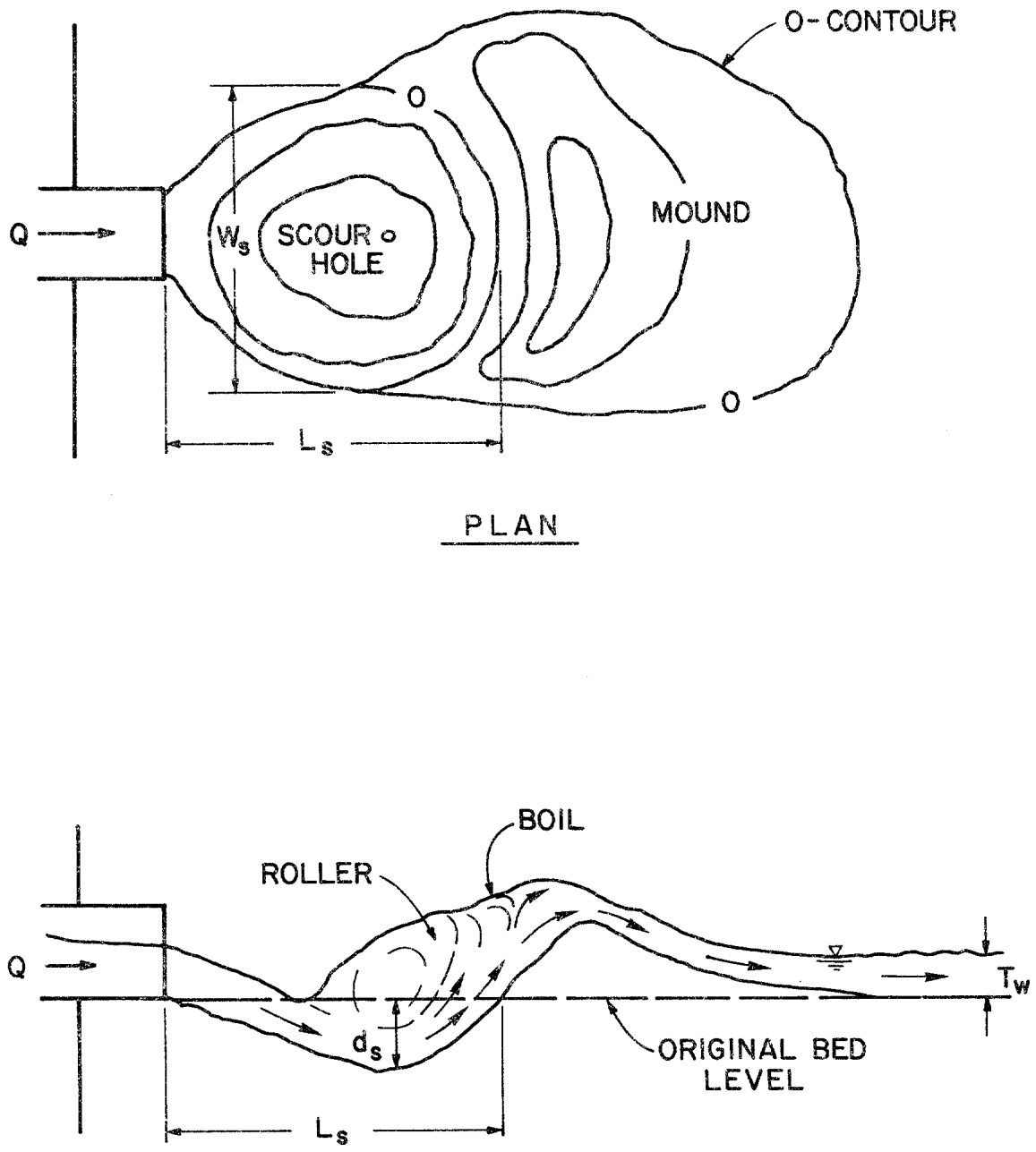

Figure 4. Definition sketch.

The experimental program was designed to formulate a series of functional relationships between these parameters applicable to local scour in noncohesive and cohesive soils at culvert outlets.

The investigations of Bohan (13), Fletcher and Grace (27), and Robinson (67) identified the variable $QD^{-5/2}$ as a significant parameters in the prediction of various scour hole characteristics. However, the parameters $QD^{-5/2}$ is not a dimensionless expression. A similar parameter which is dimensionless was derived by the π-Theorem and is the discharge intensity:

$$D.I. = \frac{Q}{g^{1/2} D^{5/2}} \tag{38}$$

The discharge intensity as utilized throughout this study is applicable to circular culverts.

Tractive Force Theory

One investigation that relates the cohesive soil characteristics with the shear stresses exerted by a moving fluid impacting upon a cohesive bed was developed in Dunn's Tractive Force Theory (23). Dunn experimented with a submerged jet impinging upon a cohesive soil sample and reasoned that a soil grain would scour when the force of the moving fluid (F_d) equaled or exceeded the soil resistive forces (F_r). Dunn's analysis of an erodible cohesive soil defined the shear force of the fluid to be

$$F_d = \tau A \tag{39}$$

where F_d is the force tending to cause erosion, τ is the stress due to the viscous drag and turbulent form drag of a moving fluid and A is the projected surface area of the soil grain.

The resisting force holding the soil grain in place is

$$F_r = (\sigma \tan \phi_h + c_h) A = S_h A \tag{40}$$

where S_h is the unit strength resisting the hydraulic shear stresses, σ is the intergranular surface stress, ϕ_h is the hydraulic stress resisting friction angle and c_h is the cohesive stress resistance. The cohesive stress resistance is defined as

$$c_h = S_v f(P) + f_1 (P) \tag{41}$$

where S_v is the vane shear strength and f(P) and f_1 (P) are functions of the plastic properties. Consolidating Eqs. (41) and (42) yields the expression

$$F_r = \tau_c = \sigma_c \tan \phi_h + S_v f(P) + f_1 (P) \quad (42)$$

When the stress exerted by the moving fluid on the bed is equal to the soil resistive force, the critical tractive shear stress is attained and the soil particles become susceptible to suspension and transport.

Dunn performed the testing phase of his experiment using a variety of cohesive soils with plasticity indexes (I_p) ranging from 2.5 to 15.6. A series of relationships were found correlating the critical tractive shear to the vane shear strength and to the plasticity index. Dunn's expression for estimating the critical tractive shear stress for a cohesive soil is given by Eq. (24) which was later modified to

$$\tau_c = 0.001 (S_v + 180) \tan (30 + 1.73 I_p) \quad (43)$$

Dunn's equation is limited in its application to cohesive soils with sand content and plastic index of 5 to 16.

Tailwater Conditions

Investigations by Smith (81,82), Doddiah (22), Laushey (44), Opie (61), Bohan (13) and Fletcher and Grace (27) identified the tailwater elevations (TW) and subsequent tailwater conditions as an important parameter in the determination of the final scour cavity geometry. Based upon preliminary tests and the Bohan (13) tailwater categorization, the condition where the tailwater elevation was less than 0.5 D but above the culvert invert produced maximum scour hole dimensions. To facilitate experimental control, a target tailwater elevation of

$$TW = 0.45 D \pm 0.05 D \quad (44)$$

above the invert was established. Tailwater elevations of zero D, 0.25 D and 0.45 D were tested in the experimental program.

Chapter V

RESULTS AND DISCUSSION

General Observations

Noncohesive Materials

A series of seventy-five scour tests were conducted, observed and documented as water discharged from a culvert outlet onto a bed of noncohesive materials. Scour holes were generally similar in geometric configuration and appearance. Scour holes were circular in shape at low discharges (D.I. $\leq$ 1.0) and elongated to an oval shape as the discharge intensities exceeded one (D.I. > 1.0).

Scour holes were created by a water jet impinging upon a horizontal bed of noncohesive material. The force of the impacting jet and subsequent turbulence lifted and entrained the material particles. Large diameter materials were transported as bed load along the bottom of the scour hole and bed downstream of the hole. Smaller materials were entrained by the flow and deposited around the rim of the hole, in the subsequent dune or mound downstream of the hole, or in the material settling basin. The mounds which formed were fan shaped for discharge intensities less than one (D.I. < 1.0) and became rectangular as the discharge intensity reached one (D.I. $\geq$ 1.0). The surface of the mounds were flat paralleling the water surface. The mound height was generally observed to be approximately 0.6-0.8 of the tailwater depth.

Cohesive Material

A series of twelve scour holes were observed and documented for the cohesive bed material. The scour holes were generally similar in geometric configuration and appearance to the holes illustrated in Figures 5 and 6. Scour holes were circular in shape at low discharges (D.I. $\leq$ 1.0). As the discharge increased (D.I. > 1.0), the holes elongated to an oval shape as displayed in Figure 5.

The force of the water jet impacting upon the bed weakened the cohesive bonds of the material and dislodged particles from the bed. The material was then lifted and entrained into the turbulent flow. Large diameter materials (sands and clods) were transported as bed load along the bottom of the scour cavity and deposited immediately downstream of the jet impact area. A mound subsequently formed downstream of the cavity. The smaller material (clay and silt particles) was entrained by the flow and trapped in void spaces along the mound or transported to the facility settling basin. Each mound was generally flat, less than 0.25 D in height and fan shaped downstream of the cavity. The mound was comprised of primarily large diameter sands and clods with fine material filling the void spaces.

Considerable deposition of sands and clods was observed around the hole rim at the conclusion of each experiment. This armouring effect consistently occurred at the downstream face and along the rim of all the scour holes. It was observed that limited armouring occurred within

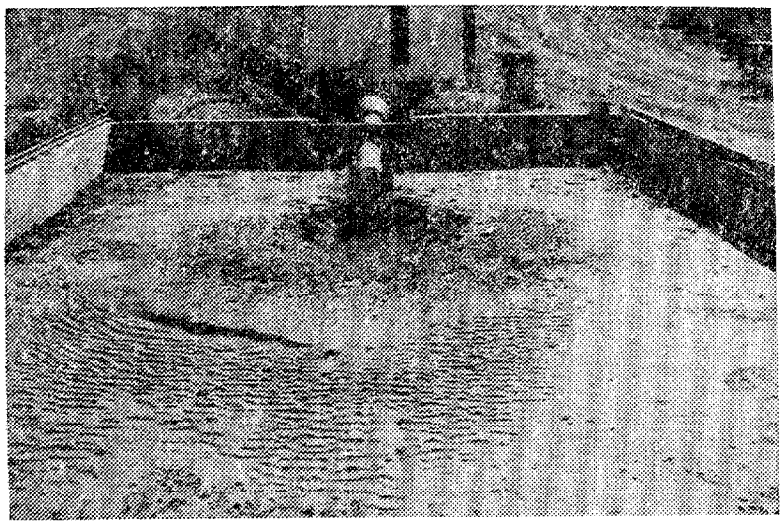

Figure 5. Scour cavity, 10-3/4 inch culvert.

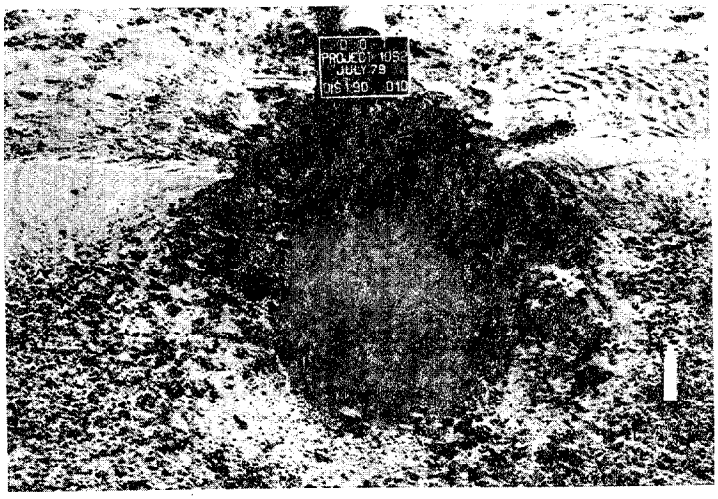

Figure 6. Scour cavity, 10-3/4 inch culvert.

the scour hole. Armouring materials could not be supported along the cavity walls due to steep side slopes and vertical sidewalls. In some cases, cantilevering occurred.

Quantitative Results

Upon completion of the scour tests, an analysis was conducted to correlate the depth, width, length and volume of scour to materials, culvert and discharge. The scour hole characteristics of depth, width, length and volume are expressed by the dimensionless parameter of d_{sm}/D, W_{sm}/D, L_{sm}/D and V_{sm}/D^3 respectively. Also, the relationships presented herein are based upon the maximum scour hole characteristic dimensions. Test durations were in accordance with times presented in Table 3-1.

Graphical representations were compiled correlating the depth, width, length and volume dimensionless parameters to the Discharge Intensity as presented in Figure 7 through Figure 11 for uniform sand (d_{50} = 1.86, σ = 1.33), graded sand (d_{50} = 2.0, σ = 4.38), uniform gravel (d_{50} = 7.62, σ = 1.32) graded gravel (d_{50} = 7.34, σ = 4.78), and the cohesive sandy clay respectively. A power regression line was fit through each logarithmic plot yielding a series of expressions of the general form

$$y = a\ x^b \tag{44}$$

where y is the dependent variable of d_{sm}/D, W_{sm}/D, L_{sm}/D or V_{sm}/D^3; a is a constant; and b is the slope of the linearized plot. A summary of equation coefficients is expressed in Table 6. From these expressions, it was evident that the maximum scour hole characteristics of depth, width, length and volume can be correlated to the culvert diameter (D) and culvert discharge (Q). Replacing the independent variable of Equation 44 with the Discharge Intensity yield the expressions:

$$\frac{d_{sm}}{D},\ \frac{W_{sm}}{D},\ \frac{L_{sm}}{D} \quad \text{or} \quad \frac{V_{sm}}{V^3} = a\ \left[\frac{Q}{g^{1/2}\ D^{5/2}}\right]^b \tag{45}$$

The Discharge Intensity relationships yield a conservative estimate of scour hole dimensions for partially filled culverts (D.I. < 1.0).

Three verification tests were conducted using a fine grained, uniform sand (d_{50} = 0.22 mm, σ = 1.27) which was similar to the material Bohan (13) tested at the Corps of Engineers Waterways Experiment Station. These tests were conducted to verify Bohan's results and were performed with Discharge Intensities of 0.3, 0.4 and 0.5 for a duration of 20 minutes.

The Bohan relationships depicting the hole dimensionless parameters versus the Froude Number is presented in Figure 12 and Figure 13. The

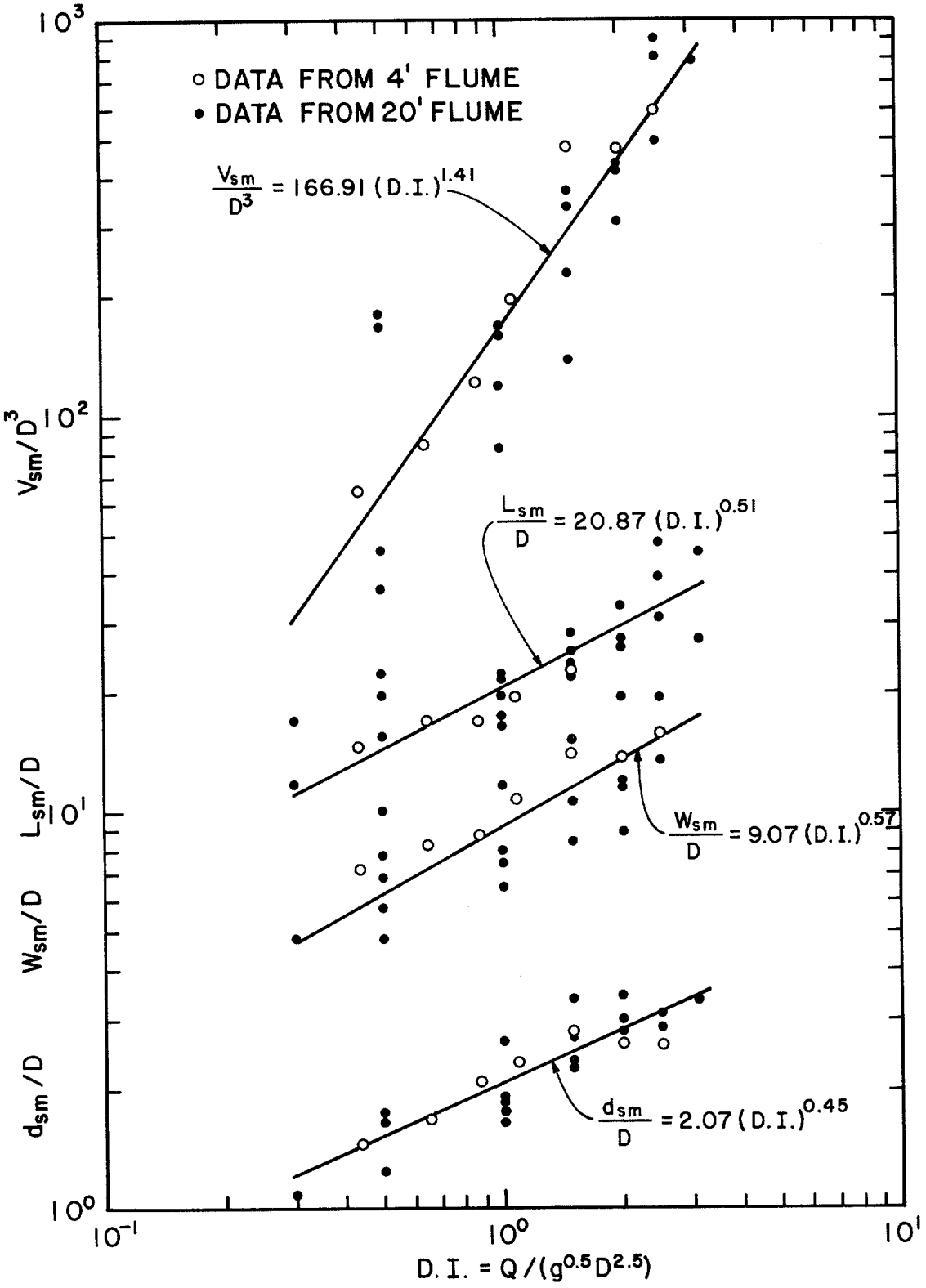

Figure 7. Scour vs. Discharge Intensity, Uniform Sand, d_{50} = 1.86 mm, σ = 1.33 t_o=1000 min.

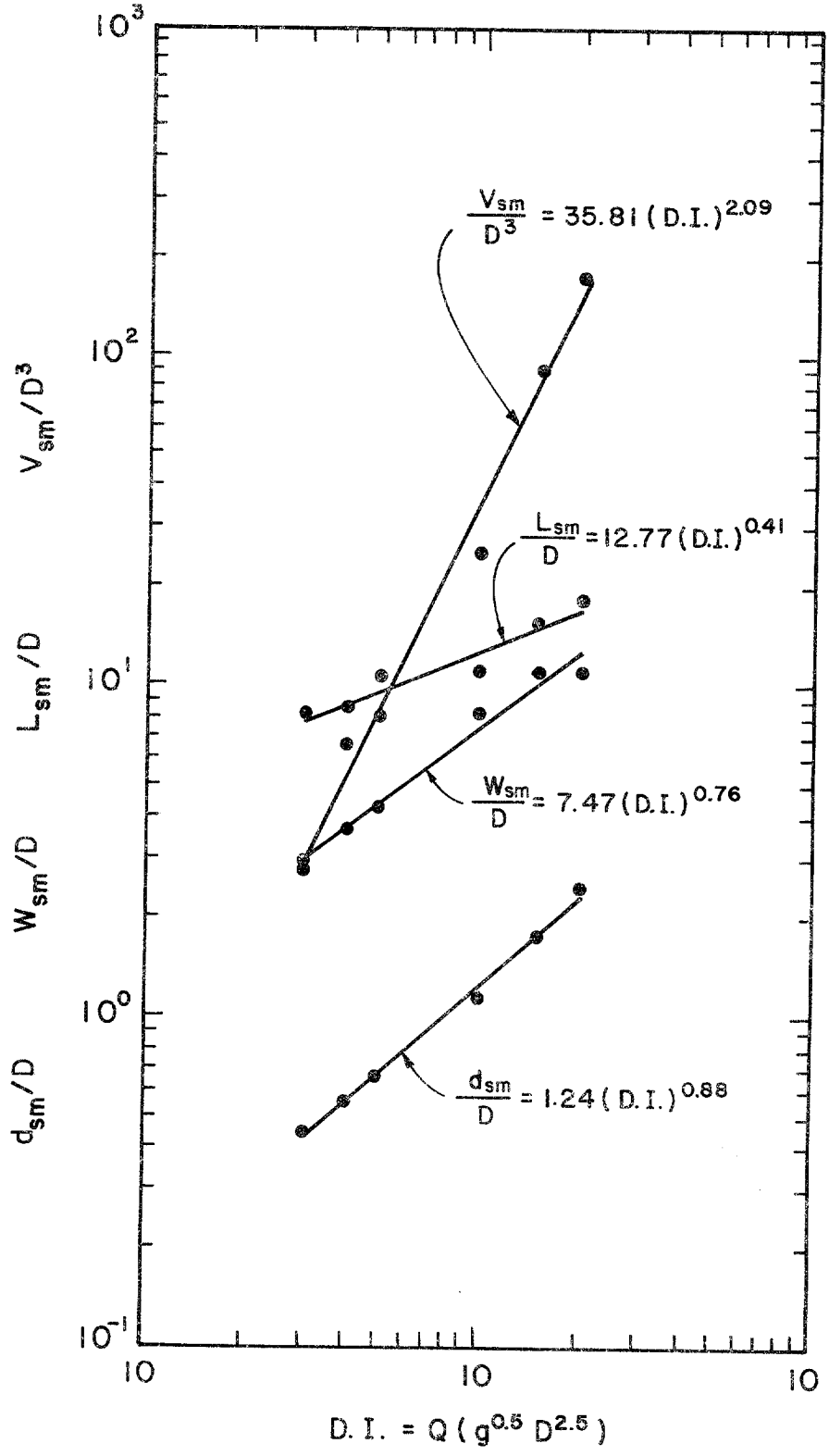

Figure 8. Scour vs. Discharge Intensity Graded sand, d_{50} = 2.00 mm, σ = t_o = 31.6 min.

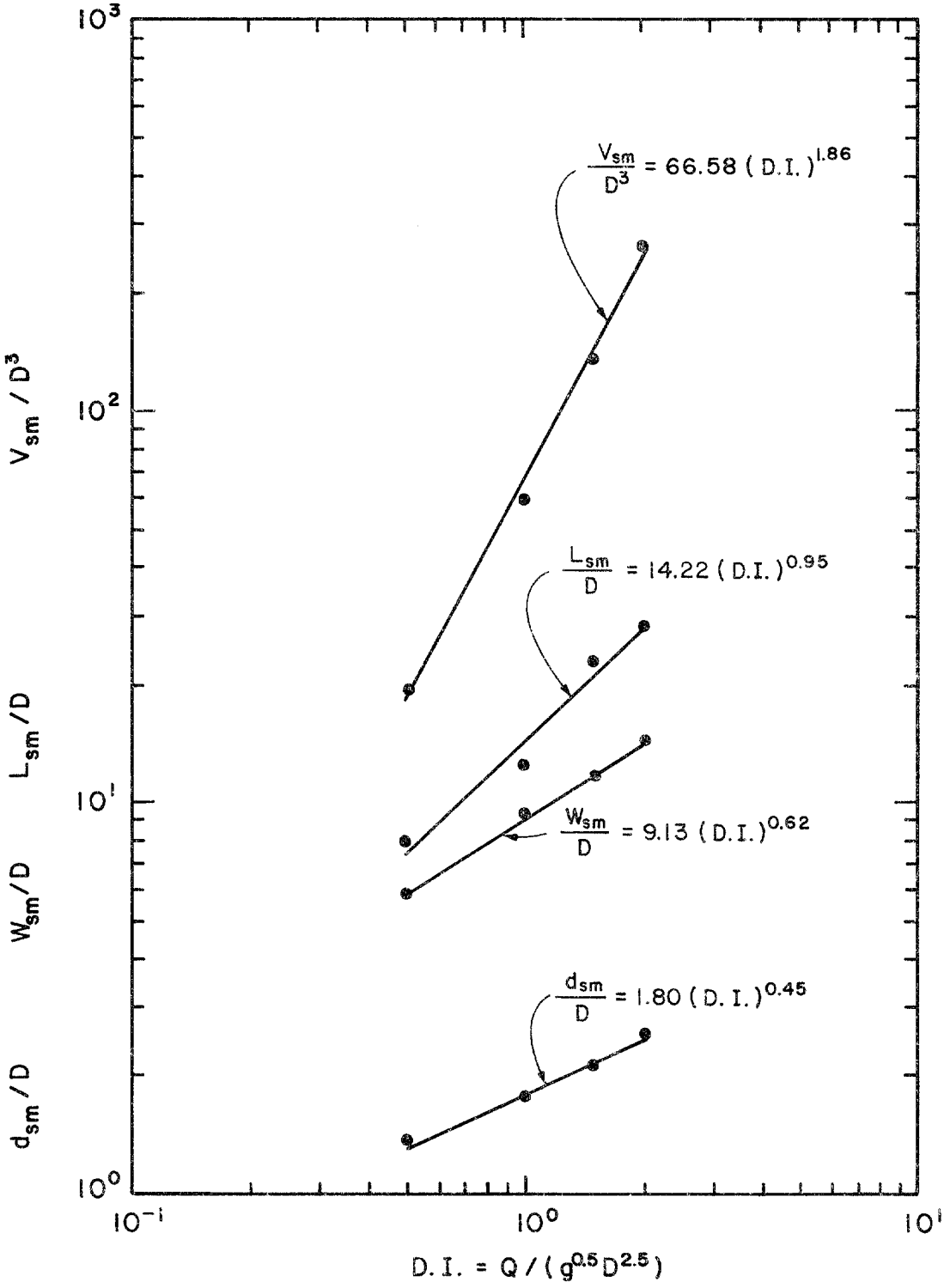

Figure 9. Scour vs. Discharge Intensity Uniform gravel, d_{50} = 7.62 mm, σ = 1.32, t_o = 316 min.

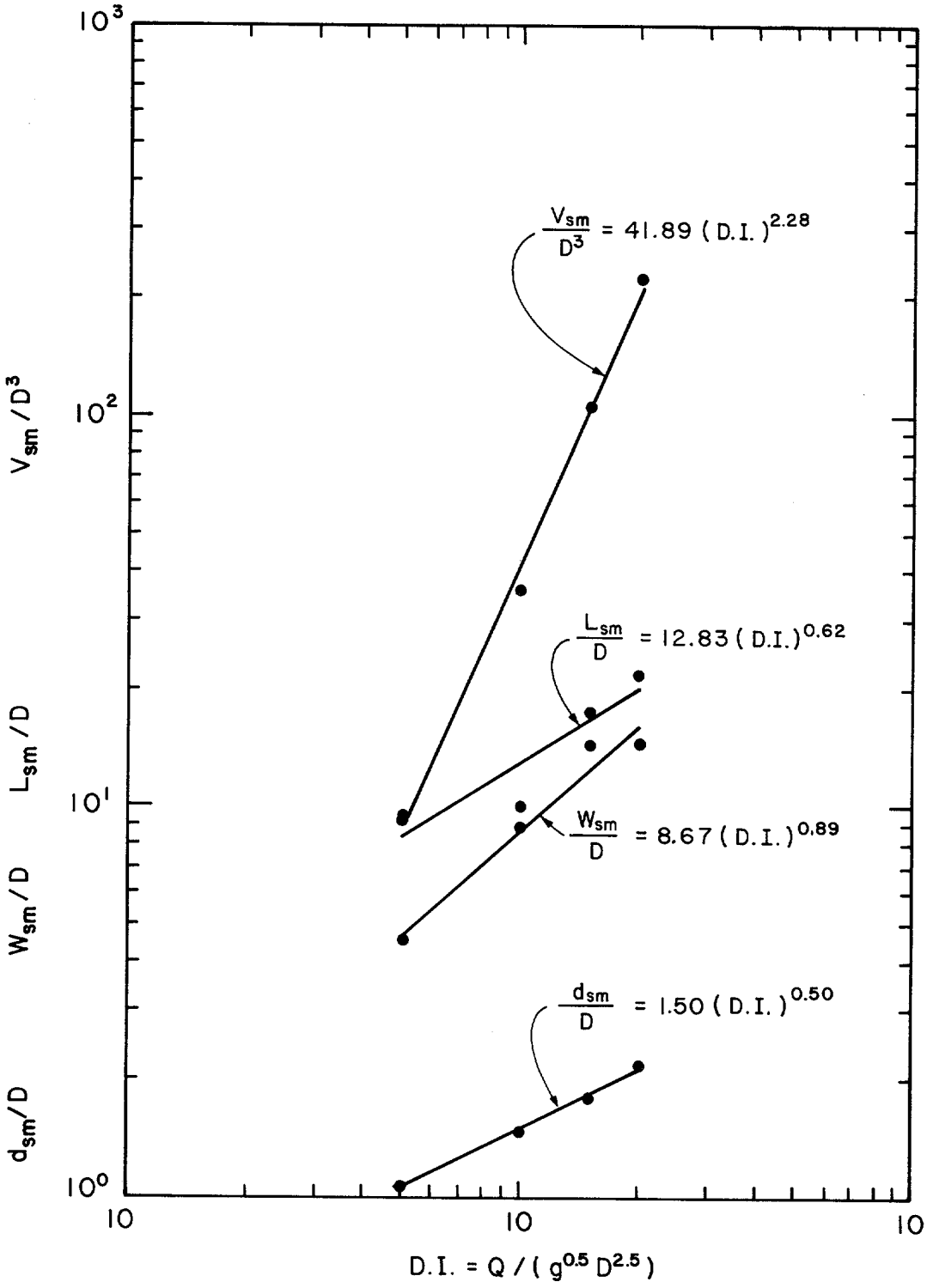

Figure 10. Scour vs. Discharge Intensity Graded gravel, d_{50} = 7.34 mm, σ = 4.78, t_o= 316 min.

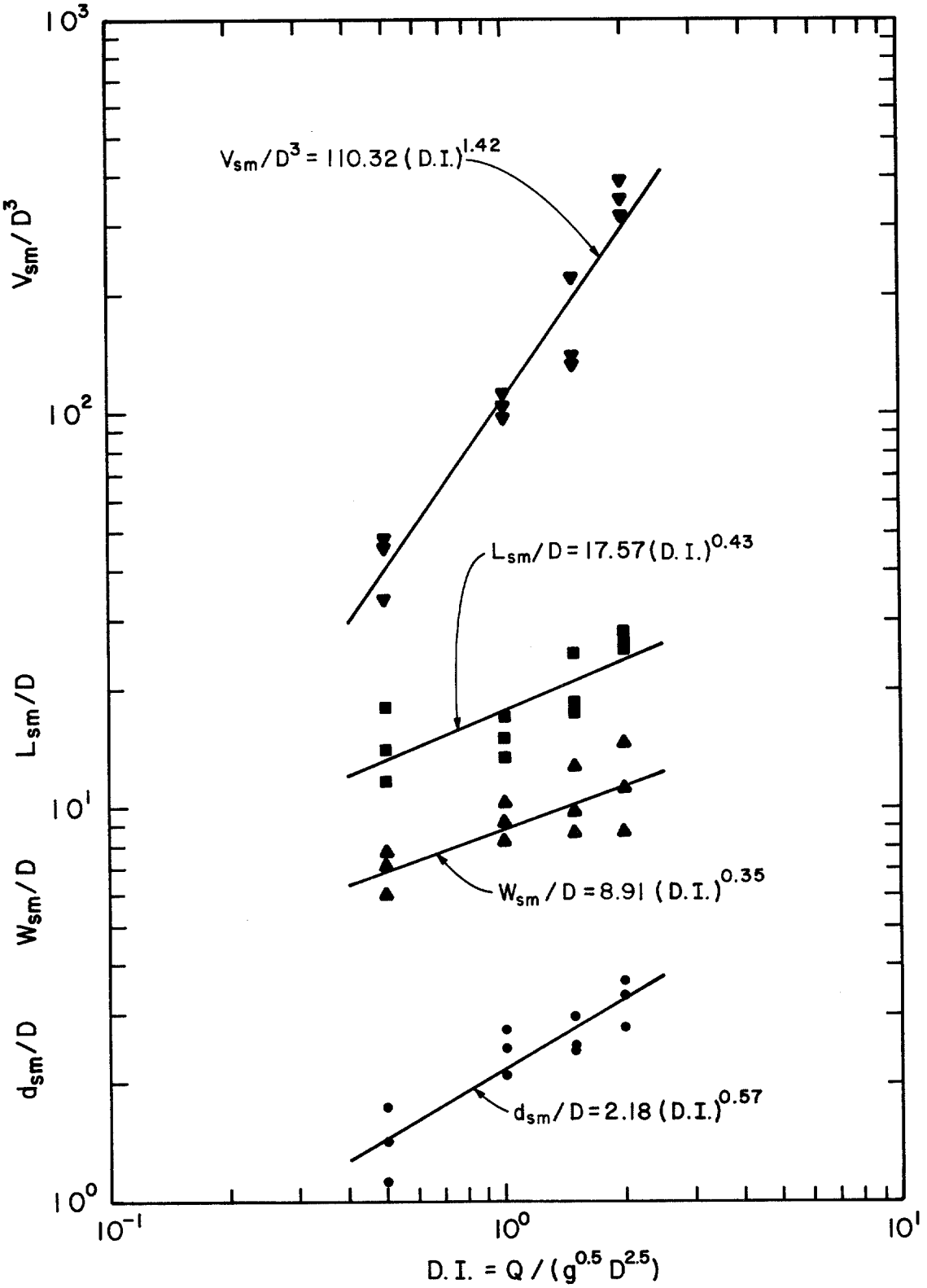

Figure 11. Scour vs. Discharge Intensity Cohesive material, t_o= 1000 min.

Table 6. Summary of Equations, Coefficients* for Estimating Maximum Hole Characteristics

Material	d_{50} (mm)	σ	(y) Dependent Variable	(x) Independent Variable	a	b
Uniform sand	1.86	1.33	d_{sm}/D	$Q\, g^{-0.5}\, D^{-2.5}$	2.07	0.45
Duration = 1000 min			W_{sm}/D	$Q\, g^{-0.5}\, D^{-2.5}$	9.07	0.57
			L_{sm}/D	$Q\, g^{-0.5}\, D^{-2.5}$	20.87	0.51
			V_{sm}/D	$Q\, g^{-0.5}\, D^{-2.5}$	166.91	1.41
Graded sand	2.00	4.38	d_{sm}/D	$Q\, g^{-0.5}\, D^{-2.5}$	1.24	0.32
Duration = 316 min			W_{sm}/d	$Q\, g^{-0.5}\, D^{-2.5}$	7.47	0.76
			L_{sm}/D	$Q\, g^{-0.5}\, D^{-2.5}$	12.77	0.41
			V_{sm}/D	$Q\, g^{-0.5}\, D^{-2.5}$	35.81	2.09
Uniform gravel	7.62	1.32	d_{sm}/D	$Q\, g^{-0.5}\, D^{-2.5}$	1.80	0.45
Duration = 316 min			W_{sm}/D	$Q\, g^{-0.5}\, D^{-2.5}$	9.13	0.62
			L_{sm}/D	$Q\, g^{-0.5}\, D^{-2.5}$	14.22	0.95
			V_{sm}/D	$Q\, g^{-0.5}\, D^{-2.5}$	66.58	1.36
Graded gravel	7.34	4.78	d_{sm}/D	$Q\, g^{-0.5}\, D^{-2.5}$	1.50	0.50
Duration = 316 min			W_{sm}/D	$Q\, g^{-0.5}\, D^{-2.5}$	8.67	0.89
			L_{sm}/D	$Q\, g^{-0.5}\, D^{-2.5}$	12.83	0.62
			V_{sm}/D	$Q\, g^{-0.5}\, D^{-2.5}$	41.89	2.28
Cohesive Material	0.15		d_{sm}/D	$Q\, g^{-0.5}\, D^{-2.5}$	2.18	0.57
Duration = 1000 min			V_{sm}/D^3	$Q\, g^{-0.5}\, D^{-2.5}$	110.32	1.42
			W_{sm}/D	$Q\, g^{-0.5}\, D^{-2.5}$	8.91	0.35
			L_{sm}/D	$Q\, g^{-0.5}\, D^{-2.5}$	17.57	0.43

*$y = a\, x^b$

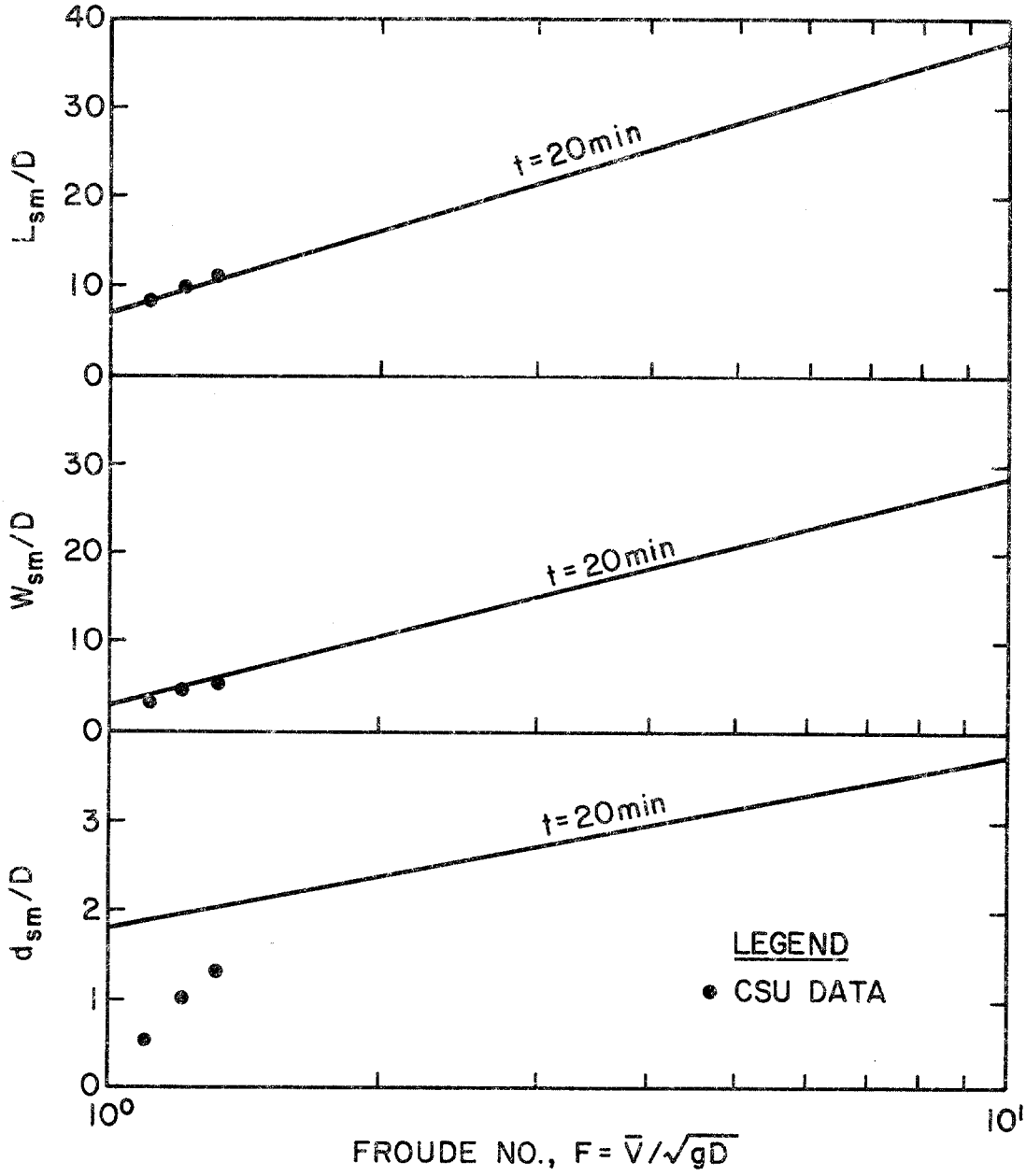

Figure 12. Bohan's equations for depth, length and width versus collected data (t_o = 20 min, d_{50} = 0.22 mm, σ = 1.26).

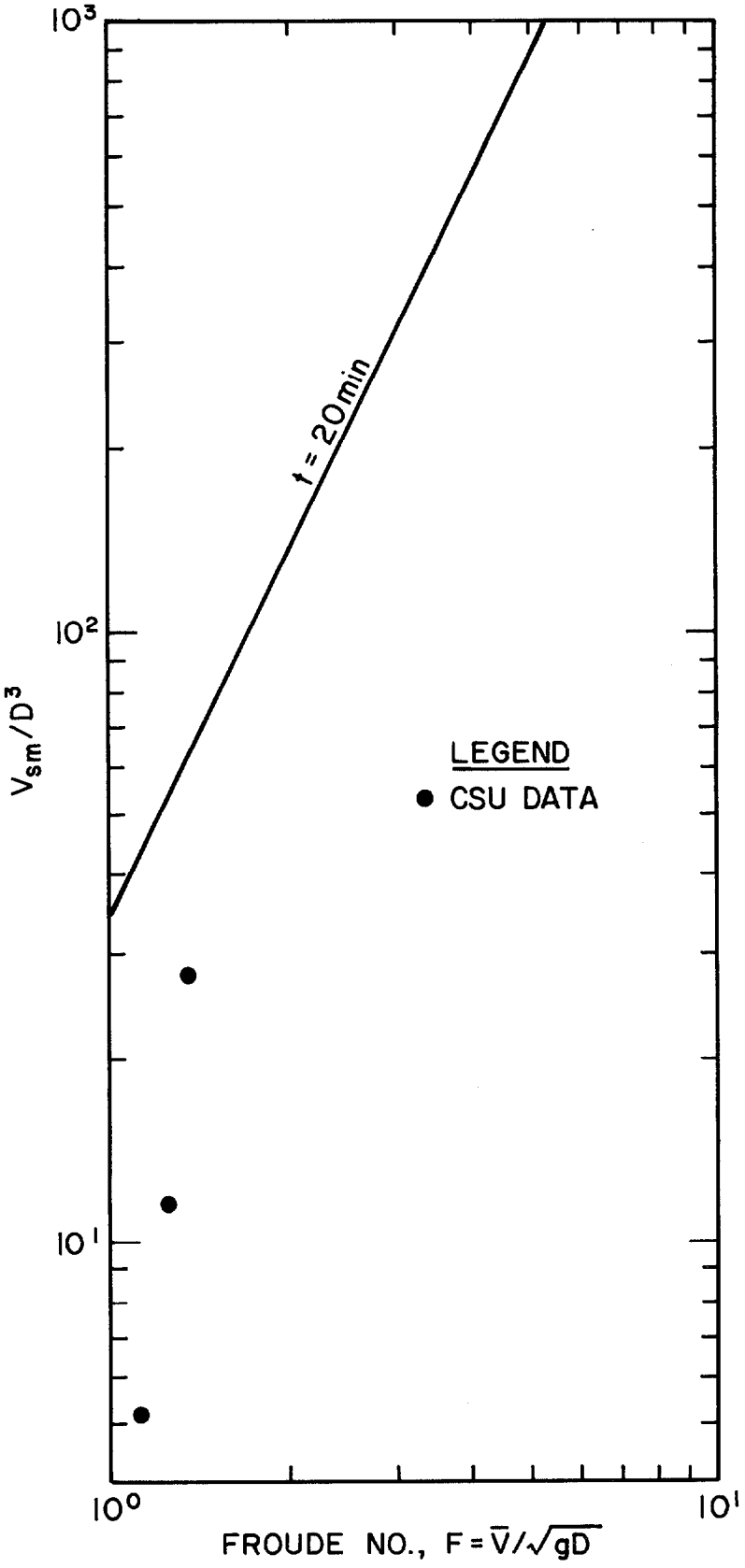

Figure 13. Bohan's equation for volume versus collected data (t_o = 20 min, d_{50} = 0.22 mm, σ = 1.26).

CSU test results are plotted on or near the Bohan findings. It is observed that the CSU data coincides with the Bohan findings for the width and length. There is a substantial difference between the CSU and Bohan depth and volume comparisons. However, the differences between the CSU and Bohan results can be explained in that the Bohan equation did not take into account partially full culverts. In most cases, the Bohan relationships give larger quantities and are more conservative than the CSU results.

For the cohesive soil, a series of empirical relationships were also formulated correlating the maximum dimensionless scour characteristics of d_{sm}/D, W_{sm}/D, L_{sm}/D and V_{sm}/D^3 to the inverted shear number. The inverted shear number is:

$$S_\eta = \frac{\rho \bar{V}^2}{\tau_c} \tag{46}$$

A graphic representation of these relationships are depicted in Figure 14.

Power regression equations were used to mathematically describe the linear plots in Figure 14 in the form presented in Equation 45. From these relationships, the maximum scour hole characteristic depth, width, length and volume can be correlated to the culvert diameter (D), culvert outlet fluid velocity ($\bar{V}$), fluid density (ρ), saturated soil shear stress (S_v) and soil platicity index (I_p). Replacing the independent variable of Equation 45 with the inverted shear number yields the equations:

$$\frac{d_{sm}}{D}, \frac{W_{sm}}{D}, \frac{L_{sm}}{D} \text{ or } \frac{V_{sm}}{D^3} = a \left[\frac{\rho \bar{V}^2}{\tau_c}\right]^b \tag{47}$$

results of this analysis are summarized in Table 7 below.

Table 7. Summary of Equation Coefficients* for Estimating Maximum Hole Characteristics for 1000 min Tests in a Sandy-clay Material

(y) Dependent Variable	(x) Independent Variable	a	b
d_{sm}/D	$[\rho\bar{V}^2 \tau_c^{-1}]$	0.87	0.18
V_{sm}/D^3	$[\rho\bar{V}^2 \tau_c^{-1}]$	3.48	0.17
W_{sm}/D	$[\rho\bar{V}^2 \tau_c^{-1}]$	2.85	0.33
L_{sm}/D	$[\rho\bar{V}^2 \tau_c^{-1}]$	0.63	0.93

*General Equation: $y = a\, x^b$

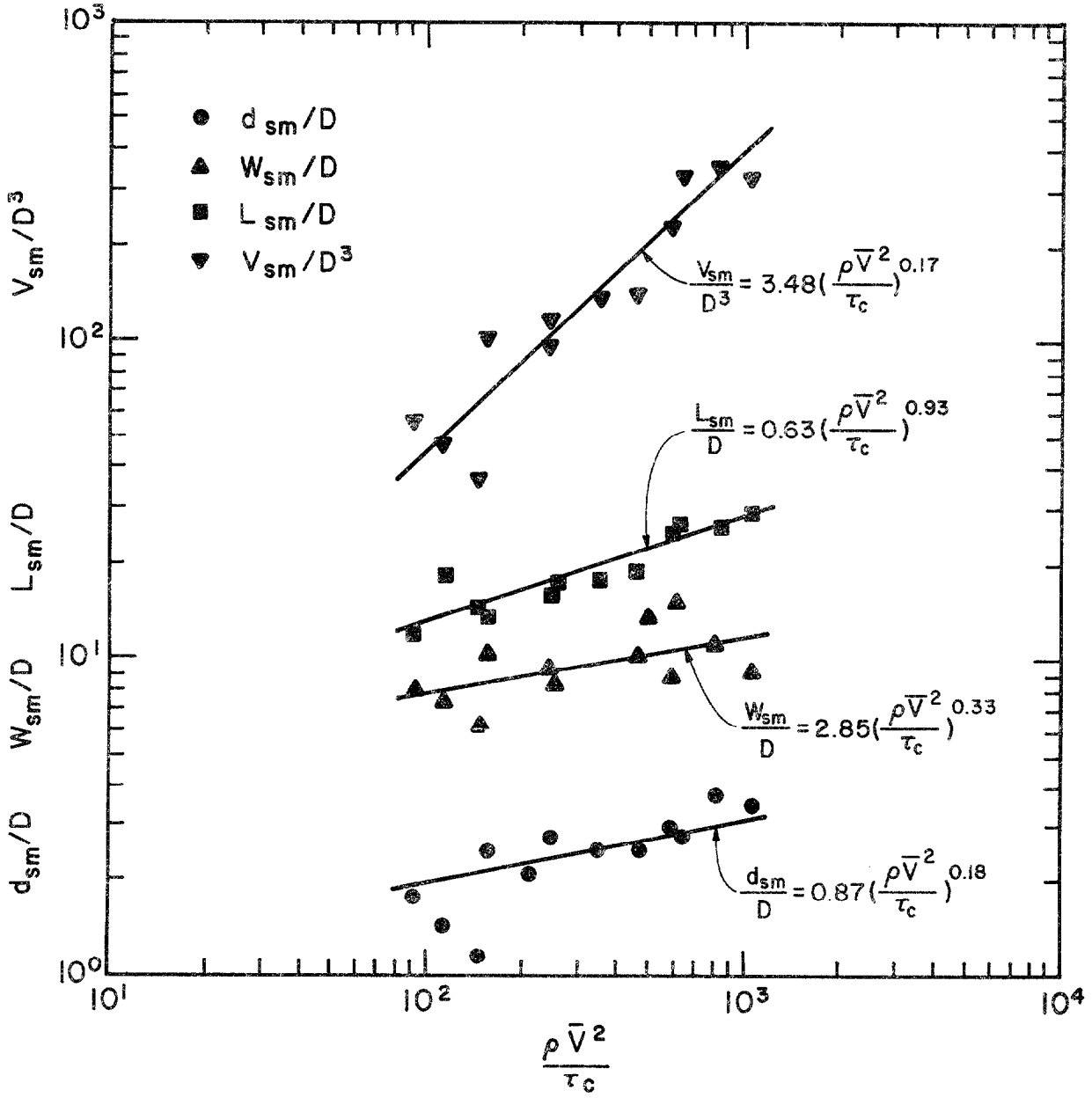

Figure 14. Characteristic dimension of scour vs. the reciprocal of the Shear number.

Time Relationships

Scour hole measurements were taken at 31, 100 and 316 minutes for all of the noncohesive materials while a portion of the uniform sand and all of the cohesive soil tests extended to 1000 minutes in duration. The observed scour hole characteristics were evaluated for each time interval. Characteristic values were normalized with reference to the final or maximum values obtained after the appropriate test durations. The normalized scour hole characteristics are presented in Table 8.

It was observed that after 31 minutes of testing, a minimum of 80.0 percent of the maximum scour depth was attained from a 316 minute scour test independent of the type of material tested. Furthermore, the 31 minute values for scour hole width, length and volume averaged 83, 80 and 61 percent of the 316 minute values respectively. The 31 minute rate of scour of the cohesive material was close to the average 31 minute rate of scour of the other material.

A comparison of the 316 minute scour hole dimensions with the 1000 minute scour hole dimensions indicates that although the duration of scour extended 684 times (216 percent) longer, the scour hole dimensions increased on an average by 14 percent in depth, 7 percent in width, 16 percent in length and 46 percent in volume. It appears that the scour mechanism approaches a state of equilibrium.

A logarithmic plot of the normalized scour hole characteristic versus time (t/t_o), where t is any time less than or equal to the duration of scour and t_o is equal to the duration of scour, is presented in Figure 15 through Figure 19. Utilizing the power relationship depicted in Equation 44, a series of regressions curves were fit to the data where time is the independent variable. Table 9 summarizes these equation coefficients.

Scour Relationships

Utilizing the dimensionless parameters and characteristic relationships thus far developed, it is possible to formulate a series of equations which estimate scour hole dimensions at any finite time between 31 minutes and the test duration of 316 to 1000 minutes. Combining Equation 44 with the time expression yields an equation which relates a desired hole characteristic to its maximum value as a function of time. The resulting equation is

$$y = a\ (x)^{b} * \left(\frac{t}{t_o}\right)^{c} \qquad (48)$$

where a is a coefficient; b is the slope of the desired characteristic curve; c is the slope of the desired time relationship; x is the independent variable of $Q\ g^{-0.5}\ D^{-2.5}$ or $\rho\ V^2(\tau_c)^{-1}$; and y is the dependent variable of d_s/D, W_s/D, L_s/D or V_s/D^3. Furthermore, since

Table 8. Normalized Scour Hole Characteristics for 316 Minutes and 1000 Minutes

Material	d_{50} mm	σ	Parameter	Time in Minutes 31	100	316	1000
Uniform sand	1.86	1.33	d_s/d_{sm}	0.81	0.81	1.00	
t_o = 316 min			W_s/W_{sm}	0.87	0.93	1.00	
			L_s/L_{sm}	0.67	0.82	1.00	
			V_s/V_{sm}	0.45	0.67	1.00	
Graded Sand	2.00	4.38	d_s/d_{sm}	0.83	0.90	1.00	
t_o = 316 min			W_s/W_{sm}	0.85	0.90	1.00	
			L_s/L_{sm}	0.91	0.96	1.00	
			V_s/V_{sm}	0.65	0.81	1.00	
Uniform gravel	7.62	1.32	d_s/d_{sm}	0.88	0.93	1.00	
t_o = 316 min			W_s/W_{sm}	0.83	0.91	1.00	
			L_s/L_{sm}	0.76	0.88	1.00	
			V_s/V_{sm}	0.63	0.80	1.00	
Graded gravel	7.34	4.78	d_s/d_{sm}	0.92	0.96	1.00	
t_o = 316 min			W_s/W_{sm}	0.80	0.90	1.00	
			L_s/L_{sm}	0.86	0.94	1.00	
			V_s/V_{sm}	0.70	0.83	1.00	
Uniform sand	1.86	1.33	d_s/d_{sm}	0.73	0.81	0.90	1.00
t_o = 1000 min			W_s/W_{sm}	0.81	0.87	0.93	1.00
			L_s/L_{sm}	0.57	0.70	0.85	1.00
			V_s/V_{sm}	0.29	0.43	0.64	1.00
Cohesive Soil Sandy Clay		0.15	d_s/d_{sm}	0.69	0.79	0.86	1.00
t_o = 1000 min			W_s/W_{sm}	0.77	0.90	0.95	1.00
			L_s/L_{sm}	0.71	0.82	0.88	1.00
			V_s/V_{sm}	0.45	0.58	0.73	1.00

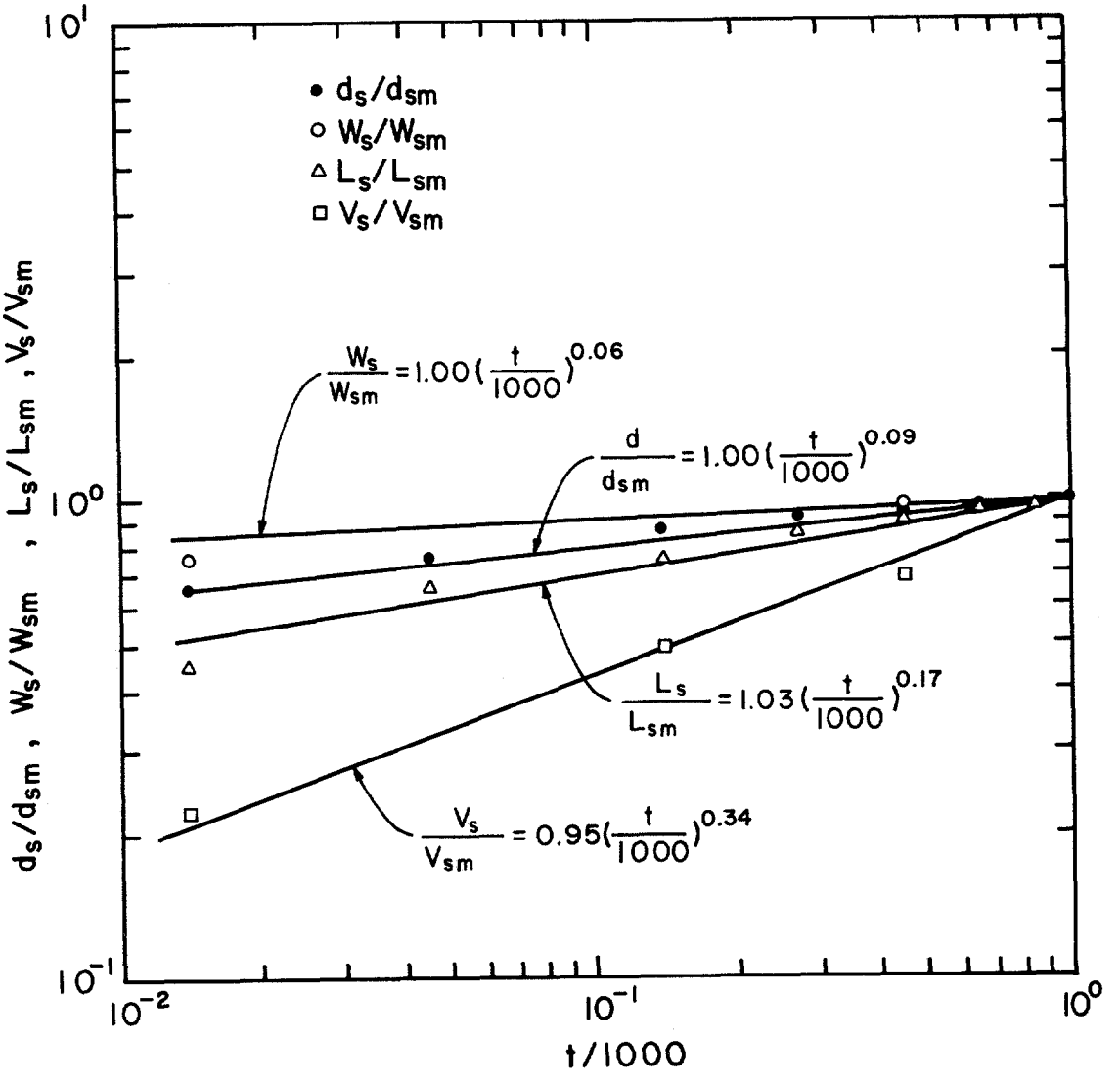

Figure 15. Uniform sand, normalized scour hole characteristics versus normalized time.

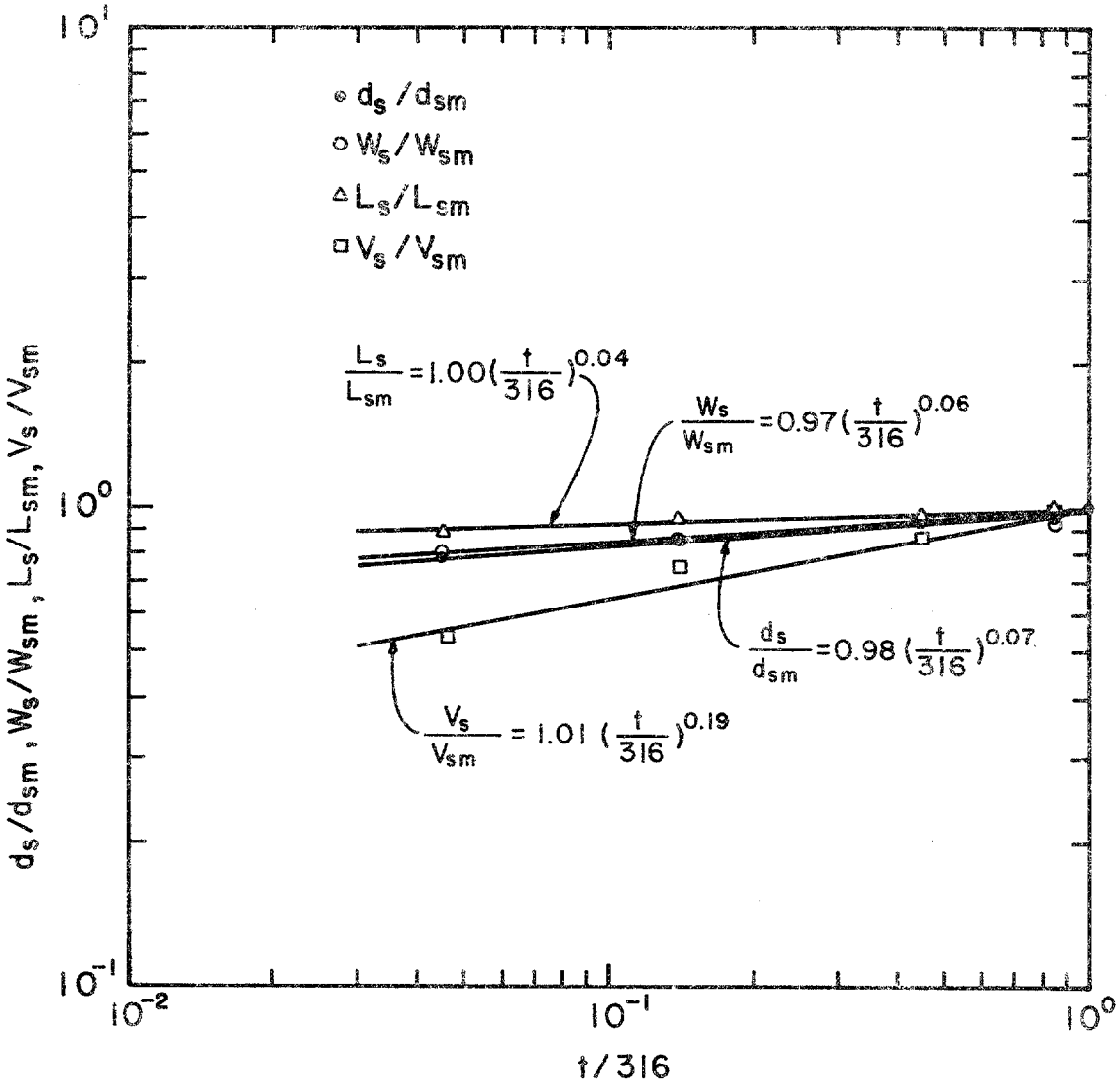

Figure 16. Graded sand, normalized scour hole characteristics versus normalized time.

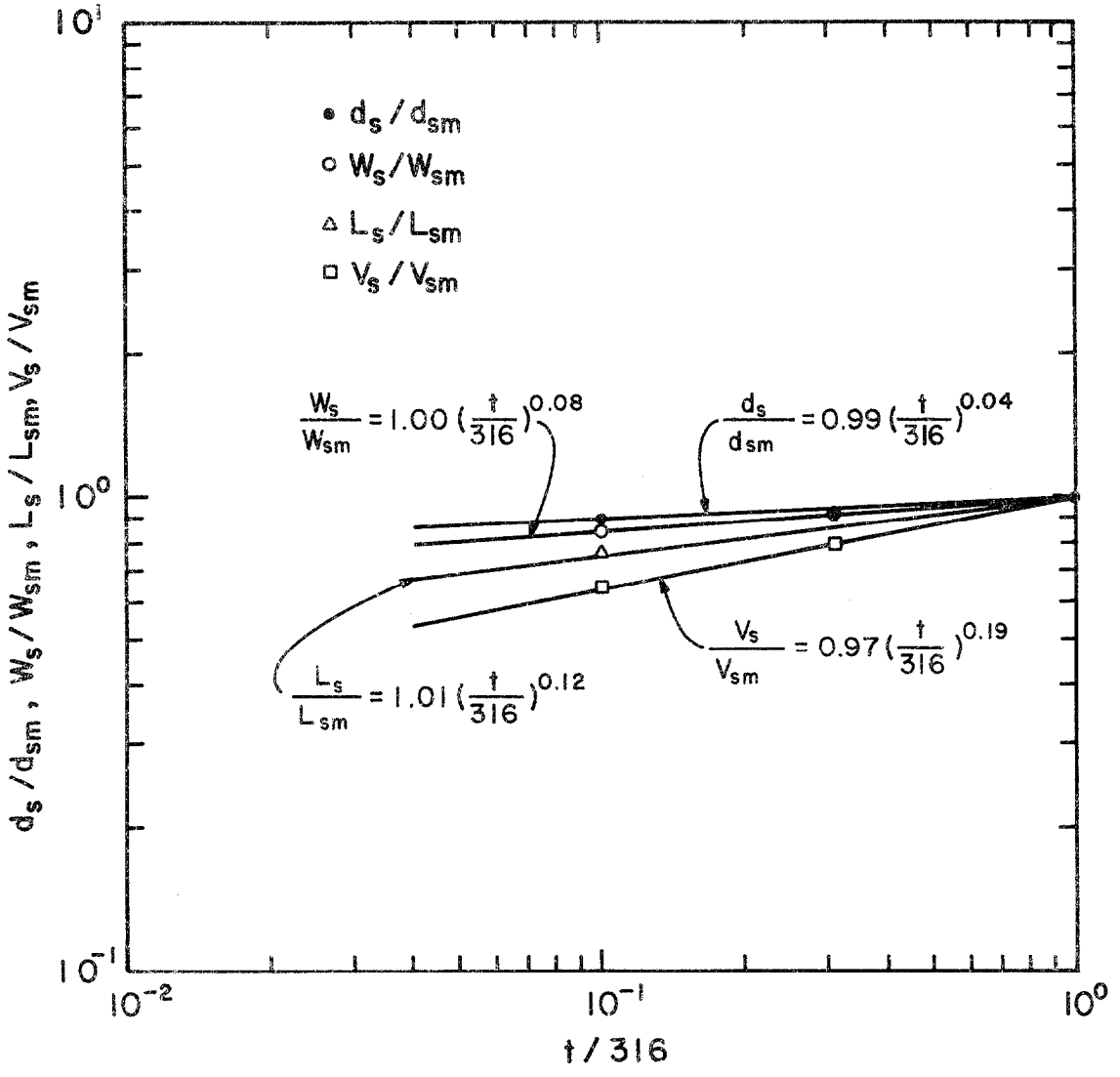

Figure 17. Uniform gravel, normalized scour hole characteristics versus normalized time.

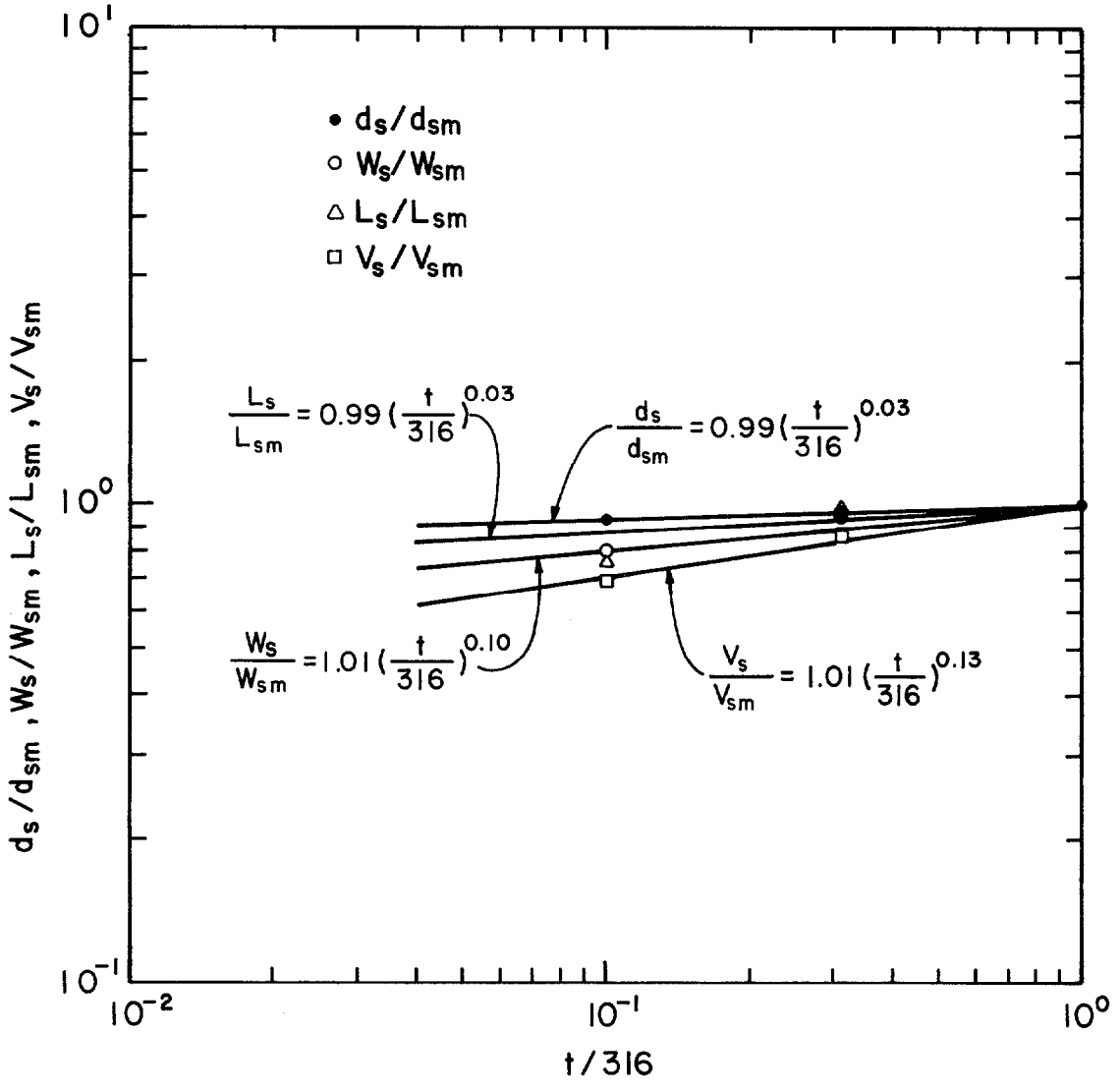

Figure 18. Graded gravel, normalized scour hole characteristics versus normalized time.

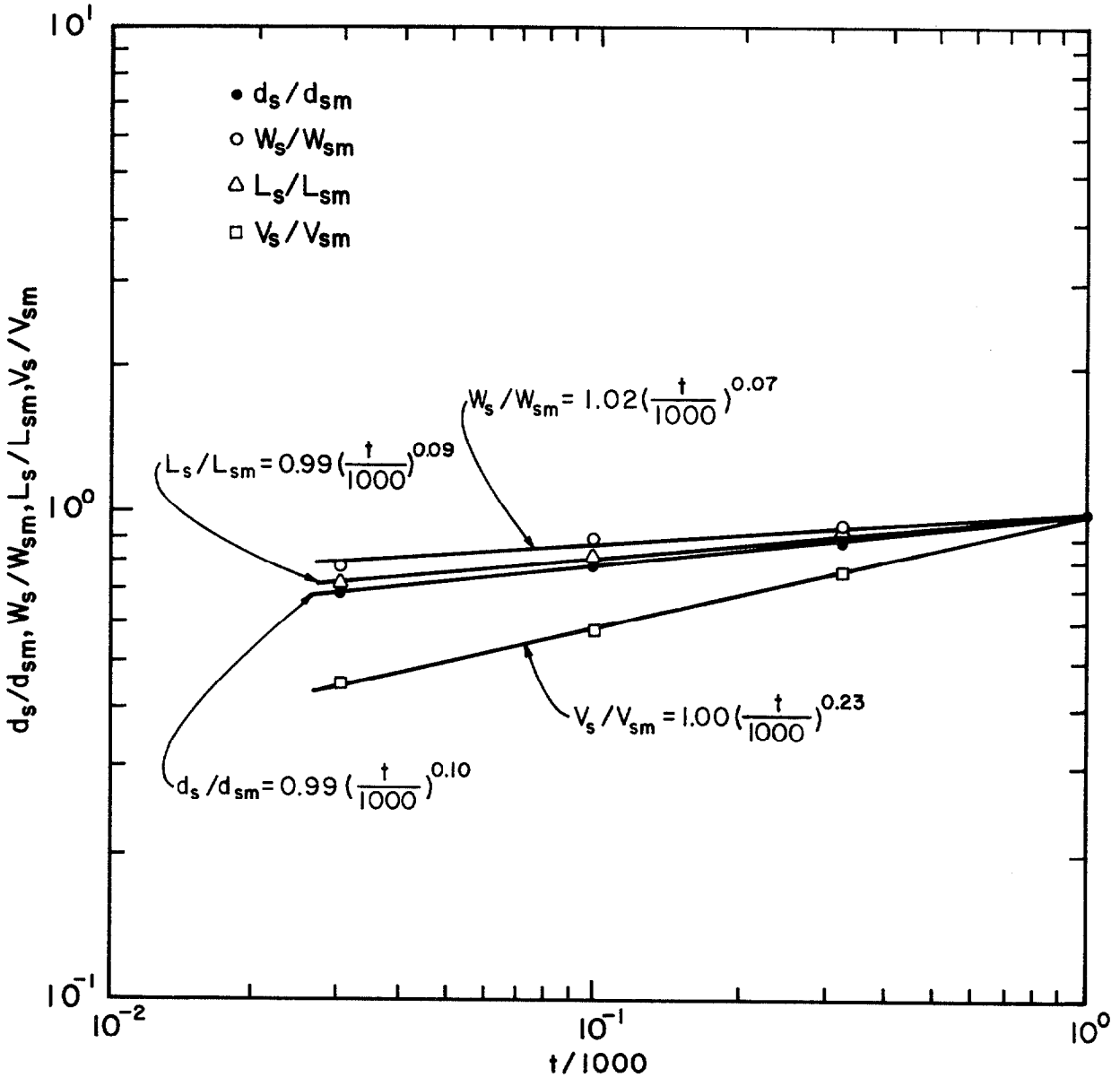

Figure 19. Cohesive material, normalized hole characteristics versus normalized time.

Table 9. Summary of Equation Coefficients* for Time versus Characteristic Lengths

Material	d_{50} (mm)	σ	(y) Dependent Variable	(x) Independent Variable	a	b
Uniform sand	1.86	1.33	d_s/d_{sm}	t/t_o	1.00	0.09
t_o = 1000 min			W_s/W_{sm}	t/t_o	1.00	0.06
			L_s/L_{sm}	t/t_o	1.03	0.17
			V_s/V_{sm}	t/t_o	0.95	0.34
Graded sand	2.00	4.38	d_s/d_{sm}	t/t_o	0.98	0.07
t_o = 316 min			W_s/W_{sm}	t/t_o	0.97	0.06
			L_s/L_{sm}	t/t_o	1.00	0.04
			V_s/V_{sm}	t/t_o	1.01	0.19
Uniform gravel	7.62	1.32	d_s/d_{sm}	t/t_o	0.99	0.04
t_o = 316 min			W_s/W_{sm}	t/t_o	1.00	0.08
			L_s/L_{sm}	t/t_o	1.01	0.12
			V_s/V_{sm}	t/t_o	0.99	0.19
Graded gravel	7.34	4.78	d_s/d_{sm}	t/t_o	0.99	0.03
t_o = 316 min			W_s/W_{sm}	t/t_o	1.01	0.10
			L_s/S_{sm}	t/t_o	1.02	0.07
			V_s/V_{sm}	t/t_o	1.01	0.17
Cohesive Sandy Clay			d_s/d_{sm}	t/t_o	0.99	0.10
t_o = 1000 min			W_s/W_{sm}	t/t_o	1.02	0.07
			L_s/L_{sm}	t/t_o	0.99	0.09
			V_s/V_{sm}	t/t_o	0.99	0.23

Equation $y = a\ x^b$

$t \leq 1000$ minutes, t_o = 1000 minutes or 316 minutes as indicated

some of the tests were run for a 316 minute duration and others were run for 1000 minutes, the coefficient "a" can be multiplied by the appropriate time normalization percentages from Table 3 so that all of the materials will have the same divisor for the time parameter. Table 10 presents a summary of the coefficients and exponents for each material and scour hole parameter. The exponents b and c are the same as the component regression analyses for each independent variable. The coeffients "a" are the product of the coefficients from the component regression analyses for each independent variable times the normalization percentages $d_{s_{316}}/d_{s_{1000}}$, $W_{s_{316}}/W_{s_{1000}}$, $L_{s_{316}}/L_{s_{1000}}$ and $V_{s_{316}}/V_{s_{1000}}$ for the runs that extended to 1000 minutes.

A compilation of maximum scour hole depths versus discharge intensity for four uniform materials and two graded materials is shown in Figure 20.

Tailwater Effects

A series of tests were run to further investigate the effects of TW depth on the scour hole dimensions. Previous tests by Bohan (13) and Fletcher and Grace of the U.S. Army Corps of Engineers demonstrated that maximum scour occurred when the TW was below the culvert center line. Current tests for TW of zero, 0.25 D and 0.45 D were run to determine where below the culvert centerline the TW tended to maximize scour.

The tests were run for a uniform sand and a uniform gravel as presented in Figure 21 through Figure 24 respectively. The results were not conclusive for the gravel. For the sand bed depicted, little difference in scour between zero tailwater and 0.25 D tailwater is observed. As the tailwater was raised from 0.25 D to 0.45 D, the depth and width of scour were lower while the length and volume of scour were larger. Overall, the 0.25 D tailwater, scour hole dimensions were no more than 10 percent greater than basic tests with the 0.45 D tailwater. Therefore, little difference was observed in the maximum scour hole dimensions as the tailwater varied from zero to 0.45 D for Discharge Intensities of 1.5 and greater.

Effects of Similitude

Throughout the investigation, two facilities were used to conduct the scour tests in the uniform sand bed material. To insure that the two facilities would generate compatible results, data from the 20-foot outdoor facility was compared with the data from the 4-foot model which was a 1:5 Froude scale model of the outdoor facility. Plotting the dimensionless scour hole parameters of d_{sm}/D, L_{sm}/D and V_{sm}/D versus the Discharge Intensity yielded Figure 25.

Observation of the dimensionless comparisons indicate that the laws of similitude relative to noncohesive materials were maintained and that data was complemented from the two sources. As illustrated in Figure 25, data from both facilities were randomly scattered with few extraneous points.

Table 10. Summary of Equation* Coefficients and Exponents in Terms of a Constant 316 Minute Duration

Material	d_{50} mm	σ	(y) Dependent Variable	(x) Independent Variable	a	b	c
Uniform sand	1.86	1.33	d_s/D	$Qg^{-0.5}D^{2.5}$	1.86	0.45	0.09
			W_s/D	$Qg^{-0.5}D^{2.5}$	8.44	0.57	0.06
			L_s/D	$Qg^{-0.5}D^{2.5}$	18.28	0.51	0.17
			V_s/D^3	$Qg^{-0.5}D^{2.5}$	101.48	1.41	0.34
Graded Sand	2.00	4.38	d_s/D	$Qg^{-0.5}D^{2.5}$	1.22	0.82	0.07
			W_s/D	$Qg^{-0.5}D^{2.5}$	7.25	0.76	0.06
			L_s/D	$Qg^{-0.5}D^{2.5}$	12.77	0.41	0.04
			V_s/D^3	$Qg^{-0.5}D^{2.5}$	36.17	2.09	0.19
Uniform gravel	7.62	1.32	d_s/D	$Qg^{-0.5}D^{2.5}$	1.78	0.45	0.04
			W_s/D	$Qg^{-0.5}D^{2.5}$	9.13	0.62	0.08
			L_s/D	$Qg^{-0.5}D^{2.5}$	14.36	0.95	0.12
			V_s/D^3	$Qg^{-0.5}D^{2.5}$	65.91	1.86	0.19
Graded Gravel	7.34	4.78	d_s/D	$Qg^{-0.5}D^{2.5}$	1.49	0.50	0.03
			W_s/D	$Qg^{-0.5}D^{2.5}$	8.76	0.89	0.10
			L_s/D	$Qg^{-0.5}D^{2.5}$	13.09	0.62	0.07
			V_s/D^3	$Qg^{-0.5}D^{2.5}$	42.31	2.28	0.17
Cohesive Sandy Clay		0.15	d_s/D	$Q\,g^{-0.5}\,D^{-2.5}$	1.86	0.57	0.10
			W_s/D	$Q\,g^{-0.5}\,D^{-2.5}$	8.63	0.35	0.07
			L_s/D	$Q\,g^{-0.5}\,D^{-2.5}$	15.30	0.43	0.09
			V_s/D^3	$Q\,g^{-0.5}\,D^{-2.5}$	79.73	1.42	0.23
Cohesive Sandy Clay		0.15	d_s/D^3	$\rho\,V^2\,\tau_c^{-1}$	0.86	0.18	0.10
			W_s/D	$\rho\,V^2\,\tau_c^{-1}$	3.55	0.17	0.07
			L_s/D	$\rho\,V^2\,\tau_c^{-1}$	2.82	0.33	0.09
			V_s/D^3	$\rho\,V^2\,\tau_c^{-1}$	0.62	0.93	0.23

*Modified Equation $y = a\,(x)^b * (t/316\ \text{min})^c$
where $t \leq 1000$ minutes and $t \geq 31$ minutes.

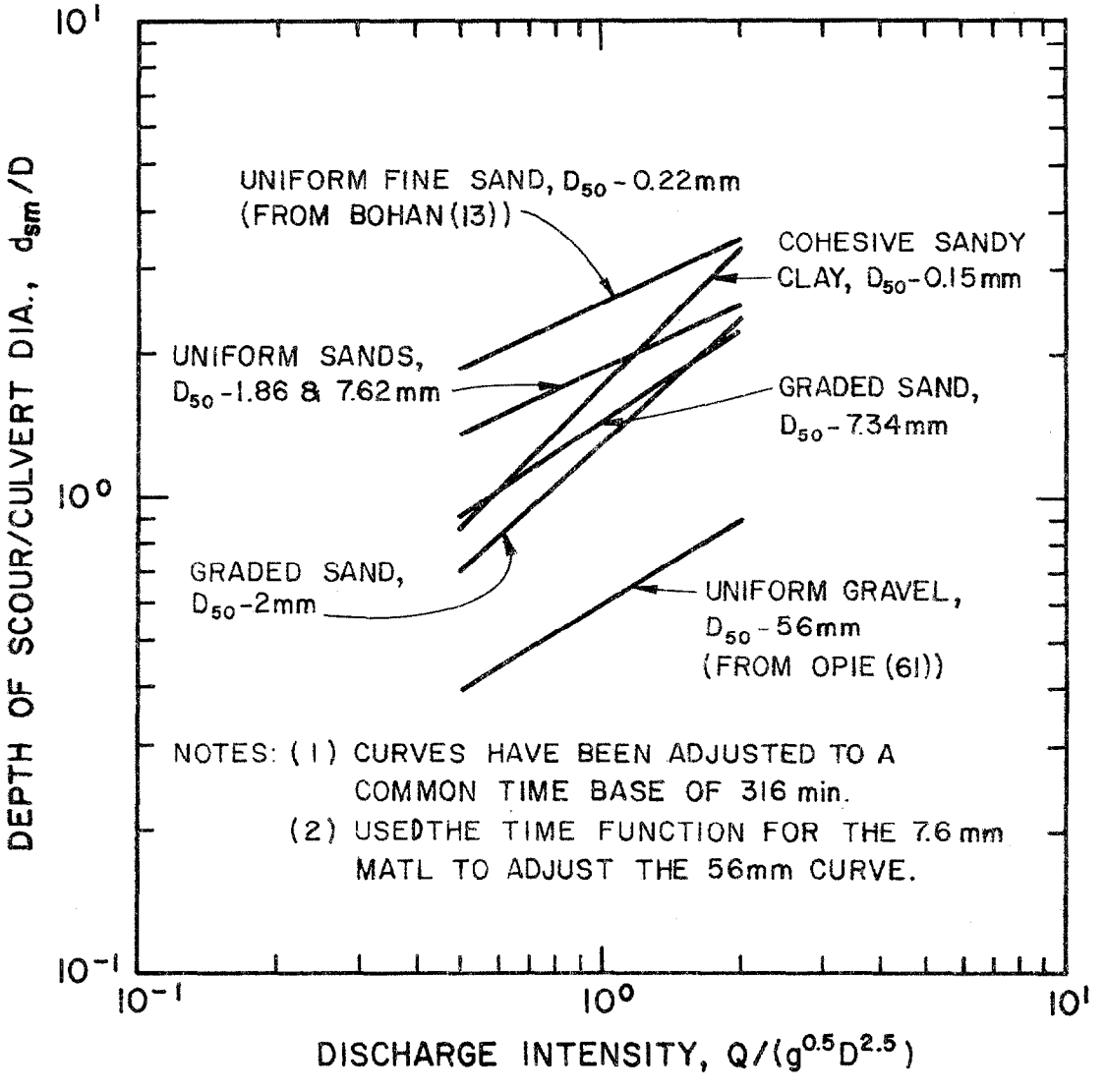

Figure 20. Cohesive and cohesionless material, d_s/D versus D.I. curves adjusted to a common time base of 316 minutes.

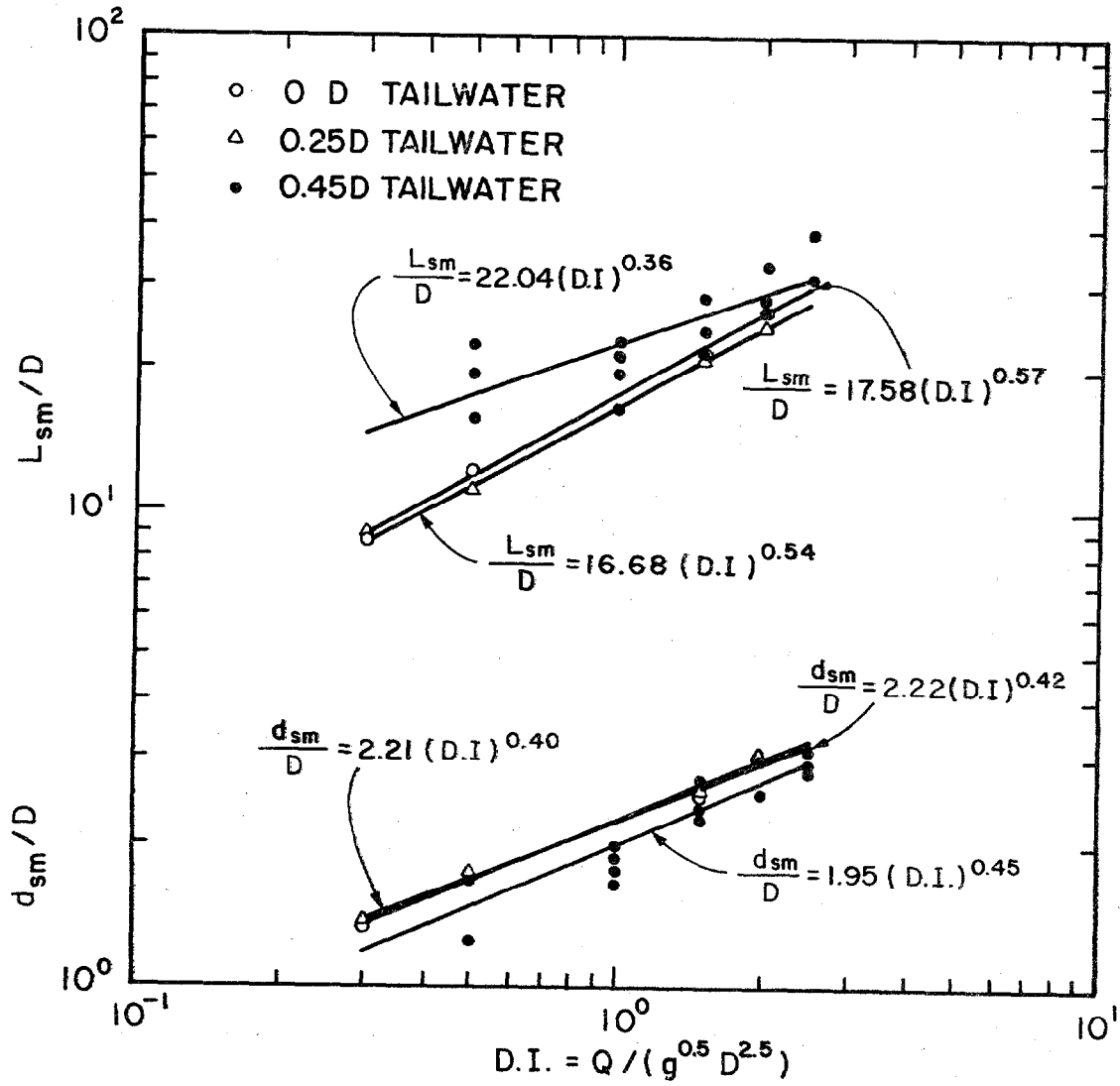

Figure 21. Uniform sand, tailwater comparison of scour hole depth and length.

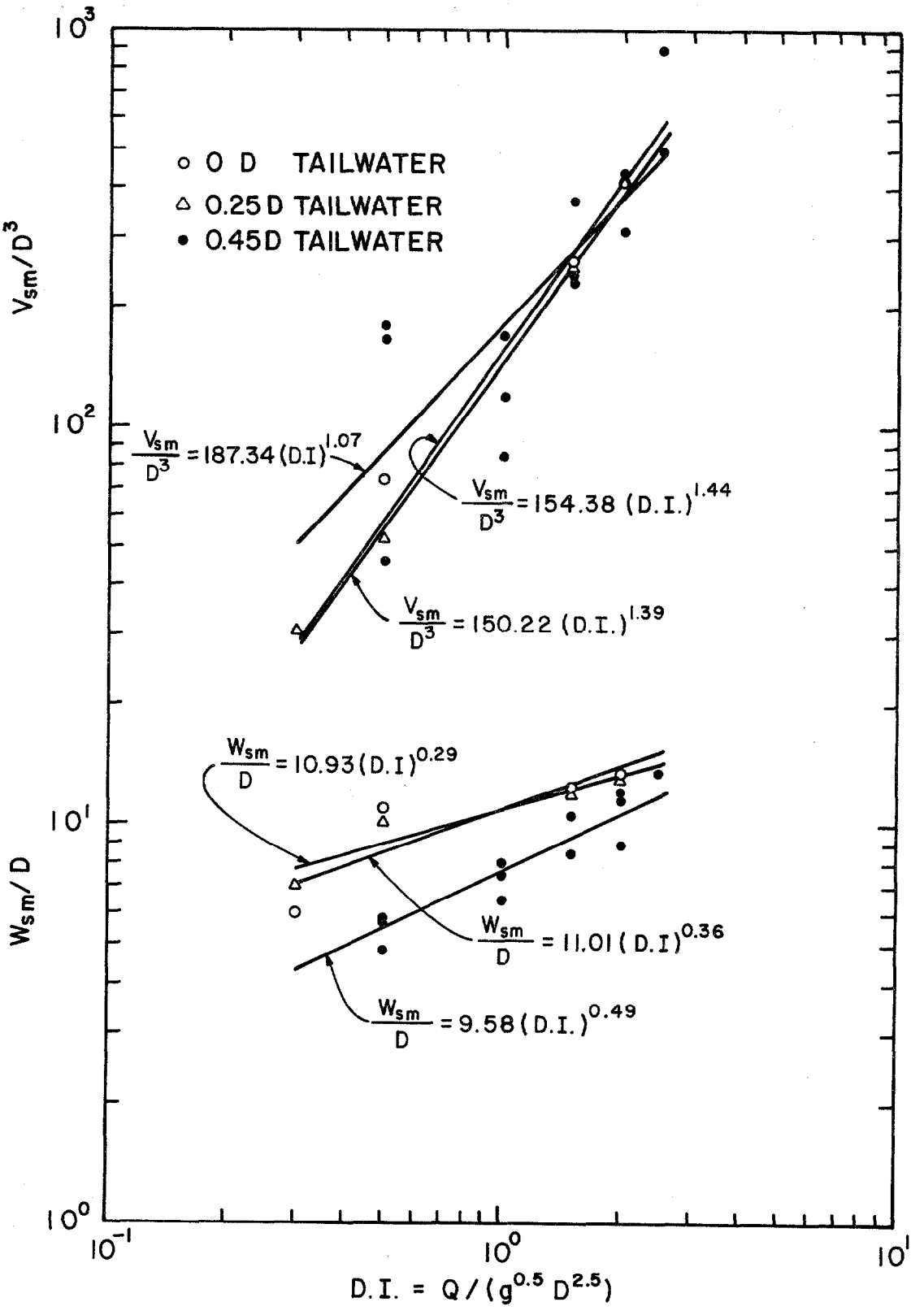

Figure 22. Uniform sand, tailwater comparison of scour hole width and volume.

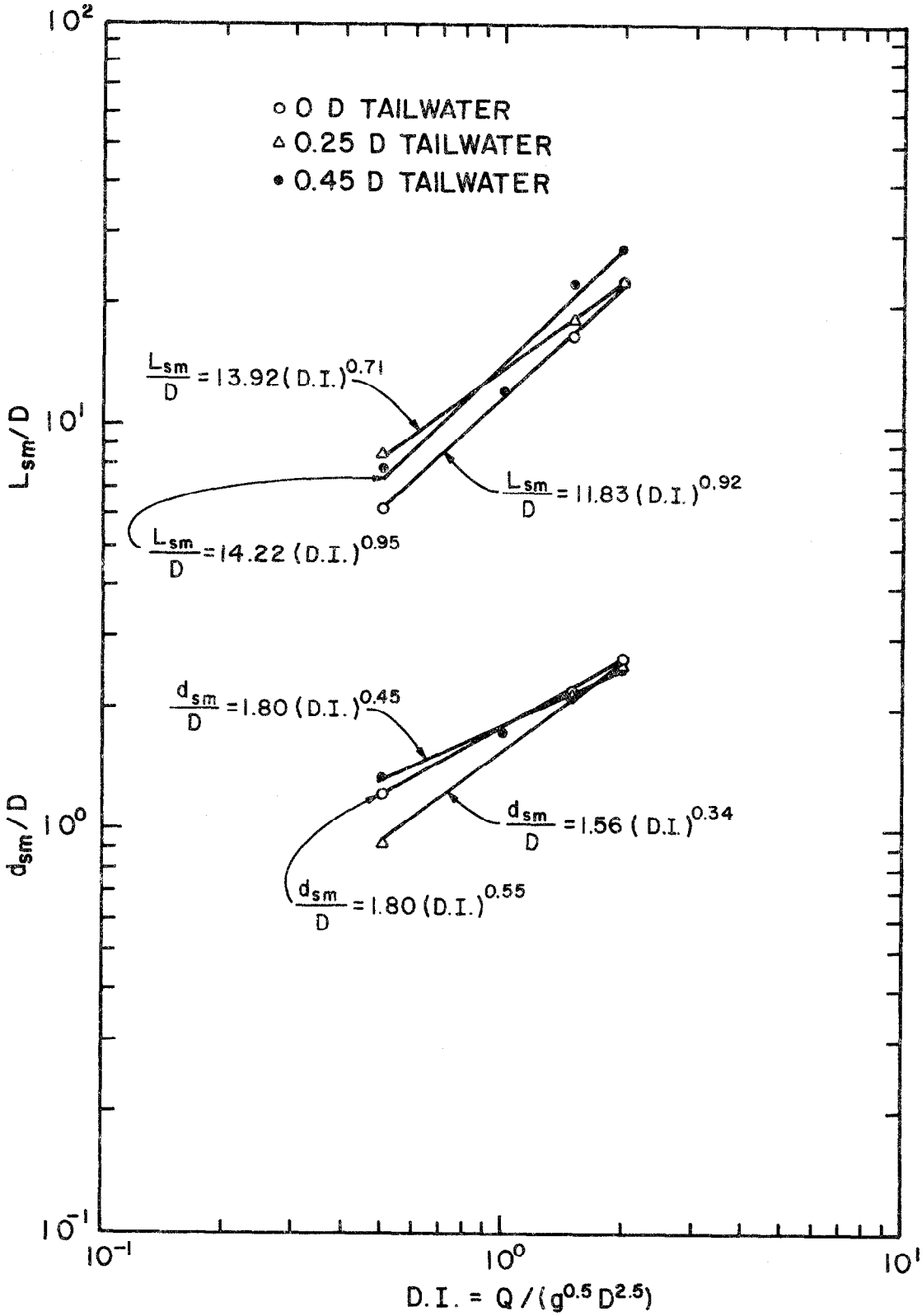

Figure 23. Uniform gravel, tailwater comparison of scour hole depth and length.

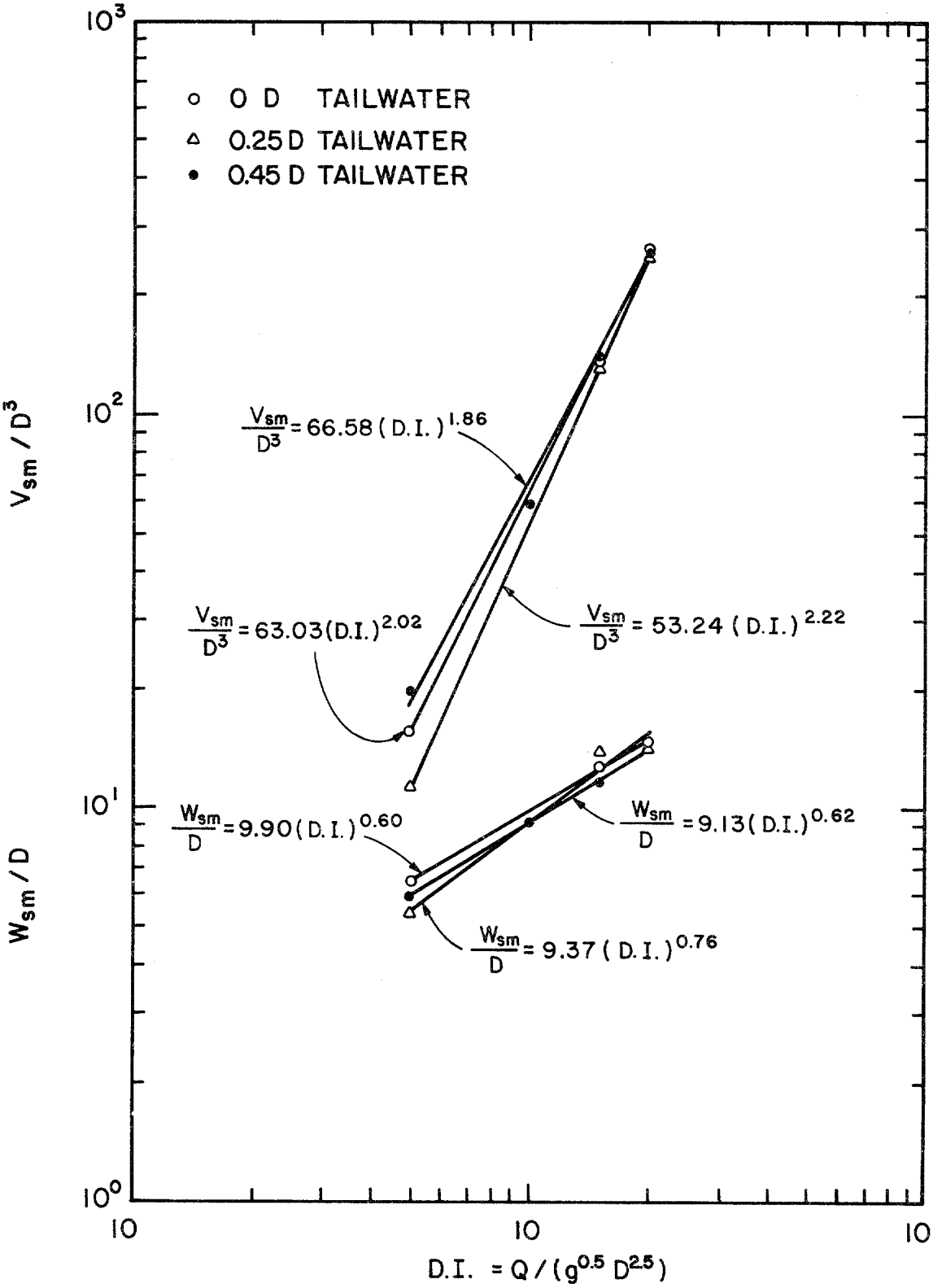

Figure 24. Uniform gravel, tailwater comparison of scour hole width and volume.

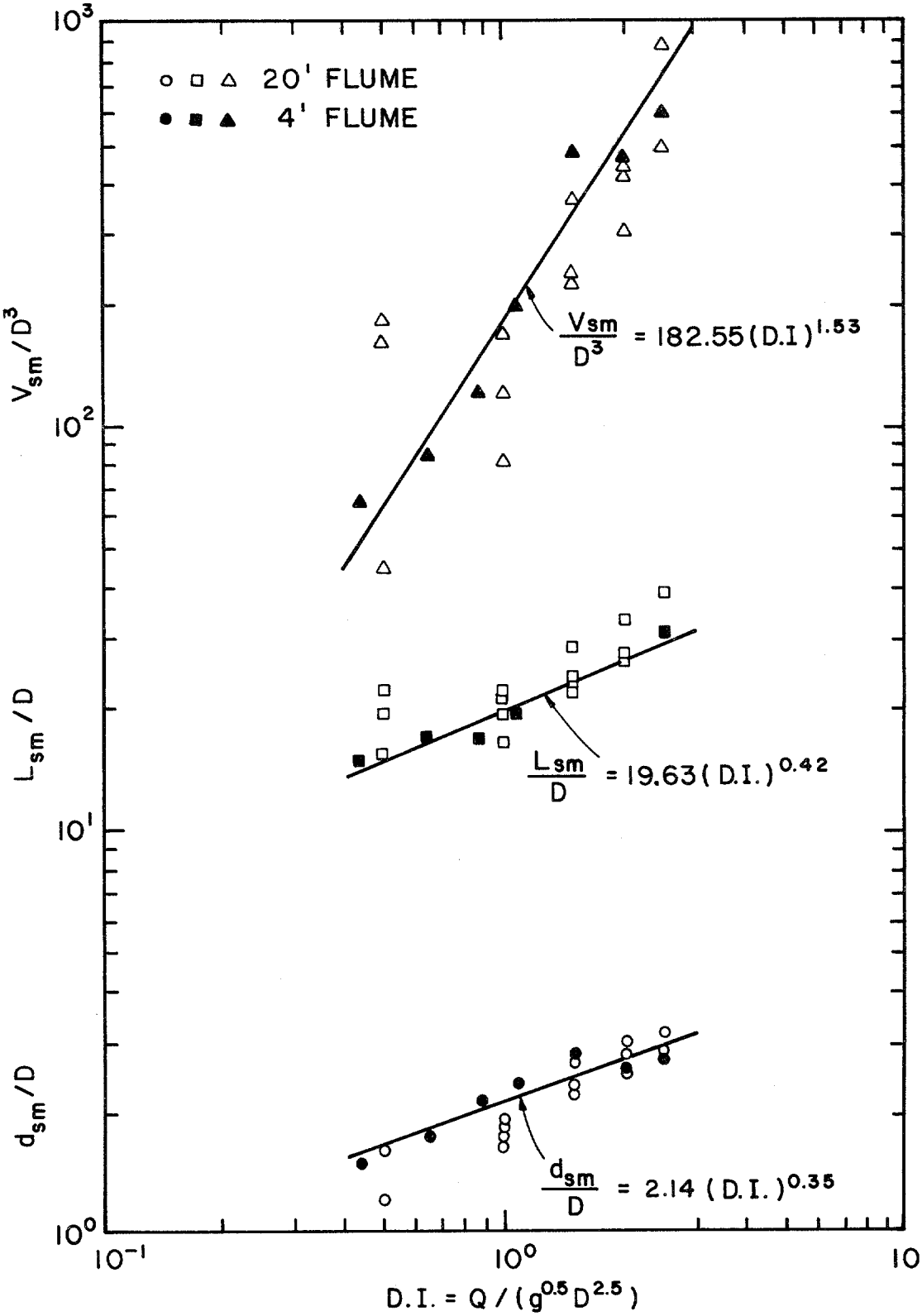

Figure 25. Similitude comparison of scour hole depth, length and volume in uniform sand.

Gradation Effects

An analysis was performed comparing noncohesive materials of similar nominal mean grain diameters (d_{50}) but different material gradation to maximum scour hole dimensions for similar testing conditions. The gradation is expressed in terms of the material standard deviation (σ) where

$$\sigma = \sqrt{d_{84}/d_{16}} \tag{49}$$

The uniform sand (σ = 1.32) and graded sand (σ = 4.38), both having nominal mean grain diameters of 2.0 mm, were compared in Figure 26. Similarly, the uniform gravel (σ = 1.33) and graded gravel (σ = 4.78), both having nominal mean grain diameters of 8.0 mm, were compared in Figure 27. It is evident that as the material uniformity increased, the maximum dimensions of the scour hole increased. Furthermore, the smaller the mean grain diameter of the material, the more significant the gradation effects. It is also evident that the graded materials tend to armour the scour hole reducing ultimate scour hole dimensions from those of more uniform materials.

The convergence of the scour curves for graded and uniform materials of the same mean diameter is limited by the resistance to motion by the soil particles and the dissipation of the erosive forces in the scour hole. At lower discharge intensities the larger fractions of a graded material resist motion and stabilize the scour hole with an effective size material that is much larger than the mean. At higher discharge intensities the dissipation of erosive forces in the scour hole becomes the dominant factor.

Graded materials were observed to have steeper slopes than those derived for uniform materials of similar mean grain diameters. Therefore, at low discharge intensities, the graded material is more desirable to maximize energy dissipation and minimize the volume of material eroded. However, at high discharge intensities, materials of similar mean grain diameters scour in a similar manner independent of the material gradation.

Effects of Culvert Shape

A series of test runs were performed investigating how the shape of a culvert influenced the scour hole dimensions of depth, length and volume. Only circular and square culverts were considered in this analysis.

Culverts were sized such that the diameter of the circular culvert was equivalent to the length of one side of the square culvert. Since the cross-sectional areas of the two culverts were not identical, it was necessary to compare the results based upon parameters other than the Discharge Intensity and culvert diameter. The Froude relationship was selected for analysis where the Froude number is defined as

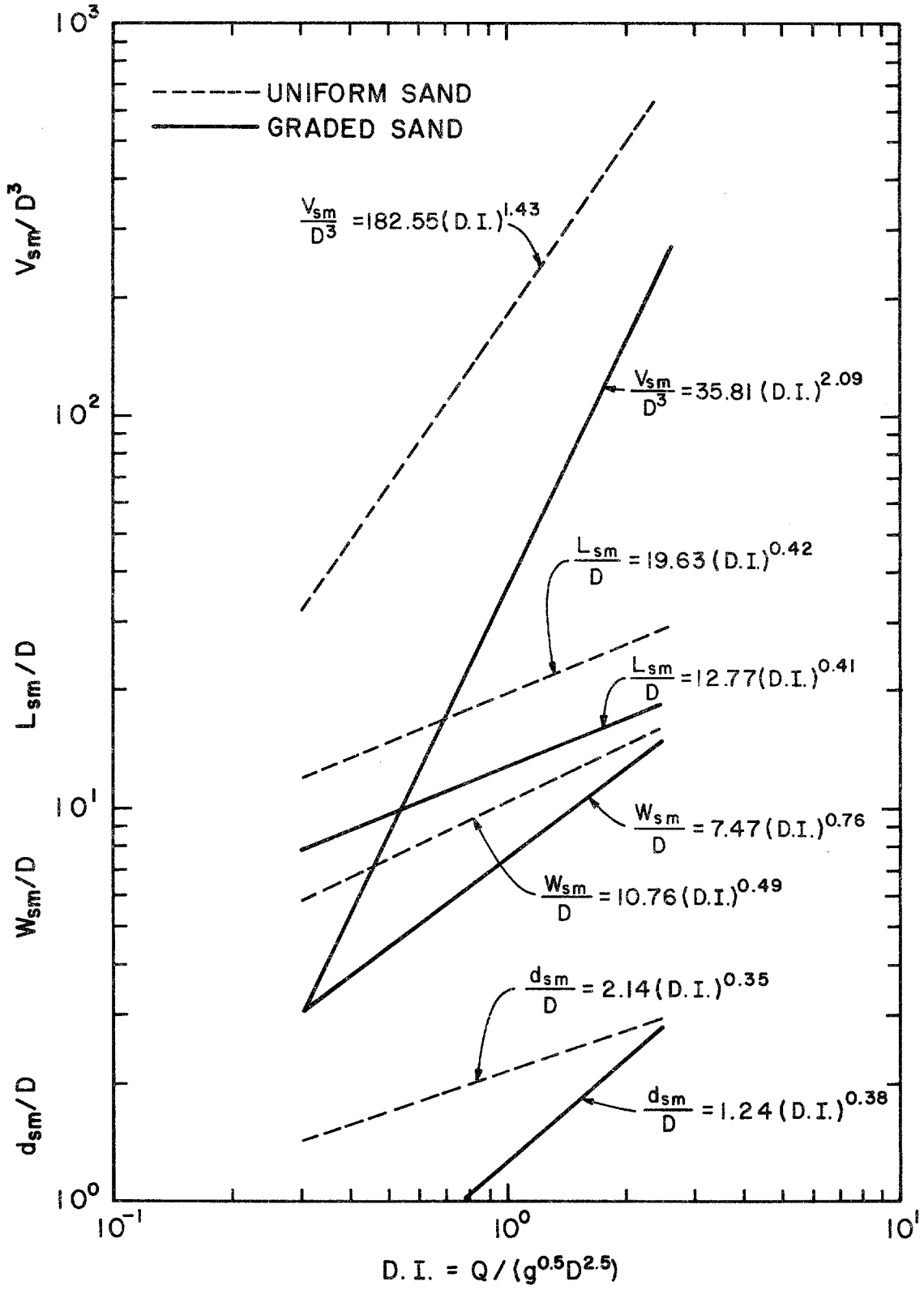

Figure 26. Effects of gradation for sand materials having similar mean grain diameter.

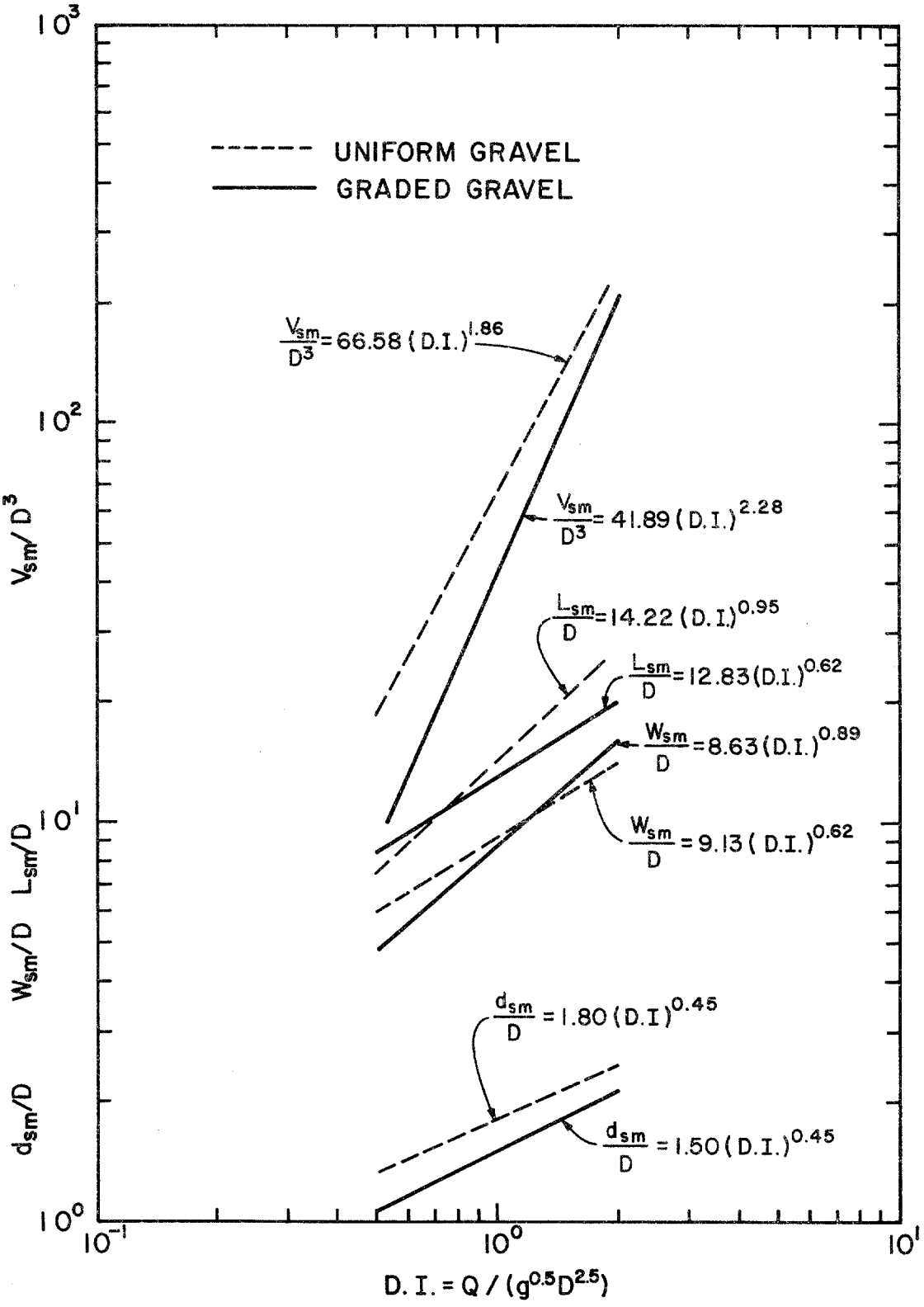

Figure 27. Effects of gradation for gravel materials having similar mean grain diameter.

$$F = \frac{\bar{V}}{\sqrt{gL}} \tag{50}$$

where g is the acceleration of gravity, L is the culvert characteristic length and $\bar{V}$ is the average fluid velocity measured at the culvert outlet. The hydraulic radius (R_H) was selected as a common denominator characteristic length and is defined as

$$R_H = \frac{A}{WP} \tag{51}$$

where A is the cross-sectional area of flow and WP is the wetted perimeter.

A series of analyses were performed using an equivalent depth parameter (Y_e). The equivalent depth is a characteristic length applicable to any shape culvert and is expressed as

$$Y_e = (A/2)^{1/2} \tag{52}$$

where A is the cross-sectional area of flow.

A comparison of the Froude number with the dimensionless scour hole parameters of d_{sm}/R_H, L_{sm}/R_H and V_{sm}/R_H^3 is presented in Figure 28. It is observed that the dimensions of scour are greater for circular shaped culverts than for square shaped culverts of similar characteristic lengths. The relationships illustrated are based on tests where Froude numbers varied from 2 to 6.5.

A comparison of the equivalent depth with the dimensionless scour hole parameters of d_{sm}/Y_e, L_{sm}/Y_e and V_{sm}/Y_e^3 is presented in Figure 29. It is again observed that the dimensions of scour are greater for circular shaped culverts than for square shaped culverts of similar characteristic lengths.

An analysis was performed evaluating which parameter, Froude number or equivalent depth, more closely predicted scour hole dimensions when culverts were flowing full. It is observed that the slopes of the equivalent depth curves are flatter than the curves using the hydraulic radius in the Froude number parameter. The slope differences between the parameters can be attributed to the spreading of data at discharge intensities of less than 1.0 in the equivalent depth parameter analysis. The resulting equations in the equivalent depth analysis yields a conservative estimate of scour hole dimensions at low discharge intensities (D.I. < 1.0) and tends to under estimate scour hole dimensions at higher discharge intensities (D.I. ≥ 1.5).

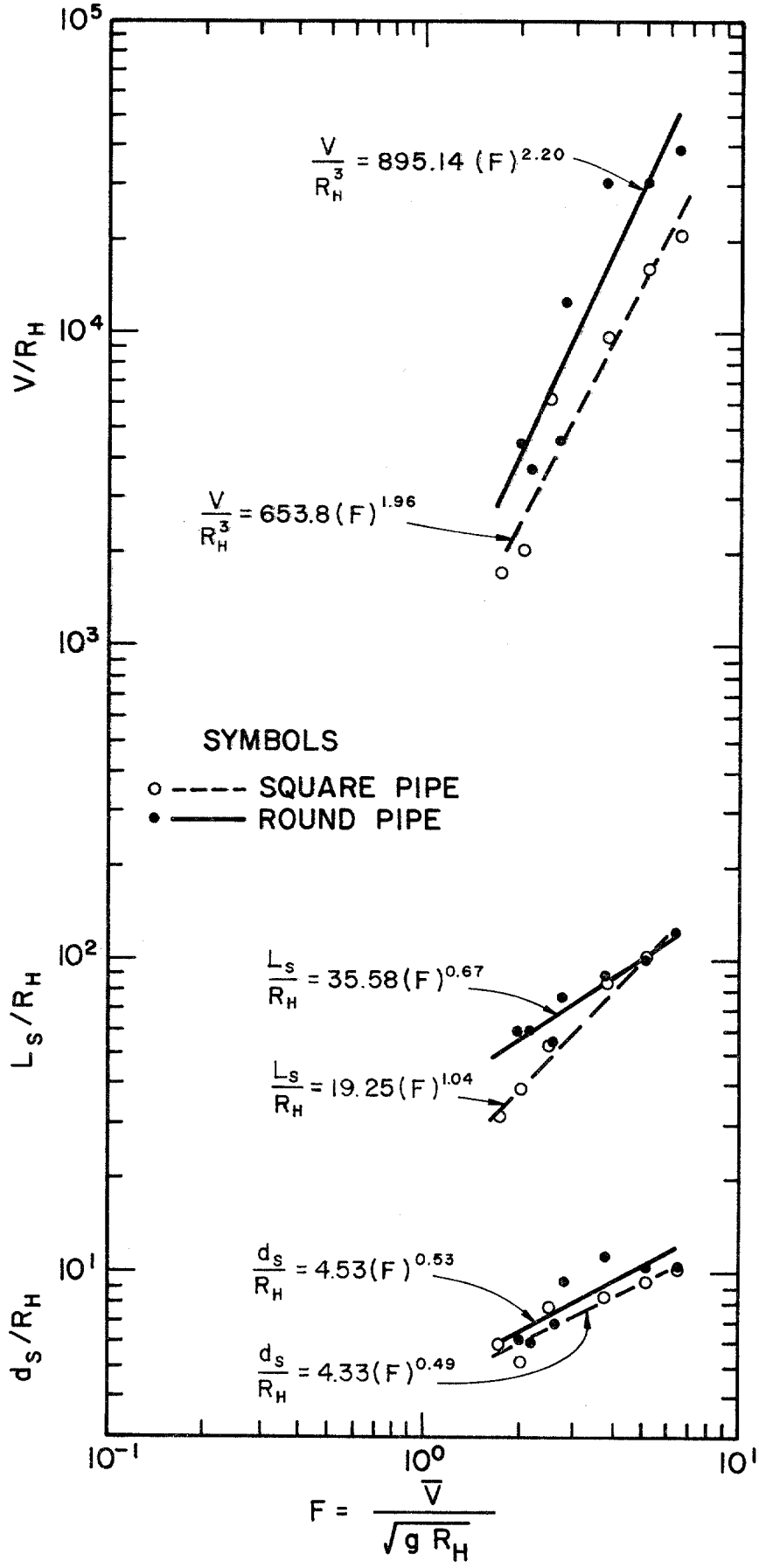

Figure 28. Froude number comparison of circular and square shaped culverts in uniform sand.

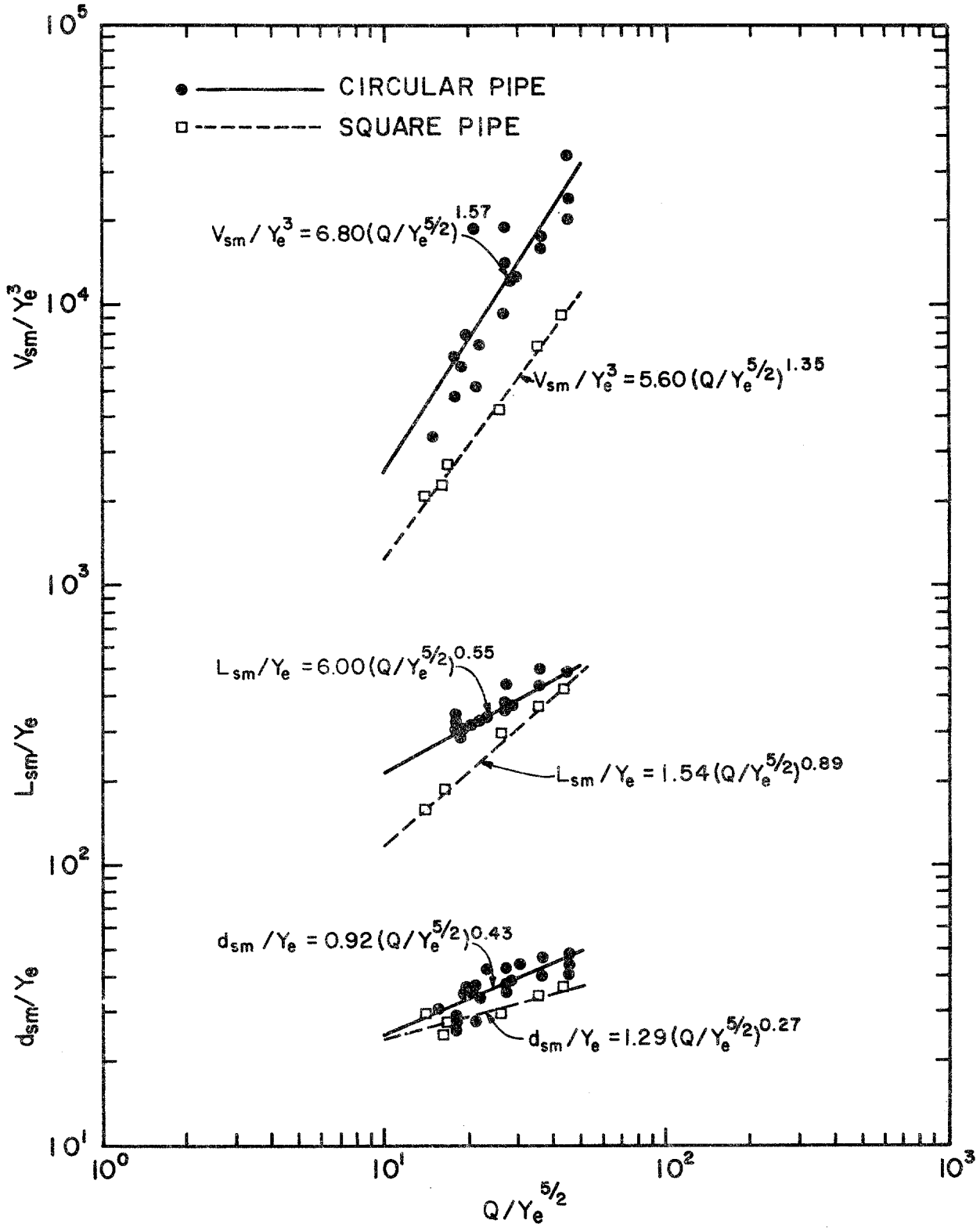

Figure 29. Equivalent depth comparison of circular and square shaped culverts in uniform sand.

It was observed that as the flow discharged from the square outlet, the jet dispersed and impacted over a wider area than the more concentrated jet from the circular culvert. Therefore, it is anticipated that rectangular culverts having width greater than height, the estimated depth of scour will be less than that predicted by circular and square shaped culverts at identical Froude numbers. In this case, the height dimension is used as the characteristic length.

These test results indicate that circular shaped culverts yield more conservative scour hole dimensions than do square shaped culverts of similar characteristic lengths. The Froude number analysis using the hydraulic radius and the equivalent depth analysis adequately predict scour hole dimensions at all Discharge Intensities.

Headwall Effects and Scour Profiles

A series of tests were performed placing a headwall adjacent to the culvert outlet in the uniform sand material. The scour hole dimensions were compared to tests performed under similar conditions without the headwall. The test results of both headwall and no headwall conditions are depicted in Figure 30.

Examination of the results indicates that little difference exists in the scour hole dimensions between the headwall and no headwall conditions.

Dimensionless profiles of the scour hole centerline are presented in Figure 31 and Figure 32 for headwall and no headwall conditions respectively. Superimposing Figure 31 and Figure 32 indicates that the scour hole depth and length are approximately the same with or without a headwall. The maximum depth of scour was observed to occur at a point between approximately $0.3\ L_{sm}$ and $0.43\ L_{sm}$ downstream of the culvert outlet where L_{sm} is the maximum length of scour. Furthermore, erosion directly under the culvert outlet was observed to be $0.4\ d_{sm}$ where d_{sm} is the maximum scour depth for the no headwall condition.

It is observed in Figure 31 that if a headwall is installed at the culvert outlet, scour can extend downward adjacent to the headwall to a depth equal to the maximum depth of scour. Therefore, the headwall should extend below the maximum expected depth of scour to prevent headwall from being undermined.

Dimensionless scour hole profiles for the gravel and cohesive sandy clay are presented in Figures 33 and 34 for the no headwall condition. The maximum depth of scour occurs at a distance ranging from $0.30\ L_{sm}$ to $0.45\ L_{sm}$ downstream from the culvert outlet where L_{sm} is the maximum length of scour. Little scour occurs directly under the culvert outlet, but the scour cavity sidewall slope is considerably steeper on the culvert side than it is on the opposite side where the water jet impacts.

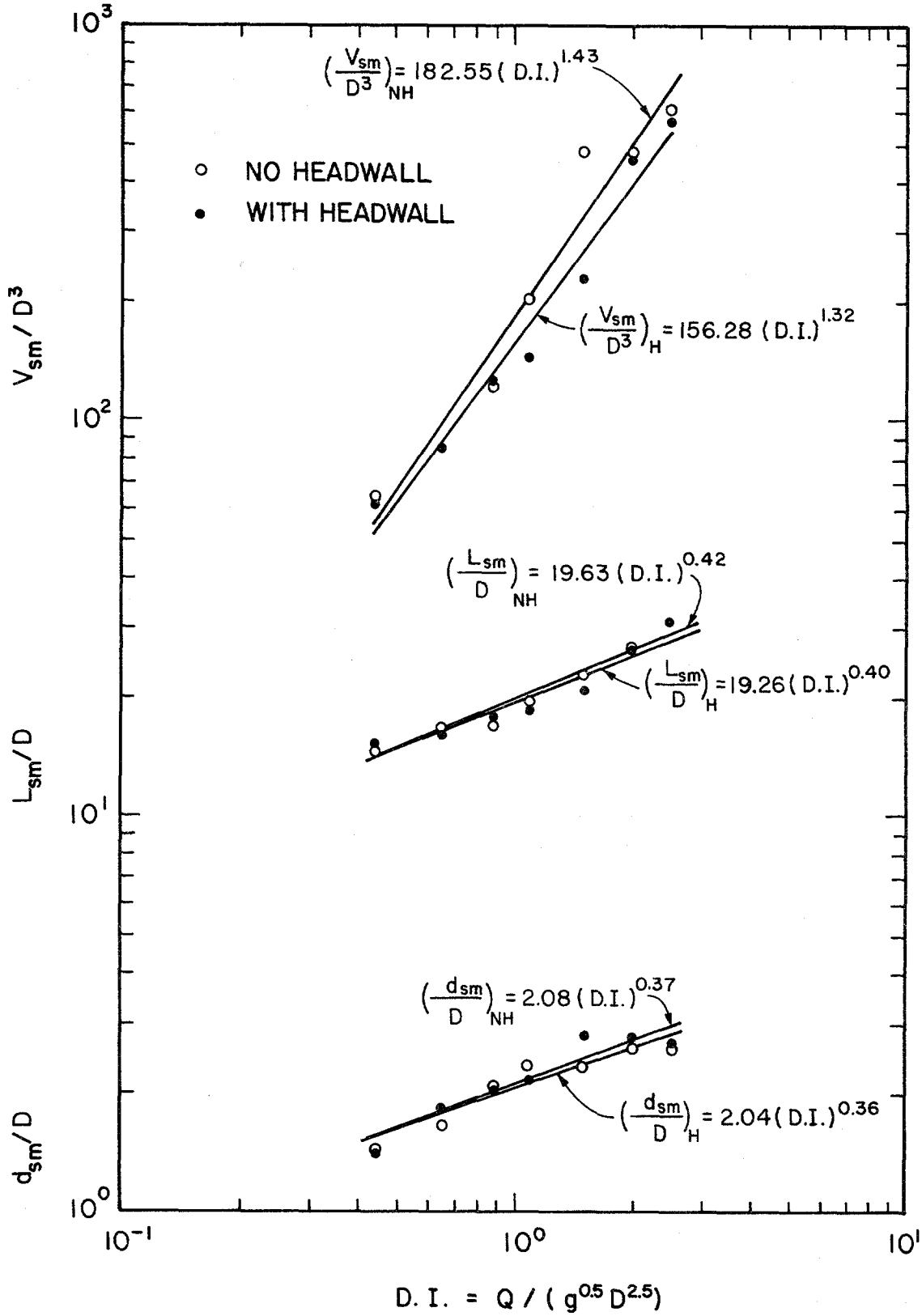

Figure 30. Comparison of headwall and no-headwall conditions in uniform sand.

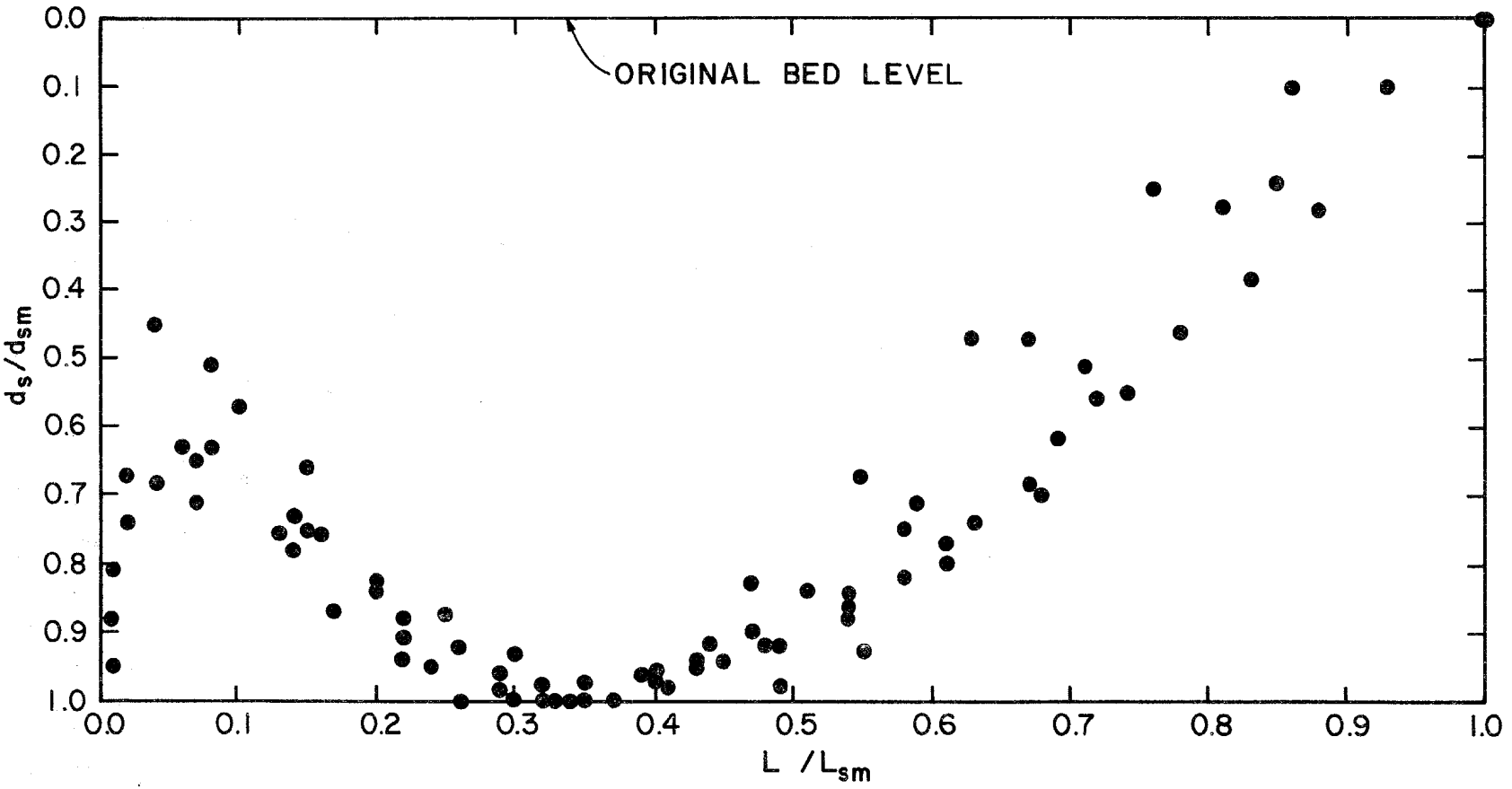

Figure 31. Centerline scour hole profile (headwall condition), uniform sand.

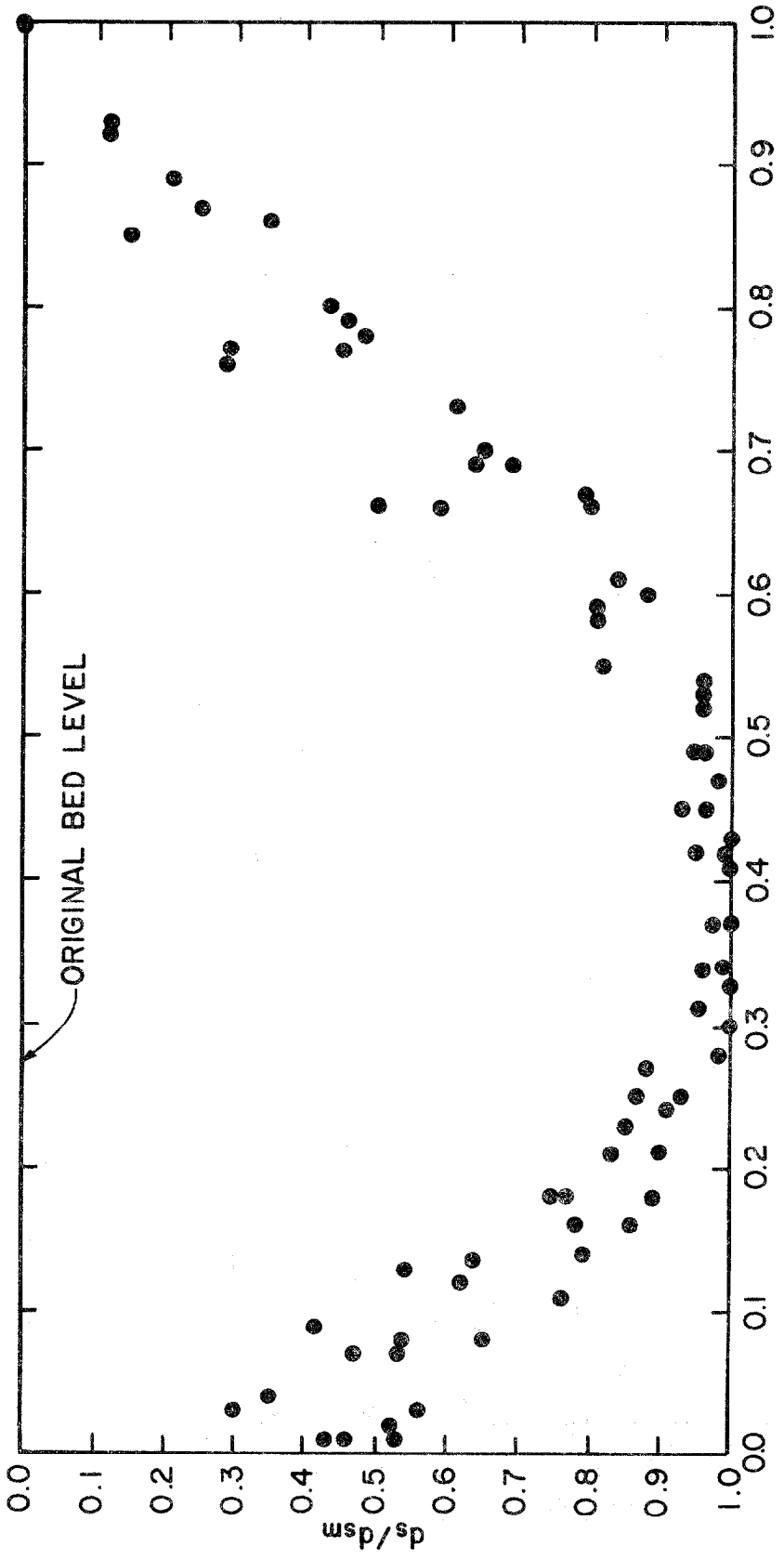

Figure 32. Centerline scour hole profile (no-headwall condition), uniform sand.

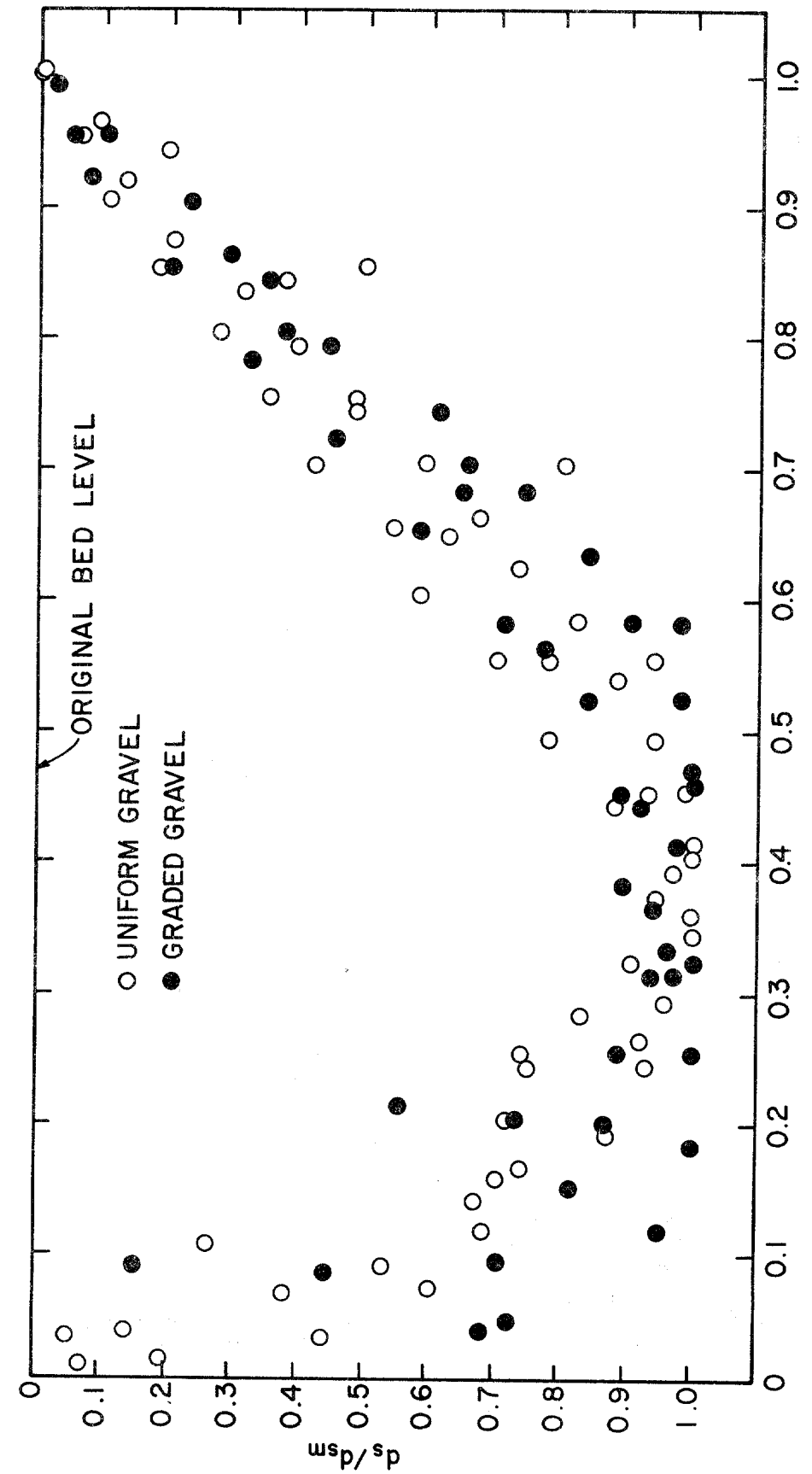

Figure 33. Dimensionless scour hole geometry in uniform and graded gravel, 316 minutes

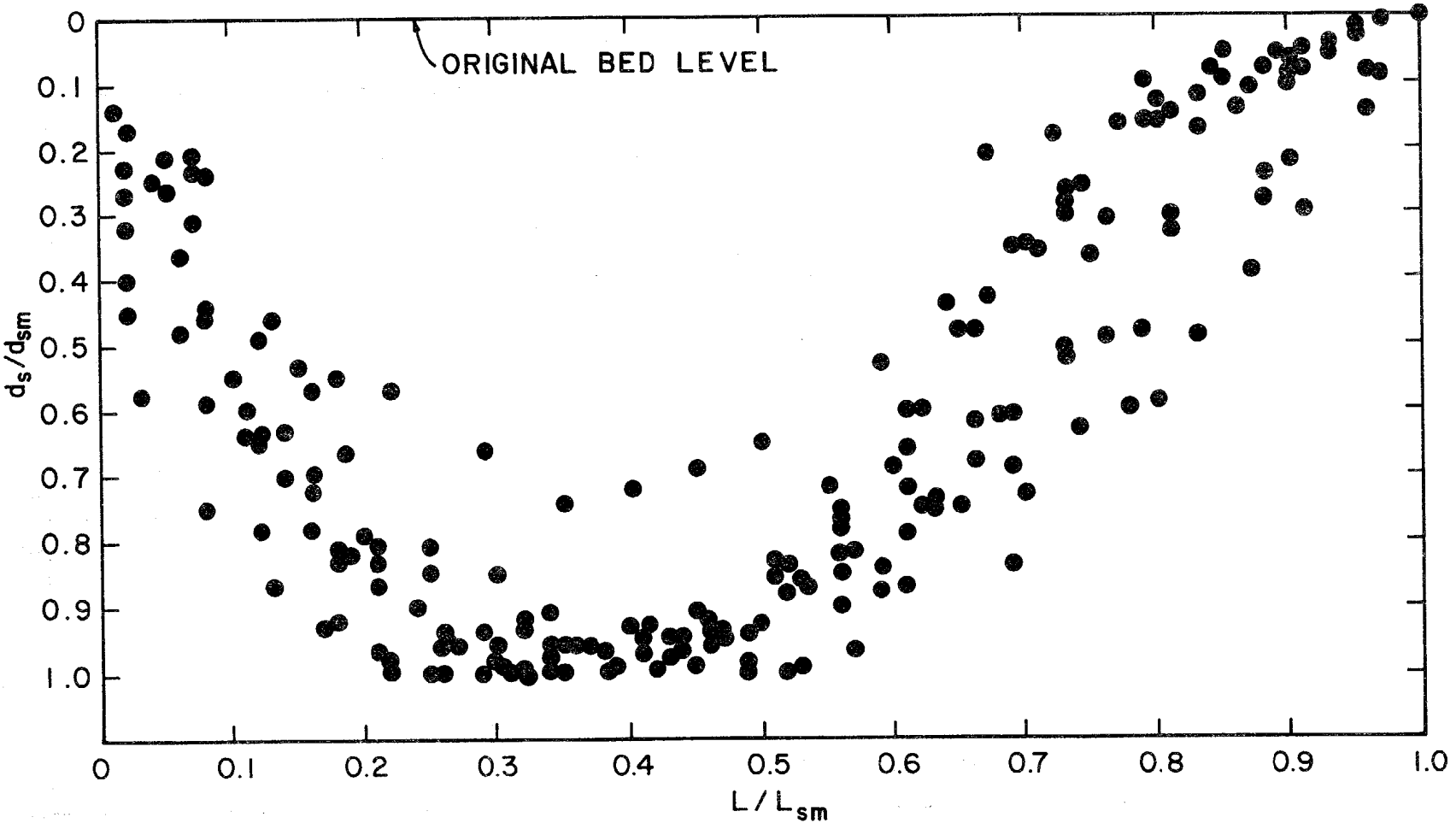

Figure 34. Scour hole dimensionless profile, cohesive bed material, 1000 minutes.

Scour Influence

It was found that the scour mechanism influences areas downstream of the scour hole through the deposition of scoured materials. The length of scour influence is defined as the length of scour hole (L_{sm}) plus the length of mound deposition (L_{mm}). The width of influence is the width of mound deposition. In order to identify the magnitude of material deposition of scour influence (SI), a series of tests were performed in uniform sand which documented the extent of mound movement. Figure 35 presents the relationship found between the Discharge Intensity and the maximum length and maximum width of scour influence expressed in culvert diameters.

An analysis indicates that the length of the mound is approximately the same length as the maximum length of scour hole for a culvert flowing full. The length of scour influence is twice the length of the scour hole measured downstream of the culvert outlet. It was observed that the width of scour influence ranges from two to three times the scour hole width for Discharge Intensities of 1.0 to 3.0. The scour influence relationships apply to culverts flowing full.

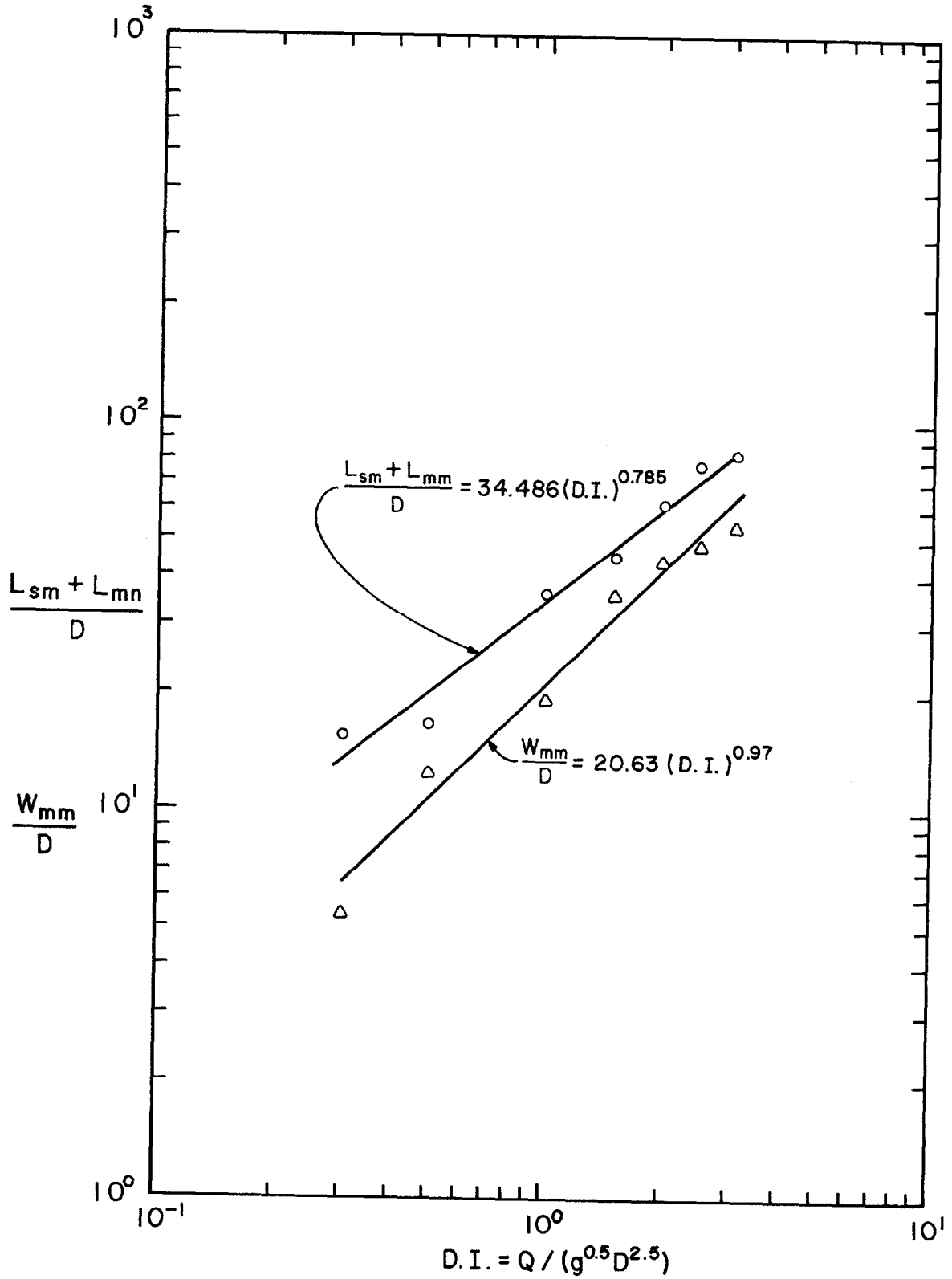

Figure 35. Influence of scour versus discharge intensity in uniform sand.

Chapter VI

CONCLUSIONS

Erosion at culvert outlets caused by disrupted flow is a major engineering problem in highway design. Severe erosion in the vicinity of culverts often results in the instability and failure of the embankment adjacent to the outlet. A method is needed to control and manage the scour phenomenon and thus prevent these damages. Selection of a control method requires an estimate of the extent of scour downstream of culvert outlets. Therefore, scour at culvert outlets in noncohesive and cohesive materials was investigated.

Scour holes produced by different discharges in varying materials were observed and contoured. Experimental results were analyzed and empirical equations and graphs were developed for estimating the maximum depth, length, width, volume and influence of scour.

Analysis of the experimental results led to the following conclusions:

Noncohesive Materials

1. Approximately 80% of the maximum depth, width and length of scour is attained in the initial 31 minutes of scour.

2. The depth, width, length and volume of scour were directly correlated to the Discharge Intensity. As the Discharge Intensity increased, the ultimate dimensions of scour increased.

3. The maximum scour depth was located approximately between 0.3 and 0.4 of the maximum scour length.

4. The headwall foundation should be placed below the predicted maximum scour depth. The headwall prevented undermining of the culvert barrel and protected the embankment.

5. The rate and magnitude of scour are the same for headwall and no headwall conditions.

6. It was observed that a circular culvert yields larger scour hole dimensions than a square shaped culvert when the circular culvert diameter is equivalent to the side of the square shaped culvert.

7. For materials having similar nominal mean grain sizes (d_{50}) but different standard deviations (σ), it was observed that as σ increased, the maximum scour hole dimensions decreased. The larger particles in the graded material appear to armor the scour hole.

8. The rate of increase of scour depth with time was approximately the same for uniform and graded soils materials having similar nominal mean grain diameters.

9. Mounds were formed downstream of the scour hole as a result of deposition of scoured materials. Mounds were generally fan shaped, flat and were approximately 0.6 TW to 0.8 TW in height where TW is the tailwater depth.

10. The area influenced by the scour process was directly related to the Discharge Intensity. It was found that the length of impacted area was approximately twice the length of scour hole while the width of impacted area was approximately 2-3 times the width of scour hole for culverts flowing full.

11. It was observed that when Discharge Intensities exceeded 1.0, undermining of the culvert became significant for culverts cantilevered.

12. Scour hole dimensions for tests conducted at tailwater depths of 0.0 D and 0.25 D were about 10 percent greater than those observed at a tailwater depth of 0.45 D. Differences of this magnitude were not considered to be significant.

13. All scour holes were observed to be similar in geometric configuration and appearance independent of the material or culvert diameter.

14. Scour hole relationships can be predicted based on relationships using the Discharge Intensity, Froude number or equivalent depth.

15. The Discharge Intensity relationships yield a conservative estimate of scour hole dimensions for partially filled culverts (D.I. < 1.0).

Cohesive Material

1. The results indicated that the soil parameters of saturated shear strength and plasticity indices, fluid parameters of density and velocity and time could be correlated to predict the depth, width, length and volume of a scour hole in an SC cohesive material.

2. The scour hole dimensions were directly related to the Discharge Intensity for an SC cohesive soil. The Discharge Intensity relationships yield a conservative estimate of scour hole dimensions for partially filled culverts (D.I. < 1.0).

3. All scour holes were observed to be similar in geometric configuration and appearance independent of culvert diameter and discharge.

4. It was observed that 70% of the maximum depth, length and width of scour occurs during the initial 31 minutes of discharge.

5. The location of the maximum depth of scour occurs at approximately 0.35 times the maximum length of scour measured downstream of the culvert outlet.

6. The mounds which formed downstream of the scour hole were generally flat and less than 0.25 D in height.

REFERENCES

1. Abdel-Rahmann, N. M., "The Effects of Flowing Water on Cohesive Beds," Contribution No. 56, Versuchsanstalt fur Wasserbau and Erdbau an der Eidgenossische, Technischen Hochschule, Zurich, Switzerland, pp. 1-114, 1964.

2. Ruff, J. F. and Abt, S. R., "Scour at Culvert Outlets in Cohesive Bed Material," Colorado State University, Civil Engineering Department, CER79-80JFR-SRA61, 1980.

3. Agricultural Research Service, "A Universal Equation for Predicting Rainfall-Erosion Losses," ARS 22-66, 1961.

4. Albertson, M. L., Barton, J. R. and Simons, D. B., "Fluid Mechanics for Engineers," Prentice Hall, Inc., 1960.

5. American Society of Civil Engineers Task Committee, "Erosion of Cohesive Sediments," Journal of the Hydraulics Division, American Society of Civil Engineers, Vol. 94, No. HY-4, July 1968.

6. American Society of Civil Engineers, "Sedimentation Engineering," Manual No. 54, 1975.

7. Anderson, H. W., "Physical Characteristics of Soil Related to Erosion," Journal of Soil and Water Conservation, July 1951.

8. Ariathurai, R. and Arulanadan, K., "Erosion Rates of Cohesive Soils," Journal of Hydraulics Division, American Society of Civil Engineers, Vol. 104, No. HY2, February 1978.

9. Arulanandan, K., Loganathan, P. and Knone, R. B., "Pore and Eroding Fluid Influence on Surface Erosion of Soil," Journal of Geotechnical Division, American Society of Civil Engineers, Vol. 101, No. GT1, January 1975.

10. Bayazit, M., "Scour of Bed Materials in very Rough Channels," Journal of Hydraulics Division, American Society of Civil Engineers, Vol. 104, No. HY9, September 1978.

11. Bilaschevsky, N. N., "The Mechanism of the Local Scour behind the Spillway Structures with the Apron and the Influence of Macroturbulence upon the Scour," Proceedings of the 12th Congress of the IAHR, Vol. 3, Colorado State University, Fort Collins, Colorado, 1967.

12. Blaisdell, F. W., Anderson, C. L. and Hebaus, G. G., "Ultimate Dimensions of Local Scour," Journal of the Hydraulics Division, American Society of Civil Engineers, Vol. 107, No. HY3, March 1981.

13. Bohan, J. P., "Erosion and Riprap Requirements at Culvert and Storm-drain Outlets," U.S. Army Engineer Waterways Experiment Station, Vicksburg, Mississippi, 1970.

14. Carstens, M. R., "Similarity Laws for Localized Scour," Journal of the Hydraulics Division, American Society of Civil Engineering, May 1966.

15. Chaug, F. M. and Yevjevich, V. H., "Analytical Study of Local Scour," Colorado State University, Civil Engineering Department, CER62FMC26, 1962.

16. Chen, Y. H., "Scour at Outlets of Box Culverts," Master's Thesis, Colorado State University, Fort Collins, Colorado, September, 1970.

17. Chow, V. T., "Open Channel Hydraulics," McGraw-Hill Book Company, 1959.

18. Christensen, R. W. and Das, B. M., "Hydraulic Erosion of Remolded Cohesive Soils," Highway Research Board Special Report, No. 135, 1973.

19. Clyde, G. G., Israelsen, C. E., Packer, P. E., Farmer, E. E., Fletcher, J. E., Israalsen, E. K., Haws, F. W., Rao, N. V. and Hansen, J., "Manual of Erosion Control Principles and Practices," Hydraulics and Hydrology Series Report H-78-002, Utah Water Research Laboratory, June 1978.

20. Colorado Department of Highway, "Erosion Control Manual," October, 1978.

21. Cunha, L. V., "Time Evolution of Local Scour," Proceedings of the 12th Congress of IAHR, Vol. 2, Sao Paulo, Brazil, 1975.

22. Doddiah, D., "Comparison of Scour caused by Hollow and Solid Jets of Water," Master's Thesis, Colorado A and M College, 1950.

23. Dunn, I. S., "Tractive Resistance of Cohesive Channels," Journal of the Soil Mechanics and Foundations, Vol. 85, No. SM5, June 1959.

24. Ettema, R., "Influence of Bed Material Gradation on Local Scour," University of Auckland, Report No. 124, 1973.

25. Field, W. G., "Effects of Density Ratio on Sedimentary Similitude," Journal of the Hydraulics Division, American Society of Civil Engineers, May 1968.

26. Flaxman, E. M., "Channel Stability in Undisturbed Cohesive Soils," Journal of Hydraulic Division, American Society of Civil Engineers, Vol. 89, No. HY6, pp. 87-96, March 1963.

27. Fletcher, B. P. and Grace, J. L., "Practical Guidance for Estimating and Controlling Erosion at Culvert Outlets," U.S. Army Waterways Experiment Station, Vicksburg, Mississippi, 1972.

28. Goncharov, V. M., "Dynamics of Channel Flow," Israel Program for Scientific Translation, Jerusalem, 1964.

29. Grass, A. J., "Initial Instability of Fine Bed Sand," Journal of the Hydraulics Division, American Society of Civil Engineers, Vol. 76, No. HY3, 1970.

30. Gray, D. M., "Handbook on the Principles of Hydrology," Water Information Center, Inc., Port Washington, N. W., reprinted 1973.

31. Grissinger, E. H., Asmussen, L. E. and Espey, W. V., "Channel Stability in Undisturbed Cohesive Soils," Journal of Hydraulic Division, American Society of Civil Engineers, November 1963.

32. Grissinger, E. H., "Ristance of Selected Clay Systems to Erosion by Water," Water Resources Research, 1st Quarter, Vol. 2, No. 1, 1966.

33. Hallmark, D. W., "Influence of Particle Size Gradation on Scour at Base of Free Overfall," M.S. Thesis, Colorado A and M College, Fort Collins, Colorado, 1955.

34. Hjorth, P., "Studies on the Nature of Local Scour," Bulletin Series A, No. 46, Department of Water Resources Engineering, Lund Institute of Technology.

35. Howard, A. D., "Effect of Slope on the Threshold of Motion and its Application to Orientation of Wind Ripples," Geological Society of America Bulletin, Vol. 88, June 1977.

36. Iwagaki, Y., Smith, G. L. and Albertson, M. L., "Analytical Study of the Mechanic of Scour for Three-Dimensional Jet," Colorado State University, Civil Engineering, CER60-GLS-9, 1959.

37. Izzard, D. F., "Flow in Culverts and Related Design Philosophies," Journal of the Hydraulics Division, American Society of Civil Engineers, Vol. , No. HY3, May 1967.

38. Jacks, W., "Scour at Culvert Outlets," Presentation at Dallas-Fort Worth Workshop on Hydraulics, 1976.

39. Keeley, J. W., "Soil Erosion in Oklahoma, Part III, Culvert Outlet Conditions and Downstream Channel Stability," Federal Highway Administration, Oklahoma Division, Oklahoma City, Oklahoma, 1963.

40. Kellechals, R. and Church, M., "Stability of Channel Beds by Armoring," Journal of the Hydraulics Division, American Society of Civil Engineers, HY9, July 1977.

41. Kuti, E. O. and Yen, C. L., "Scouring of Cohesive Soils," Journal of the Hydraulics Research, Vol. 14, No. 3, 1976.

42. Lambe, T. W. and Whitman, R. V., "Soil Mechanics," John Wiley and Son, Inc., 1969.

43. Laursen, E. M., "Observations on the Nature of Scour," Proceedings of the Fifth Hydraulic Conference, June 9-11, 1952.

44. Laushley, L. M., Kappus, V., and Otwona, M. P., "Magnitude and rate of Erosion at Culvert Outlets," Proceedings of the 12th Congress of the IAHR, Vol. 3, Fort Collins, Colorado, 1967.

45. Le Feuvre, A. R., "Sediment Transport Functions with Special Emphasis on Localized Scour," Ph.D. Dissertation, Georgia Institute of Technology, Atlanta, Georgia, 1965.

46. Liou, Y., "Effects of Chemical Additives on Hydraulic Erodibility of Cohesive Soil," M.S. Thesis, Colorado State University, August 1967.

47. Liou, Y., "Hydraulic Erodibility of Two Pure Clay Systems," Ph.D. Dissertation, Colorado State University, August 1970.

48. Little, W. C. and Mayer, P. G., "Stability of Channel Beds by Armoring," Journal of Hydraulic Division, American Society of Civil Engineers, Vol. 102, No. HY11, November 1976.

49. Louisiana Department of Highways, "... Scour Predictive Methodology...," Working Papers, 1976.

50. Lyle, W. M. and Smerdon, E. T., "Relation of Compaction and other Soil Properties to Erosion Resistance of Soils," Transactions of the American Society of Agricultural Engineers, Vol. 8, No. 3, 1965.

51. Martin, T. R., discussion of, "Experiments on the Scour Resistance of Cohesive Sediments," Journal of Geophysical Research, Vol. 67, No. 4, pp. 1447-49, Washington, D.C., April 1962.

52. Mendoza, C. and Ruff, J. R., "Headwall Influence on Scour at Culvert Outlets," Colorado State University, Civil Engineering Department, CER79-80JFR-CM63, 1980.

53. Middleton, H. E., "Properties of Soils which influence Soil Erosion," U.S. Department of Agriculture Technical Bulletin No. 178, pp. 16, 1930.

54. Middleton, H. E., Slater, C. S. and Byers, H. G., "Physical and Chemical Characteristics of the Soils from the Erosion Experiment Station," U.S. Department of Agriculture Technical Bulletin No. 316, pp. 51, 1932.

55. Middleton, H. E., Slater, D. S. and Byers, H. G., "The Physical and Chemical Characteristics of the Soils from the Erosion Experiment Stations - Second Report," U.S. Department of Agriculture Technical Bulletin No. 430, pp. 62, 1934.

56. Mirtskhulava, Ts, E., "Mechanism and Computation of Local and General Scour in Noncohesive Soils and Rock Bed."

57. Mirtskhulava, Ts, E., "Erosional Stability of Cohesive Soils," Journal of the Hydraulic Research, No. 1, 1966.

58. Moore, W. L. and Masch, F. D., "Experiments on the Scour of Cohesive Sediments," Journal of Geophysical Research, Vol. 67, No. 4, April 1962.

59. Murray, W. A., "Erodibility of Coarse Sand-Clayey Silt Mixtures," Journal of the Hydraulics Division, American Society of Civil Engineers, Vol. 103, No. HY10, October 1977.

60. Musgrave, G. W., "The Quantitative Evaluation of Factors in Water Erosion," Journal of Soil and Water Conservation, Vol. 2, pp. 133-138, July 1947.

61. Opie, T. R., "Scour at Culvert Outlets," M.S. Thesis, Colorado State University, Fort Collins, Colorado, December 1967.

62. Paaswell, R. E., "Causes and Mechanisms of Cohesive Soil Erosion," Highway Research Board Special Report 135, pp. 52-74, 1973.

63. Partheniades, E., "Erosion and Deposition of Cohesive Soils," Journal of Hydraulics Division, American Society of Civil Engineers, Vol. 91, No. HY1, January 1965.

64. Peele, T. C., "The Relation of Certain Physical Characteristics to the Erodibility of Soils," Soil Science Society of America, Vol. II, November 30-December 4, 1937.

65. Prins, J. E., "Phenomena Related to Turbulent Flow in Water Control Structures," Delft Hydraulics Laboratory, Publication No. 76, III, Delft, The Netherlands, 1971.

66. Raudkivi, A. J. and Ettema, R., "Effects of Sediment Gradation on Clear Water Scour," Journal of Hydraulics Division, American Society of Civil Engineers, Vol. 103, No. HY10, October 1977.

67. Robinson, A. R., "Model Study of Scour from Cantilevered Outlets," Transactions of the American Society of Agricultural Engineers, 1971.

68. Romkens, M. J. M., Nelson, D. W. and Roth, C. B., "Soil Erosion on Selected High Clay Subsoils," Journal of Soil and Water Conservation, Vol. 30, No. 4, July-August 1975.

69. Rouse, H., "Experiments on the Mechanics of Sediment Suspension," Proceedings, Fifth International Congress for Applied Mechanics, Vol. 55, John Wiley and Sons, Inc., New York, NY, 1938.

70. Rouse, H., "Criteria for Similarity in the Transportation of Sediment," Proceedings of 1st Hydraulic Conference, Bulletin 20, State University of Iowa, Iowa City, Iowa, pp. 33-49, March 1940.

71. Sargunam, A., Riley, P. and Arulanandan, F., "Physio-Chemical Factors in Erosion of Cohesive Soils," Journal of the Hydraulics Division, American Society of Civil Engineers, Vol. 99, HY3, March 1973.

72. Scheer, A. C., "Large Culvert Studies in Montana," Department of Civil Engineering and Engineering Mechanics, Montana State University, Missoula, Montana, 1968.

73. Schneider, V. R., "Mechanics of Local Scour," Ph.D. Dissertation, Colorado State University, Fort Collins, Colorado, December 1968.

74. Seed, H. B. and Chan, C. K., "Structure and Strength Characteristics of Compacted Clays," Journal of Soil and Mechanics and Foundation Division, American Society of Civil Engineers, Vol. 85, No. SM5, October 1959.

75. Sargent, Hauskins and Beckwith, "Stability and Integrity Assessment," Church Rock Tailings Dam, Church Rock, New Mexico, Vol. 3, pp. 35-36, August 1979.

76. Shaikh, A. and Ruff, J. F., "Scour in Uniform and Graded Gravel at Culvert Outlets," Colorado State University, Civil Engineering Department, CER80-81AS-JR7, 1980.

77. Shields, A., "Application of Similarity Principles and Turbulence Research to Bed-load Movement, Berlin, 1936.

78. Simons, D. B., Li, R. M. and Ward, T. J., "A Simple Procedure for Estimating On-site Soil Erosion," Proceedings of International Symposium on Urban Hydrology, Hydraulics and Sediment Control, University of Kentucky, Lexington, Kentucky, July 18-21, 1977.

79. Simons, D. B., Li, R. M. and Ward, T. J., "Equation and Computer Program that Develop Design Tables for Estimating Road Sediment Yield," prepared for USDA, Forest Service, Flagstaff, Arizona, 1978.

80. Simons, D. B. and Sentürk, F., "Sediment Transport Technology," Water Resources Publications, Fort Collins, Colorado, 1976.

81. Smerdon, E. T. and Beasley, R. P., "Critical Tractive Forces in Cohesive Soils," Agricultural Engineering, January 1961.

82. Smith, G. L., "An Analysis of Scour below Culvert Outlets," M.S. Thesis, Colorado A and M College, Fort Collins, Colorado, 1957.

83. Smith, G. L., "Scour and Energy Dissipation below Culvert Outlets," Colorado A and M College, Fort Collins, Colorado, CER57-GLS-16, April 1957.

84. Smith, G. L. and Hallmark, D. E., "New Development for Erosion Control at Culvert Outlets," Working Papers, Colorado State University, 1959.

85. Soil Conservation Service, "Preliminary Guidance for Estimating Erosion on Area Disturbed by Surface Mining Activities in the Interior Western United States," Interim Final Report, EPA-908/4-77-055, July 1977.

86. Stevens, M. A., "Scour in Riprap at Culvert Outlets," Ph.D. Dissertation, Colorado State University, Fort Collins, Colorado, January 1969.

87. Sundorg, A., "The River Klaraluen, A Study of Fluvial Processes," Geoprafiska Annaler, pp. 127-133, 1956.

88. Thomas, R. K., "Scour in a Gravel Bed at the Base of a Free Overfall," M.S. Thesis, Colorado A and M College, Fort Collins, Colorado, May 1953.

89. Tsuchiya, Y. and Iwazaki, Yl, "On the Mechanism of the Local Scour from Flows Downstream of an Outlet," Proceedings of the 12th Congress of the IAHR, Vol. 3, Colorado State University, Fort Collins, Colorado, 1967.

90. U.S. Department of Agriculture, "Prevention and Control of Gullies," Farmers Bulletin No. 1313, September 1939.

91. U.S. Department of Transportation, "Hydraulic Design of Energy Dissipators for Culverts and Channels," Hydraulic Engineering, Circular No. 14, SN 050-002-00102-F, December 1975.

92. Valentin, F., "Considerations Concerning Scour in the Case of Flow Under Gates," Proceedings of the 12th Congress of the IAHR, Vol. 3, Colorado State University, Fort Collins, Colorado, 1967.

93. Varga, L. and Lanshey, L. H., "Application of the Wall Jet Theory to Erosion at the Outlet of Hydraulics Structures," Proceedings of the 12th Congress of the IAHR, Vol. 3, Colorado State University, Fort Collins, Colorado, 1967.

94. Vinje, J. J., "On the Flow Characteristics of Vortices in Three-dimensional Local Scour," Delft Hydraulics Laboratory, Publication No. 48, Delft, 1969.

95. White, C. M., "The Equilibrium of Grains on the Bed of a Stream," Royal Society, Proceedings A174, 1940.

96. Wischmeier, W. H. and Smith, D. D., "Rainfall Erosion Losses from Crop Land East of the Rocky Mountains," Agriculture Handbook No. 282, Reprinted December 1972.

97. Wischmeier, W. H. and Mannering, J. V., "Relation of Soil Properties to its Erodibility," Soil Science Society of America Proceedings, Vol. 33, No. 1, January-February, 1968.

98. Wischmeier, W. H., Johnson, C. B. and Cross, B. V., "A Soil Erodibility Nomograph for Farmland and Construction Sites," Journal of Soil and Water Conservation, Vol. 26, No. 5, September-October, 1971.

99. Wischmeier, W. H. and Meyer, L. D., "Soil Erodibility on Construction Acres," Proceedings Highway Research Board Soil Erosion Workshop, January 1973.

100. Wyoming State Highway Department, "Culvert Outlet Protection Design," Report No. FHWA-RD-74-501, January 1974.

101. Yalin, M. S., "Theory of Hydraulics Models," Macmillan, London, 1941.

APPENDIX I

SUMMARY OF DATA

Appendix I. Summary of Data

Soil	Model	Dia. (ft)	Part Full A Flow (sq-ft)	Part Full V (fps)	Time of Scour (min)	D.I.	Q (cfs)	D_s (ft)	W_s (ft)	L_s (ft)	V_s (cu-ft)
Uniform Sand	4' W/O	.33	.038	4.16	14	0.44	0.16	0.39		2.40	0.67
	Headwall	.33	.054	4.41		0.65	0.24	0.42		2.65	0.85
d_{50}=1.86		.33	.075	4.22		0.87	0.32	0.32		3.00	1.21
						1.09	0.40	0.47		2.80	1.25
σ = 1.33	TW/D=.45					1.50	0.55	0.51		3.70	1.92
						2.00	0.73	0.56		4.30	3.39
						2.50	0.91	0.66		5.30	6.25
		.33	.038	4.16	141	0.44	0.16	0.42		4.50	1.93
		.33	.054	4.41		0.65	0.24	0.46		5.00	1.80
		.33	.075	4.22		0.87	0.32	0.59		4.20	2.31
						1.09	0.40	0.63		4.00	3.13
						1.50	0.55	0.73		5.20	5.01
						2.00	0.73	0.76		6.30	8.20
						2.50	0.91	0.84		7.20	12.15
		.33	.038	4.16	1000	0.44	0.16	0.50	2.73	4.9	2.41
		.33	.054	4.41		0.65	0.24	0.58	2.74	5.7	3.16
		.33	.075	4.22		0.87	0.32	0.70	2.90	5.6	4.54
						1.09	0.40	0.79	3.62	6.5	7.33
						1.50	0.55	0.93	4.66	7.6	17.75
						2.00	0.73	0.87	4.61	8.6	17.65
						2.50	0.91	0.89	5.27	10.9	22.45

Summary of Data (continued)

Soil	Model	Dia. Ft.	Part Full A Flow (sq-ft)	Part Full V (fps)	Time of Scour (min)	D.I.	Q (cfs)	d_s (ft)	W_s (ft)	L_s (ft)	V_s (cu-ft)
Uniform Sand	4' W/	.33	.038	4.16	14	0.44	0.16	0.37		2.40	0.59
	Headwall	.33	.054	4.41		0.65	0.24	0.37		2.70	0.59
d_{50}=1.86		.33	.075	4.22		0.87	0.32	0.44		3.00	1.18
						1.09	0.40	0.44		3.10	1.12
σ = 1.33	TW/D=.45					1.50	0.55	0.50		3.65	2.05
						2.00	0.73	0.52		4.50	3.88
						2.50	0.91	0.62		5.50	5.71
		.33	.038	4.16	141	0.44	0.16	0.43		4.30	1.35
		.33	.054	4.41		0.65	0.24	0.53		3.70	1.50
		.33	.075	4.22		0.87	0.32	0.56		4.70	2.47
						1.09	0.40	0.54		4.50	2.50
						1.50	0.55	0.68		5.10	4.40
						2.00	0.73	0.78		6.30	8.53
						2.50	0.91	0.80		7.30	12.35
		.33	.038	4.16	1000	0.44	0.16	0.47	2.75	5.0	2.31
		.33	.054	4.41		0.65	0.24	0.61	3.50	5.4	3.18
		.33	.075	4.22		0.87	0.32	0.68	3.25	5.9	4.68
						1.09	0.40	0.71	3.45	6.2	5.29
						1.50	0.55	0.78	3.90	6.9	8.50
						2.00	0.73	0.92	4.00	8.5	16.68
						2.50	0.91	0.88	4.00	10.3	21.61

Summary of Data (continued)

Soil	Model	Dia. (ft)	Part Full A Flow (sq-ft)	Part Full V (fps)	Time of Scour (min)	D.I.	Q (cfs)	d_s (ft)	W_s (ft)	L_s (ft)	V_s (cu-ft)
Uniform Sand	4'				14	2.48	0.45	0.41	3.7	3.6	0.70
						3.82	0.69	0.46	3.7	4.3	1.68
	4"x4"					5.11	0.93	0.59	3.7	5.8	3.34
d_{50}=1.86	Square					6.37	1.16	0.67	3.7	6.3	5.92
	pipe	.33	.080	3.15		1.76	0.25	0.48	2.0	2.6	0.85
σ = 1.33		.33	.091	3.77		2.06	0.35	0.41	3.7	3.6	0.70
	TW/D=.45										
					141	2.48	0.45	0.53	3.7	4.0	2.16
						3.82	0.69	0.66	3.7	6.1	4.42
						5.11	0.93	0.75	3.7	7.3	7.68
						6.37	1.16	0.82	3.7	7.7	10.99
		.33	.080	3.15		1.76	0.25	0.59	2.7	3.0	1.31
		.33	.091	3.77		2.06	0.35	0.51	3.7	4.0	1.80
					316	2.48	0.45	0.65	3.7	4.5	3.53
						3.82	0.69	0.69	3.7	7.2	5.66
						5.11	0.93	0.80	3.7	8.7	9.32
						6.37	1.16	0.88	3.7	10.2	12.05
		.33	.080	3.15		1.76	0.25	0.59	3.7	3.2	1.69
		.33	.091	3.77		2.06	0.35	0.54	3.7	4.1	2.28

Summary of Data (continued)

Soil	Model	Dia. (ft)	Part Full A Flow (sq-ft)	Part Full V (fps)	Time of Scour (min)	D.I.	Q (cfs)	d_s (ft)	W_s (ft)	L_s (ft)	V_s (cu-ft)
Uniform Sand	20'	.33	.030	3.67	14	0.3	0.11	0.22	1.20	2.40	0.17
		.33	.044	4.09		0.5	0.18	0.16	1.04	3.20	0.15
	TW/D=.45					1.0	0.36	0.61	2.46	3.76	1.86
d_{50}=1.86						1.5	0.55	1.09	4.08	8.00	10.456
						2.0	0.73	0.82	3.37	7.50	6.25
σ = 1.33						2.5	0.91	0.76	2.80	9.00	4.961
						3.13	1.14	0.96	8.89	13.69	20.53
		.33	.030	3.67	141	0.3	0.11	0.28	1.43	3.70	0.49
		.33	.044	4.09		0.5	0.18	0.55	2.14	3.30	1.19
						1.0	0.36	0.79	3.57	4.37	3.00
						1.5	0.55	1.03	3.09	5.87	4.026
						2.0	0.73	1.15	4.08	10.83	10.37
						2.5	0.91	1.08	6.10	15.00	24.247
						3.13	1.14	1.09	8.34	14.06	27.94
		.33	.030	3.67	316	0.3	0.11	0.36	1.60	3.90	0.63
		.33	.044	4.09		0.5	0.18	0.56	2.58	3.10	1.16
						1.0	0.36	0.88	3.96	3.90	5.90
						1.5	0.55	1.11	5.04	8.50	12.30
						2.0	0.73	1.13	6.56	11.20	15.20
						2.5	0.91	1.01	6.50	16.00	28.60
						3.13	1.14	1.12	9.14	15.00	29.10

Summary of Data (continued)

Soil	Model	Dia. (ft)	Part Full A Flow (sq-ft)	Part Full V (fps)	Time of Scour (min)	D.I.	Q (cfs)	d_s (ft)	W_s (ft)	L_s (ft)	V_s (cu-ft)
Uniform Sand	20'	.85	0.15	7.67	31	0.3	1.15	.96	4.28	5.50	8.29
d_{50}=1.86		.85	0.29	6.58		0.5	1.91	1.50	7.10	8.06	24.26
						1.5	5.74	1.75	12.50	13.56	100.35
σ = 1.33	TW/D=0					2.0	7.65	1.86	15.00	16.68	131.41
		.85	0.15	7.67	100	0.3	1.15	1.10	6.00	6.68	11.46
		.85	0.29	6.58		0.5	1.91	1.58	8.63	9.68	78.58
						1.5	5.74	1.93	12.50	15.68	156.10
						2.0	7.65	2.18	20.00	19.15	178.97
		.85	0.15	7.67	316	0.3	1.15	1.10	5.13	7.43	14.18
		.85	0.29	6.58		0.5	1.91	1.49	9.40	10.32	45.39
						1.5	5.74	2.19	10.59	18.48	161.94
						2.0	7.65	2.55	11.53	22.77	259.09

Summary of Data (continued)

Soil	Model	Dia. Ft.	Part Full A Flow (sq-ft)	Part Full V (fps)	Time of Scour (min)	D.I.	Q (cfs)	d_s (ft)	W_s (ft)	L_s (ft)	V_s (cu-ft)
Uniform Sand	20'	.85	0.15	7.67	31	0.3	1.15	1.28	5.47	6.43	13.66
d_{50}=1.86	TW/D=.25	.85	0.29	6.58		0.5	1.91	1.49	7.35	7.28	27.12
						1.5	5.74	1.93	14.64	14.46	137.35
σ = 1.33						2.0	7.65	2.25	17.56	19.15	197.95
		.85	0.15	7.67	100	0.3	1.15	1.35	7.27	6.65	20.18
		.85	0.29	6.58		0.5	1.91	1.64	9.79	10.16	34.57
						1.5	5.74	2.22	14.64	17.19	177.19
						2.0	7.65	2.44	23.42	21.87	285.99
		.85	0.15	7.67	316	0.3	1.15	1.10	5.13	7.43	14.18
						0.5	1.91	1.49	9.40	10.32	45.39
						1.5	5.74	2.19	10.59	18.48	161.94
						2.0	7.65	2.55	11.53	22.77	259.09

Summary of Data (continued)

Soil	Model	Dia. (ft)	Part Full A Flow (sq-ft)	Part Full V (fps)	Time of Scour (min)	D.I.	Q (cfs)	d_s (ft)	W_s (ft)	L_s (ft)	V_s (cu-ft)
Uniform Sand	20'	.85	.29	6.58	31	0.5	1.89	0.85	2.30	8.0	-
						1.0	3.78	1.17	4.00	8.0	-
d_{50}=1.86	TW/D=.45					1.0	3.78	1.17	4.67	9.0	-
						1.5	5.67	1.44	4.93	9.5	-
σ = 1.33						2.0	7.56	1.68	5.93	13.5	-
						2.5	9.45	1.96	8.29	17.0	-
		.85	.29	6.58	100	0.5	1.89	0.98	3.00	9.0	-
						1.0	3.78	1.12	-	8.5	-
						1.0	3.78	1.15	4.00	7.5	-
						1.5	5.67	1.73	6.33	11.5	-
						2.0	7.56	1.95	6.00	15.0	-
						2.5	9.45	2.05	8.00	18.0	-
		.85	.29	6.58	1000	0.5	1.89	1.40	4.9	19.0	112.28
						1.0	3.78	1.50	6.3	19.0	-
						1.0	3.78	1.41	5.5	18.0	104.67
						1.5	5.67	1.91	7.2	24.0	226.15
						2.0	7.56	2.15	9.8	28.0	256.25
						2.5	9.45	2.41	11.6	33.0	550.04

Summary of Data (continued)

Soil	Model	Dia. (ft)	Part Full A Flow (sq-ft)	Part Full V (fps)	Time of Scour (min)	D.I.	Q (cfs)	d_s (ft)	W_s (ft)	L_s (ft)	V_s (cu-ft)
Uniform Sand	20'	1.13	.50	7.62	31	0.5	3.85	1.14	3.13	12.5	-
d_{50}=1.86	TW/D=.45					1.0	7.70	1.61	5.20	9.5	-
						1.5	11.55	1.98	7.40	14.5	-
σ = 1.33						2.0	15.40	2.23	8.90	17.5	-
						2.5	19.26	2.65	11.25	22.0	-
		1.13	.50	7.62	100	0.5	3.85	1.85	5.13	13.5	-
						1.0	7.70	-	-	10.5	-
						1.5	11.55	2.10	7.53	16.5	-
						2.0	15.40	2.20	9.14	19.0	-
						2.5	19.26	3.25	13.50	22.5	-
		1.13	.50	7.62	1000	0.5	3.85	1.89	7.70	22.0	239.75
						1.0	7.70	2.08	7.40	22.0	172.61
						1.5	11.55	2.66	12.00	27.0	343.29
						2.0	15.40	3.38	13.50	31.0	635.52
						2.5	19.26	3.51	-	35.0	721.11

Summary of Data (continued)

Soil	Model	Dia. Ft.	Part Full A Flow (sq-ft)	Part Full V (fps)	Time of Scour (min)	D.I.	Q (cfs)	d_s (ft)	W_s (ft)	L_s (ft)	V_s (cu-ft)
Uniform Sand	20'	1.46	.83	8.77	31	0.5	7.31	1.41	5.07	13.5	-
d_{50}=1.86	TW/D=.45					1.0	14.62	1.98	7.07	13.0	-
						1.5	21.91	2.40	9.80	18.0	-
σ = 1.33						2.0	29.23	2.55	12.00	22.0	-
						2.0	29.23	3.00	13.00	22.0	-
		1.46	.83	8.77	100	0.5	7.31	1.62	5.40	11.5	-
						1.0	14.62	1.67	8.00	14.0	-
						1.5	21.91	2.80	12.33	20.0	-
						2.0	29.23	3.30	12.00	23.0	-
						2.0	29.23	3.22	12.86	23.5	-
		1.46	.83	8.77	1000	0.5	7.31	1.81	6.99	22.5	141.91
						1.0	14.62	2.80	11.61	24.0	256.65
						1.5	21.91	3.91	12.29	32.0	716.88
						2.0	29.23	4.07	12.91	38.0	958.88

Summary of Data (continued)

Soil	Model	Dia. Ft.	Part Full A Flow (sq-ft)	Part Full V (fps)	Time of Scour (min)	D.I.	Q (cfs)	d_s (ft)	W_s (ft)	L_s (ft)	V_s (cu-ft)
Uniform Sand	4'	0.33	0.030	3.6	20	0.3	0.11	0.18	1.0	2.8	0.19
d_{50} = .22	TW/D=.45		0.038	3.8	20	0.4	0.15	0.33	1.3	3.3	0.40
			0.043	4.2	20	0.5	0.18	0.42	1.7	3.7	0.84

Summary of Data (continued)

Soil	Model	Dia. (ft)	Part Full A Flow (sq-ft)	Part Full V (fps)	Time of Scour (min)	D.I.	Q (cfs)	d_s (ft)	W_s (ft)	L_s (ft)	V_s (cu-ft)
Graded Sand	4'	.33	.044	4.09	14	0.5	.18	.177	.924	2.6	.131
d_{50}=2.00	TW/D=.45	.33	.030	3.67		0.3	.11	.177	.691	2.7	.057
						1.0	.36	.348	2.16	3.1	.703
σ = 4.38		.33	.035	4.17		0.4	.15	.113	.874	2.7	.085
						1.5	.55	.486	3.7*	4.0	1.736
						2.0	.73	.649	3.7*	5.4	4.049
		.33	.044	4.09	141	0.5	.18	.228	1.237	3.5	.244
		.33	.030	3.67		0.3	.11	.123	.863	2.7	.080
						1.0	.36	.378	2.86	3.2	.933
		.33	.035	4.17		0.4	.15	.165	1.742	3.8	.236
						1.5	.55	.535	3.7*	5.0	2.802
						2.0	.73	.718	3.7*	6.4	5.797
		.33	.044	4.09	316	0.4	.18	.23	1.41	3.5	.30
		.33	.030	3.67		0.3	.11	.15	.97	2.7	.10
						1.0	.36	.38	2.97	3.6	.93
		.33	.035	4.17		0.4	.15	.19	2.27	3.8	.26
						1.5	.55	.58	3.70	5.3	3.36
						2.0	.73	.82	3.70	6.4	6.44

*Exceeded Facility Boundaries

Summary of Data (continued)

Soil	Model	Dia. (ft)	Part Full A Flow (sq-ft)	Part Full V (fps)	Time of Scour (min)	D.I.	Q (cfs)	d_s (ft)	W_s (ft)	L_s (ft)	V_s (cu-ft)
Uniform Gravel	20'	.85	.29	6.58	31	0.5	1.91	0.75	4.00	5.01	4.70
d_{50}=7.62	TW/D=.25					1.5	5.74	1.62	10.60	12.81	57.77
σ = 1.32						2.0	7.65	2.03	12.50	15.48	93.90
		.85	.29	6.58	100	0.5	1.91	0.79	4.00	6.97	6.32
						1.5	5.74	1.73	11.38	13.98	67.86
						2.0	7.65	2.12	12.50	13.60	121.65
		.85	.29	6.58		0.5	1.91	0.79	4.61	7.28	7.09
						1.5	5.74	1.85	12.21	15.68	81.88
						2.0	7.65	2.17	12.39	19.68	155.09

Summary of Data (continued)

Soil	Model	Dia. (ft)	Part Full A Flow (sq-ft)	Part Full V (fps)	Time of Scour (min)	D.I.	Q (cfs)	d_s (ft)	W_s (ft)	L_s (ft)	V_s (cu-ft)
Uniform Gravel d_{50}=7.62 σ = 1.32	20' TW/D=.45	.85	.29	6.58	31	0.5	1.91	0.71	3.31	8.86	8.53
						1.0	3.83	1.35	7.39	7.29	20.97
						1.5	5.74	1.55	7.80	15.29	48.42
						2.0	7.65	1.95	11.05	17.24	88.84
		.85	.20	6.58	100	0.5	1.91	1.00	4.05	7.19	9.25
						1.0	3.83	1.35	7.70	8.03	27.03
						1.5	5.74	1.66	8.83	16.87	60.46
						2.0	7.65	2.05	11.31	20.17	118.90
		.85	.29	6.58	316	0.5	1.91	1.15	5.04	9.09	12.25
						1.0	3.83	1.49	7.94	10.35	36.41
						1.5	5.74	1.84	9.79	19.58	86.13
						2.0	7.65	2.15	12.11	23.64	164.28

Summary of Data (continued)

Soil	Model	Dia. Ft.	Part Full A Flow (sq-ft)	Part Full V (fps)	Time of Scour (min)	D.I.	Q (cfs)	d_s (ft)	W_s (ft)	L_s (ft)	V_s (cu-ft)
Uniform Gravel	20'	.85	0.29	6.58	31	0.5	1.91	1.05	4.58	5.48	8.14
d_{50}=7.62	TW/D=0					1.5	5.74	1.54	11.01	11.68	51.23
σ = 1.32						2.0	7.65	1.99	12.50	15.68	101.73
		.85	0.29	6.58	100	0.5	1.91	1.06	5.37	5.35	9.62
						1.5	5.74	1.75	12.50	12.68	71.41
						2.0	7.65	2.16	12.50	17.51	130.19
		.85	0.29	6.58	316	0.5	1.91	1.05	5.55	5.34	9.78
						1.5	5.74	1.89	11.02	14.41	84.33
						2.0	7.65	2.27	12.64	19.53	166.98

Summary of Data (continued)

Soil	Model	Dia. Ft.	Part Full A Flow (sq-ft)	Part Full V (fps)	Time of Scour (min)	D.I.	Q (cfs)	d_s (ft)	W_s (ft)	L_s (ft)	V_s (cu-ft)
Grad. Gravel	20'	.85	.29	6.58	31	0.5	1.91	0.67	2.50	9.07	3.07
d_{50}=7.34	TW/D=.45					1.0	3.83	1.08	6.50	7.25	14.82
						1.5	5.74	1.50	8.89	11.93	46.42
σ = 4.78						2.0	7.65	1.65	11.25	15.29	86.32
		.85	.29	6.58	100	0.5	1.91	0.82	3.31	8.46	4.26
						1.0	3.83	1.17	7.28	7.44	19.65
						1.5	5.74	1.44	11.60	14.32	54.83
						2.0	7.65	1.77	10.73	16.84	105.77
		.85	.29	6.58	316	0.5	1.91	0.91	3.82	9.30	5.84
						1.0	3.83	1.24	7.61	8.31	22.11
						1.5	5.74	1.54	12.21	14.9	65.02
						2.0	7.65	1.87	12.21	18.57	139.78

Summary of Data (continued)

Soil	Model	Dia. Ft.	Part Full A Flow (sq-ft)	Part Full V (fps)	Time of Scour (min)	D.I.	Q (cfs)	d_s (ft)	W_s (ft)	L_s (ft)	V_s (cu-ft)
Cohesive	20'	.85	.29	6.58	31	0.5	1.91	1.16	5.5	7.5	16.1
						1.0	3.83	1.56	6.0	8.5	25.2
d_{50}=.15	TW/D=.45					1.5	5.74	1.78	10.0	12.5	62.0
						2.0	7.65	2.08	12.0	16.0	97.6
		.85	.29	6.58	100	0.5	1.91	1.43	7.0	8.0	17.3
						1.0	3.83	1.62	7.0	9.0	33.0
						1.5	5.74	1.95	10.0	14.0	67.4
						2.0	7.65	2.08	12.0	17.0	107.1
		.85	.29	6.58	1000	0.5	1.91	1.50	6.6	9.8	28.9
						1.0	3.83	2.11	8.6	11.5	61.6
						1.5	5.74	2.07	11.0	19.9	84.4
						2.0	7.65	2.32	12.5*	22.1	209.5

*Exceeded Facility Boundaries

Summary of Data (continued)

Soil	Model	Dia. Ft.	Part Full A Flow (sq-ft)	Part Full V (fps)	Time of Scour (min)	D.I.	Q (cfs)	d_s (ft)	W_s (ft)	L_s (ft)	V_s (cu-ft)
Cohesive	20'	1.13	.50	7.62	31	0.5	3.81	1.03	7.0	11.5	44.8
						1.0	7.62	1.43	6.0	12.5	29.3
d_{50}=.15	TW/D=.45					1.5	11.43	2.04	12.5	15.5	121.4
						2.0	15.23	2.27	13.0	20.0	174.0
		1.13	.50	7.62	100	0.5	3.81	1.14	7.0	14.0	53.3
						1.0	7.62	1.43	7.0	14.0	42.4
						1.5	11.43	2.09	12.0	17.0	149.1
						2.0	15.23	2.43	13.0	23.0	225.4
		1.13	.5	7.62	1000	0.5	3.81	1.60	8.0	20.3	66.3
						1.0	7.62	3.07	10.4	16.9	139.3
						1.5	11.43	2.75	11.0	20.9	198.2
						2.0	15.23	4.09	12.5*	28.7	554.5

*Exceeded Facility Boundaries

*U.S. GOVERNMENT PRINTING OFFICE: 1982-0-361-428/2263

FEDERALLY COORDINATED PROGRAM (FCP) OF HIGHWAY RESEARCH AND DEVELOPMENT

The Offices of Research and Development (R&D) of the Federal Highway Administration (FHWA) are responsible for a broad program of staff and contract research and development and a Federal-aid program, conducted by or through the State highway transportation agencies, that includes the Highway Planning and Research (HP&R) program and the National Cooperative Highway Research Program (NCHRP) managed by the Transportation Research Board. The FCP is a carefully selected group of projects that uses research and development resources to obtain timely solutions to urgent national highway engineering problems.*

The diagonal double stripe on the cover of this report represents a highway and is color-coded to identify the FCP category that the report falls under. A red stripe is used for category 1, dark blue for category 2, light blue for category 3, brown for category 4, gray for category 5, green for categories 6 and 7, and an orange stripe identifies category 0.

FCP Category Descriptions

1. Improved Highway Design and Operation for Safety

Safety R&D addresses problems associated with the responsibilities of the FHWA under the Highway Safety Act and includes investigation of appropriate design standards, roadside hardware, signing, and physical and scientific data for the formulation of improved safety regulations.

2. Reduction of Traffic Congestion, and Improved Operational Efficiency

Traffic R&D is concerned with increasing the operational efficiency of existing highways by advancing technology, by improving designs for existing as well as new facilities, and by balancing the demand-capacity relationship through traffic management techniques such as bus and carpool preferential treatment, motorist information, and rerouting of traffic.

3. Environmental Considerations in Highway Design, Location, Construction, and Operation

Environmental R&D is directed toward identifying and evaluating highway elements that affect the quality of the human environment. The goals are reduction of adverse highway and traffic impacts, and protection and enhancement of the environment.

4. Improved Materials Utilization and Durability

Materials R&D is concerned with expanding the knowledge and technology of materials properties, using available natural materials, improving structural foundation materials, recycling highway materials, converting industrial wastes into useful highway products, developing extender or substitute materials for those in short supply, and developing more rapid and reliable testing procedures. The goals are lower highway construction costs and extended maintenance-free operation.

5. Improved Design to Reduce Costs, Extend Life Expectancy, and Insure Structural Safety

Structural R&D is concerned with furthering the latest technological advances in structural and hydraulic designs, fabrication processes, and construction techniques to provide safe, efficient highways at reasonable costs.

6. Improved Technology for Highway Construction

This category is concerned with the research, development, and implementation of highway construction technology to increase productivity, reduce energy consumption, conserve dwindling resources, and reduce costs while improving the quality and methods of construction.

7. Improved Technology for Highway Maintenance

This category addresses problems in preserving the Nation's highways and includes activities in physical maintenance, traffic services, management, and equipment. The goal is to maximize operational efficiency and safety to the traveling public while conserving resources.

0. Other New Studies

This category, not included in the seven-volume official statement of the FCP, is concerned with HP&R and NCHRP studies not specifically related to FCP projects. These studies involve R&D support of other FHWA program office research.

* The complete seven-volume official statement of the FCP is available from the National Technical Information Service, Springfield, Va. 22161. Single copies of the introductory volume are available without charge from Program Analysis (HRD-3), Offices of Research and Development, Federal Highway Administration, Washington, D.C. 20590.